Joana Barbosa Henriques e Queiroz Machado

Genetic analysis of *tef*: a mutation in *Drosophila melanogaster* that causes abnormal telomere behaviour

Porto
2001

Joana Barbosa Henriques e Queiroz Machado

Genetic analysis of *tef*: a mutation in *Drosophila melanogaster* that causes abnormal telomere behaviour

Porto

2001

Joana Barbosa Henriques e Queiroz Machado

Genetic analysis of *tef*: a mutation in *Drosophila melanogaster* that causes abnormal telomere behaviour

Dissertação realizada para a candidatura a grau de Doutor em Ciências Biomédicas submetida ao Instituto de Ciências Biomédicas Abel Salazar da Universidade do Porto

Supervisor: Professor Doutor Claudio E. Sunkel

Porto

2001

Este trabalho foi financiado pela Fundação para a Ciência e a Tecnologia

Declaração

De acordo com o disposto no nº2 do Artigo 8º do Decreto Lei nº388/70, nesta dissertação foram utilizados resultados das publicações abaixo indicadas. No cumprimento do disposto no referido Decreto-Lei, a autora desta dissertação declara que interveio na concepção e na execução do trabalho experimental, na interpretação dos resultados e na redacção dos manuscritos publicados ou em preparação, sob o nome de Quieroz-Machado J.

Queiroz-Machado J, Perdigão J, Simões-Carvalho P, Herrmann S and Sunkel CE (2001) *tef*: a mutation that causes *telomere fusion* and severe genome rearrangements in *Drosophila melanogaster*. Chromosoma 110: 10-23

Queiroz-Machado J, Sousa S, Salcedo S, Simões-Carvalho P, Coelho PA and Sunkel CE (2001) Chromosome painting in *Drosophila melanogaster* mitotic chromosomes (in preparation)

Aos meus Pais

Agradecimentos/Acknowledgements

Em primeiro lugar gostaria de manifestar a minha admiração pelo Professor Doutor Claudio Sunkel e expressar a minha profunda gratidão pela oportunidade que me concedeu em trabalhar sob sua supervisão. Não esqueço o enorme gosto que me incutiu pela ciência através do entusiasmo que transmitiu ao longo destes anos. Agradeço também todas as discussões construtivas, os conselhos e a sua disponibilidade constante.

I would like to express my gratitude to Professor Sergio Pimpinelli, for accepting me in his lab to perform HP1 protein analysis in the *tef* mutant and for the valuable discussions. I would also like to thank Laura Fanti for her constant help and for the thoughtful advises. To all the members of the lab, thank you for the hospitality and availability.

O meu agradecimento é também dirigido:

À Paula Almeida Coelho pela sua participação no projecto de "Chromosome painting" e acima de tudo pelo seu constante espírito crítico, apoio e amizade ao longo destes anos. Não esqueço também as discussões acesas e construtivas que sempre nos levavam um passo mais à frente.

Ao Pedro Simões Carvalho pela sua valiosa colaboração neste trabalho, e por ter sido tão fácil trabalharmos em conjunto.

À Siegrun Herrman pela importante participação na análise da espermatogénese do mutante *tef*, e pela preciosa ajuda e tempo que concedeu durante a execução desta tese.

À Sandra Sousa e Susana Salcedo pelo seu contributo no trabalho "chromosome painting" e pela constante disponibilidade e boa disposição.

À Joana Perdigão por me ter ajudado nos primeiros passos deste trabalho, pelos seus conselhos e críticas.

À Carla Lopes, Catarina Lemos, Elsa Bronze, Elsa Logarinho, Hassan Bousbaa, Paula Sampaio e Tatiana Moutinho pelas críticas que me fizeram em diferentes alturas deste percurso, pelos conselhos pertinentes durante a execução desta tese e pela agradável companhia ao longo destes anos.

À Alexandra Moreira, Isabel Amorim e ao João Almeida Santos, Ana Nóvoa, Madalena Costa, Pedro Pinto, Pedro Castelo-Branco, Helder Maiato, Søren Steffensen e Daniel Perez pela colaboração e conselhos.

Não posso também deixar de manifestar a minha gratidão às pessoas que apesar de não terem participado na execução desta tese contribuiram para a minha formação profissional e pessoal também:

My deepest thanks to the late Professor Harry Hoge who taught me the "begginings" and showed me the beauty of science.

À Inês Lopes Cardoso gostava de agradecer por me ter acompanhado nos primeiros passos no laboratório e pela amizade ao longo destes anos.

Agradeço também em particular à Senhora D. Adelaide Santos, Senhora D. Maria João e Senhora D. Teresa pela disponibilidade sempre constantes.

Ao Instituto de Biomédicas Abel Salazar agradeço por me ter aceite como aluna de doutoramento.

Agradeço e dedico também este trabalho à Maria Isabel Oliveira, a minha outra Mãe, confidente e conselheira por excelência em todas as ocasiões, que sem ter qualquer noção de Biologia Molecular vai sempre dizer que esta é a melhor tese do mundo.

Com profunda saudade dedico também esta tese à memória dos meus Avós paternos.

Aos meus Pais, Avós maternos e Irmãos gostava de manifestar a minha mais sentida gratidão e carinho que se estendem muito para além do que aqui fica escrito. Sem o seu apoio nada seria possível, pelo que esta tese também lhes pertence.

CONTENTS

ABSTRACT

Telomeres are the stable ends of linear chromosomes in eukaryotes. These complex protein-nucleic acid structures are essential to maintain genomic stability and the integrity of linear chromosomes. Chromosome fusions have been reported in a variety of human tumours, ageing cells and several instability syndromes. Telomeres are composed of simple repetitive sequences, which exhibit high homology within most species, except in *Drosophila*. Studies in *Drosophila* have demonstrated that specific retrotransposons, Het-A and TART, are present in chromosome ends and that protection of telomere ends is achieved by a capping mechanism that may be sequence independent.

This study reports a new *Drosophila* mutation that causes high frequency of end-to-end fusions of chromosomes during mitosis and meiosis. The mutation, causes chromosome fusions that do not resolve, leading to cycles of chromosome breakage and rejoining and severe genome rearrangements. Linear chromosome ends appear to be essential for fusions to take place. The gene is essential for normal cell proliferation and mutant tissue shows significant apoptosis. This study suggests that the function encoded by the mutant gene is required to protect the linear ends of chromosomes.

Progress in mapping the *tef* mutation by meiotic recombination analysis and further complementation with various deficiency strains is also reported. The *tef* gene is located in the 88B8-C4 cytological division. Molecular analysis of a P1 clone mapped within these limits was performed, and cDNAs were isolated from phage libraries. Several coding regions from the "Berkeley *Drosophlia* Genome Project" were selected from this analysis as potential candidates of the *tef* gene. Further analysis will have to be performed in order to test these sequences.

Chromosome painting in *Drosophila* was also developed. This technical approach will enable analysis of mitotic phenotypes concerning chromosome structure or genome rearrangements.

SUMÁRIO

Os telómeros são estruturas formadas por um conjunto de proteínas específicas associadas às sequências teloméricas, e são essenciais para a estabilidade e correcta segregação dos cromossomas durante a divisão celular. Fusões entre as extremidades de cromossomas foram já observadas em vários tipos de tumores humanos, células envelhecidas e uma série de síndromes caracterizados por instabilidade cromossómica. Os telómeros são constituídos por sequências repetitivas simples que apresentam elevada homologia entre a maioria dos eucariotas excepto *Drosophila*. Estudos neste organismo revelaram que os telómeros são constituídos por dois tipos de transposão, Het-A e TART, e que o mecanismo de protecção da extremidade dos cromossomas é eventualmente independente do tipo de sequência de DNA presente.

Este estudo reporta a caracterização de um novo mutante de *Drosophila* que exibe uma elevada taxa de fusões entre todos os cromossomas em mitose e em meiose. Esta mutação induz a fusão das extremidades dos cromossomas que resulta na formação de pontes de DNA em anafase, conduzindo a ciclos de quebra da cromatina e de nova fusão. Os cromossomas apresentam também uma elevada taxa de rearranjos cromossomais eventualmente associados a esses ciclos de quebra e fusão. Chromossomas lineares parecem ser essenciais para a existência de fusões. O gene é essencial para a proliferação celular normal e os tecidos mutantes apresentam um elevado índice de apoptose. O presente estudo sugere que a função codificada pelo gene *tef* é necessária para a protecção das extremidades dos cromossomas.

O progresso do mapeamento do gene *tef* foi também realizado através de recombinação meiótica e de testes de complementação com estirpes de *Drosophila* deficientes em determinadas porções do genoma. O gene *tef* está mapeado na zona citológica 88B8-C4. Foi efectuada a análise molecular de um clone P1 mapeado entre esses limites. Este clone foi utilizado como sonda para efectuar o rastreio de várias bibliotecas de cDNA, tendo-se isolado vários cDNAs que foram sequenciados e analizados. Foram seleccionados algumas regiões codificantes do "Berkeley *Drosophlia* Genome Project" como potenciais genes que codificam a função *tef*.

Neste trabalho foi também desenvolvida a técnica de "chromosome painting" em *Drosophila* que permitirá mais facilmente a análise de fenótipos mitóticos que afectem a estrutura cromossómica, nomeadamente com rearranjos genómicos.

RÉSUMÉ

Les télomères sont les extrémités stables des chromosomes linéaires des eucaryotes. Ces structures protéine-acide nucléique complexes sont essentielles pour le maintien de la stabilité génomique et l'intégrité des chromosomes linéaires. Des fusions entre chromosomes ont été rapportées dans de nombreuses tumeurs humaines, dans les cellules sénescentes et dans une variété de syndromes d'instabilité. Les télomères sont composés de simples séquences répétitives présentant une grande homologie entre les espèces sauf chez *Drosophila*. Des études chez *Drosophila* ont montré que des rétrotransposants spécifiques, Het-A et TART, sont présents dans les extrémités des chromosomes et que la protection des extrémités des télomères est assurée par un mécanisme de capping probablement séquence indépendant.

Le présent travail décrit une nouvelle mutation chez *Drosophila* causant une grande incidence de fusions entre les extrémités des chromosomes durant la mitose et la méiose. Les fusions provoquées par cette mutation ne se défont pas, donnant origine à des cycles de cassures et unions chromosomiques ainsi qu'à des réarrangements génomiques sévères. Les extrémités des chromosomes linéaires paraissent être essentielles pour que les fusions aient lieu. Le gène est essentiel pour la prolifération cellulaire normale et les tissus des mutants montrent une intense activité d'apoptose. Ces résultas suggèrent que la fonction codée par le gène muté *tef* est de protéger les extrémités des chromosomes linéaires.

Un progrès significatif a été réalisé dans le but de cartographier la mutation *tef* à travers l'analyse de recombinaisons méiotique et les tests de complémentation avec des souches déficientes. Le gène *tef* est localisé au niveau de la division cytologique 88B8-C4. L'analyse moléculaire d'un clone P1 couvrant cette région a été effectuée et le cDNA a été isolé à partir d'une bibliothèque de phages. Plusieurs régions codantes ont été sélectionnées à partir de « Berkeley Drosophila Genome Project » comme potentiels candidats du gène *tef*. Des analyses ultérieures devraient tester ces séquences.

Des expériences de chromosome painting chez *Drosophila* ont été aussi effectuées. Cette approche technique permettrait l'analyse des phénotypes mitotiques concernant la structure des chromosomes ou les réarrangements génomiques.

PART I: *tef*, a mutation that causes *telomere fusion* and severe genome rearrangements in *Drosophila melanogaster*

1. INTRODUCTION

1. INTRODUCTION

1.1 The Cell Cycle: General Description

Cells are able to proliferate by dividing in two identical daughter cells. The cell division cycle consists of an ordered and highly controlled series of specific events. Most eukaryotic cells never proceed to the next stage of the cycle without successfully completing the previous event. Therefore, to produce a pair of genetically identical daughter cells the DNA must be faithfully replicated and sister chromatids must be correctly segregated into two separate cells. The vast majority of cell types also doubles their mass and duplicates all cytoplasmic organelles in each cell cycle. In multicellular organisms loss of cell division control ultimately leads to cancer or cell death.

The eukaryotic cell cycle is divided into distinct phases with variable time-lengths depending on the cell type and the development stage of the organism (Fig. 1).

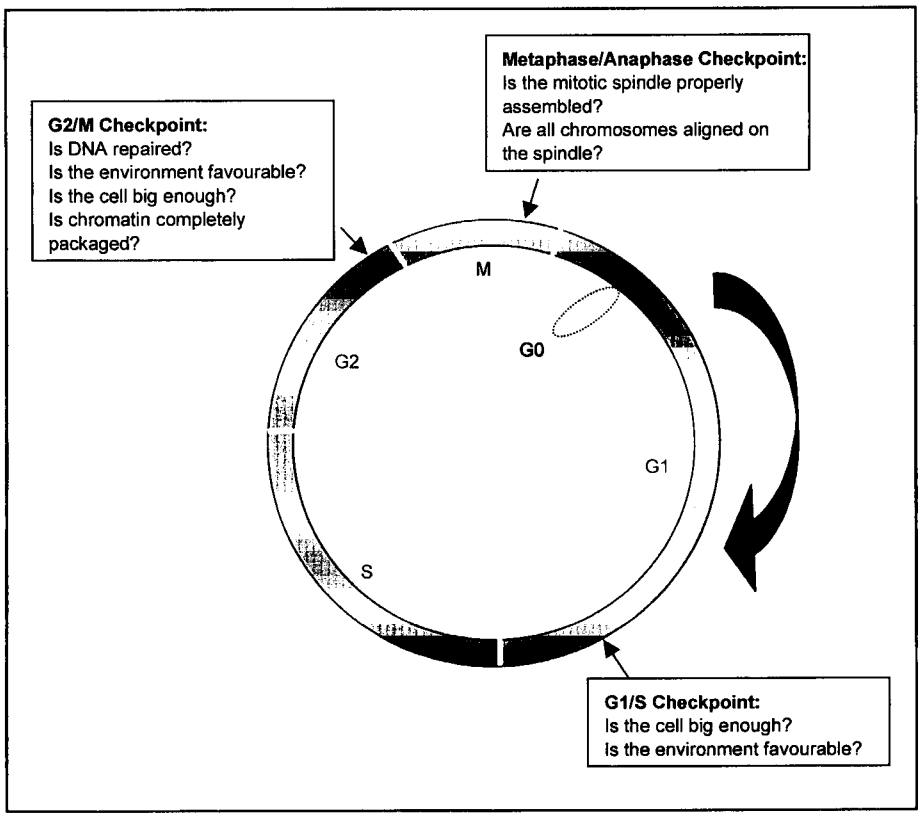

Figure 1: The cell cycle stages. The relative duration of each phase is variable and depends on the cell type and the development stage of the organism. During G1, cells can also exit the cell cycle into a G0 stationary phase and later return to G1. Checkpoint controls take place in several points of the cell cycle and are referred inside boxes.

During interphase, which takes place after mitotic division (M phase), the cell continuously grows and DNA is replicated. DNA replication is confined to the part of interphase known as S phase. G1 is the gap phase between M and S phase, and G2 corresponds to the gap between S and M phase. Throughout G1 phase, cells increase in size. During this stage, cells can exit the cell cycle and enter a specialised resting state called G0 where they can remain for days, weeks or years before returning to G1 and continue proliferation. Alternatively, they may not divide at all. During S phase, the DNA is duplicated in a semi-conservative process, so that in the end, two sister chromatids associated at the centromeric region compose each chromosome. G2 provides a safety gap, where DNA repair takes place to ensure faithful transmission of genetic information to daughter cells arising from the next mitotic division, and where synthesis of proteins required for cell division takes place. Centrosome duplication takes place during G1/S phase but they do not separate until G2.

During mitosis cells divide after completing a series of events (Fig.2). Mitosis is generally short and subdivided into six sequential events. Prophase is characterised by chromosomal condensation and the beginning of mitotic spindle assembly, during which centrosomes migrate to opposite sides of the nucleus where they will establish the spindle poles. Prometaphase starts with nuclear envelope disassembly. Spindle microtubules are able to reach the chromosomes and bind them at specialised protein complexes called kinetochores. When sister kinetochores of a chromosome attach to microtubules of opposite ends the cell reaches the metaphase stage. At this point all chromosomes are aligned at the equatorial region of the mitotic spindle. Anaphase is characterised by segregation of sister chromatids to opposite poles. This phase can be subdivided in Anaphase A, where kinetochore microtubules shorten as the chromosomes approach the poles, and in Anaphase B, which is characterised by polar microtubule elongation. In telophase kinetochore microtubules disassemble and polar microtubules continue to elongate. Chromatin decondenses and the nuclear envelope reforms around each group of daughter chromosomes. Finally, during cytokinesis the membrane between the two daughter nuclei is drawn inward to form a cleavage furrow, which ends up separating the two new daughter cells.

There are many exceptions to the cell cycle pattern described above. For example, early embryonic cell cycles are normally much faster and in many animals do not involve gap phases. Accordingly, no cell growth occurs and consequently cells decrease in volume as they divide. Other embryos as those of *Drosophila* undergo early cell cycles of syncytial nuclear multiplication in the absence of cytokinesis. Endoreplication cycles observed in salivary glands of *Drosophila melanogaster* are

another exception. This process consists of successive S phases not intercalated by cell division, thus forming cells with multiple copies of the genome.

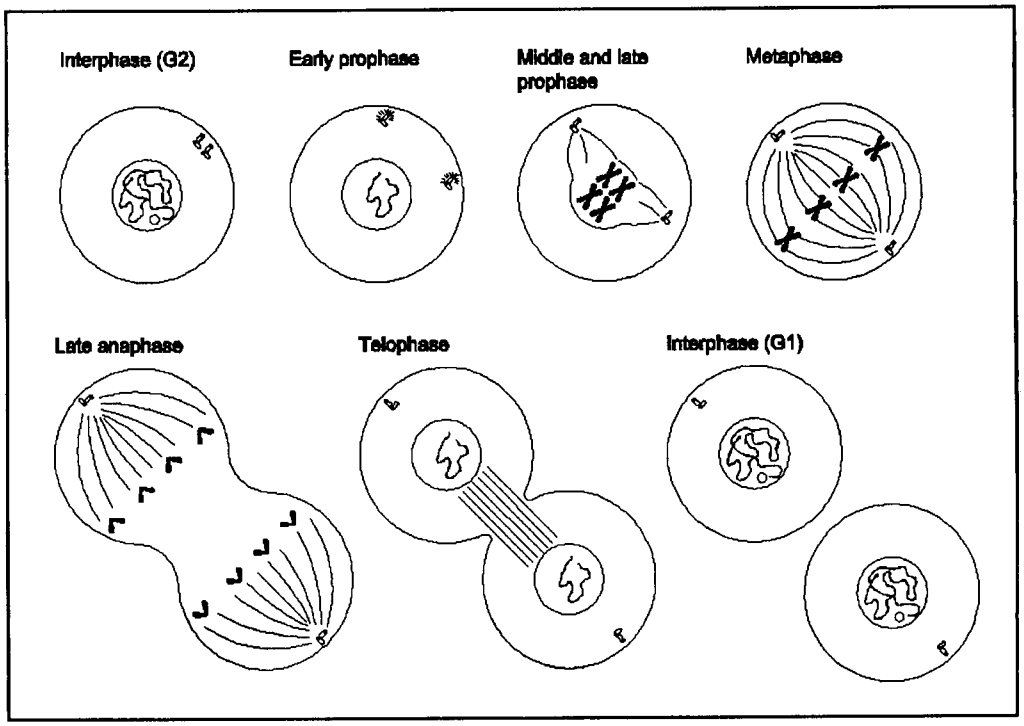

Figure 2: The cell cycle and mitosis specific stages.

1.2. The Cell Cycle Control

The cell cycle control mechanism is a biochemical machinery constituted by several interacting proteins that induce and control essential ordered events responsible for duplicating and dividing the cell contents. The exact duplication of cellular components is not a limiting process, since either all components exist in a high number or there is always the possibility of synthesising them *de novo* through the information contained in the genetic material. In contrast, DNA and the microtubule organising centres have to be identically duplicated in each cell division. Various feedback control systems can stop the cell cycle at specific checkpoints (Fig. 1). Feedback signals are thought to delay the progress throughout the cell cycle in order to complete previous events. Additionally, these checkpoint controls may react to environmental factors, such as growth factors and hormones, integrating cell proliferation with cell growth and differentiation (Murray and Hunt, 1993 and Muller *et al.*, 1993). The most prominent checkpoints occur in the G1/S, the G2/M and the metaphase/anaphase transitions.

The first evidence that trans-acting factors were involved in the regulation of the cell cycle came from cell fusion experiments with cultured mammalian cells. These experiments showed that when cells in G1, S or G2 stage were fused to cells in mitosis, they were also induced to progress into mitosis (Johnson and Rao, 1970). These experiments suggested that a factor present in mitotic cells was driving interphase cells to undergo mitosis. Since nuclei in any stage of the cell cycle are sensitive to this factor, mitosis was suggested as the dominant phase in relation to the other cell cycle stages. Similarly, when cells in G1 were fused to cells in S phase and the fused cells were exposed to radioactive thymidine, the label was incorporated into the DNA of the G1 nucleus, suggesting that DNA replication was induced by a cytoplasmic factor present in cells in S phase. However, similar experiments involving fusion of cells in G2 and cells in S phase, showed that no DNA replication took place in the G2 nuclei, suggesting the existence of a control mechanism responsible to inhibit DNA re-replication before mitosis took place, thus maintaining a suitable cellular DNA content (Rao and Johnson, 1970).

Biochemical studies in developing frog oocytes and early embryos, enabled the purification of the protein complex called "Maturation Promoting Complex" (MPF), constituted by a 34 kDa and a 45 kDa protein, which promotes the entry of an oocyte into meiosis (Lohka *et al.,* 1988). Other important studies with *S. pombe* and *S. cerevisiae* enabled the isolation of several cdc (cell division cycle) mutants, which showed cell division defects. The high homology of a cloned *S. pombe* Cdc2 gene product and the *S. cerevisiae* CDC28 with the *Xenopus* p34 protein (Dunphy *et al.,* 1988; Gautier *et al.,* 1988), enabled to identify the p34 protein as the catalytic subunit with a serine/threonine kinase activity. The 45 kDa protein was found to be a cyclin (called cyclin B), that regulates the MPF kinase activity by recognising suitable substrates. Cyclins were described as proteins that cyclically oscillate throughout the cell cycle, accumulating in mitosis and drastically decreasing at the end of this phase.

These observations suggested a model where the accumulation of cyclin B at the entry into mitosis would be necessary to activate the Cdc2 kinase. Later studies also demonstrated that this kinase activity is dependent on the phosphorylation or de-phosphorylation of specific residues of this protein. The discovery of protein homologues in several organisms including man, suggested that this is a conserved control mechanism.

1.2.1. The cell cycle control is based on protein kinase activities

New forms of the serine/threonine protein kinases (known as CDKs - Cyclin Dependent Kinases) were identified in higher eukaryotes and were shown to be responsible for the entry into S phase, and other stages of the cell cycle. All CDKs are structurally related and require transient associations with regulator cyclin proteins, binding of inhibitory polypeptides and reversible phosphorylation reactions for driving the cell cycle. Eight different CDKs have already been identified in mammals, involved in different phase transitions of the cell cycle (Nigg, 1995). Similarly, the cyclin family of proteins is also extent. There are two main classes of cyclins: mitotic cyclins, which bind to CDK proteins during G2 and are necessary for the entry into mitosis, and G1 cyclins, which associate to CDK molecules during G1 and are required for entry into S phase (Fig.3).

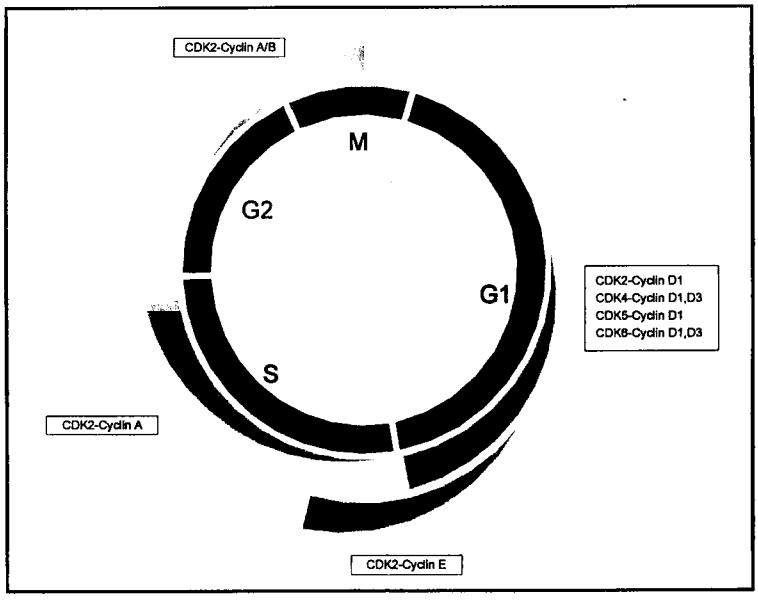

Figure 3: Distinct CDK/cyclin complex activities required for the different stages of a mammalian cell cycle.

1.2.1.1. The G1/S Transition

Most of the genetic studies that contributed to the understanding of the molecular mechanisms controlling the entry into S phase were performed in yeast cells. These organisms have been especially useful for isolation of temperature-sensitive mutants with defects in specific proteins required for the cell cycle machinery. To promote progression towards DNA replication, CDK/cyclin complexes phosphorylate

proteins (e.g. transcription factors) required for the activation of genes involved in DNA synthesis, as well as components of the DNA replication machinery. In budding yeast, at least three conditions limit the entry to S phase – the cell size, availability of nutrients and the demands of mating. However, once G1 cells reach the critical size, they become committed to completing the cell cycle even if they are shifted to a medium low in nutrients. This point, where cells become irreversibly committed to enter the S phase is called START, which is equivalent to the restriction point in mammals.

When *cdc28* temperature-sensitive mutants are shifted to the non-permissive temperature they behave like wild-type cells suddenly deprived of nutrients, that is, they cannot pass Start and enter the S-phase.

The G1 cyclins Cln1, Cln2 and Cln3 were shown to drive cells through G1 by activating the CDC28 kinase, forming the S-phase promoting factor (SPF). Gene knockout experiments showed that *S. cerevisiae* cells grow if they carry one of the three *CLN* genes, but arrest in G1 and die if all of them are deleted. Over-expression of one Cln protein drives cells through Start point. Cln1 and Cln2 levels increase during G1 and fall as cells enter S phase. Distinct cyclins, Clb5 and Clb6, promote DNA replication in S phase.

Mammalian cells in G1 react to external growth factors and to agents that induce cell differentiation that determine the G1/S transition, in contrast to yeast cells that arrest in G1 in the presence of mating-type factors. Similarly to yeast, these cells are sensitive to external factors until a certain restriction point in G1, after which they are forced to complete the division cycle (Pardee, 1989). Unlike yeast cells, which have a single Cdk to regulate the cell cycle progression, metazoan cells require a small family of related Cdks in the different cell cycle transitions. Higher eukaryotes contain cyclin functional homologues that act similarly (Fig. 3): cyclins D (D1, D2 and D3 cyclin complexes) and E during G1 and cyclins E and A during S phase. The specificity of Cdc2 activity therefore depends on the type of cyclin associated with it (Pan *et al.,* 1993). Additionally, a given cyclin may associate with multiple CDK partners and vice versa. Over-expression of cyclins D and E lead to a decrease in the time cells spend in G1, thus inhibiting cell growth (Resnitzy *et al.,* 1994). Entry into S phase requires cyclin E degradation, and the activation of the cdk2/cyclin A complex that initiates DNA replication, by acting upon specific substrates. This was possible to demonstrate by injecting anti-cyclin A antibodies into cells, that inhibited entry into S phase (Girard *et al.,* 1991). In mammalian cells, cyclin B is first synthesised during the S-phase and its levels increase as cells proceed through G2.

1.2.1.2. The G2/M transition

In the G2/M transition major checkpoint controls take place and an abrupt activation of the cyclin B/Cdc2 complex is observed. This kinase activity will result in chromosome condensation, mitotic spindle assembly and chromosome alignment in the metaphase plate. Entry into mitosis (prophase) requires accumulation of cyclin B to a certain level, for subsequent MPF activation (Solomon *et al.*, 1990). However, over-expression of cyclin B does not accelerate the G2/M transition, suggesting that over a certain level of cyclin B the MPF kinase activity still requires other positive and negative regulating mechanisms (Hagan *et al.*, 1988). Thus, MPF activation may be inhibited by phosphorylation/ dephosphorylation mechanisms. In fact, MPF catalytic subunit contains activating and inhibitory sites that are phosphorylated.

1.2.1.2.1. Regulation of the MPF complex

It is well known that the activation process of the cyclin B/Cdc2 complex requires the phosphorylation of threonine-161 aminoacid residue (numbers relative to the human Cdc2) (Fig. 4). This residue is localised in the T-loop domain, present in several kinases, which is involved in the control of the substrate accessibility to the catalytic subunit (Nigg, 1995). Phosphorylation of Cdc2 Thr161 is thought to cause the Cdc2 T loop to bend away from the active site, thereby allowing Cdc2 to bind protein substrates at the active site. The kinase responsible for the Cdc2 threonine-161 phosphorylation and corresponding residues in other Cdks was named as Cdk-Activating kinase (CAK) (Fesquet *et al.*, 1993; Poon *et al.*, 1993; Solomon *et al.*, 1993). Analysis of its catalytic subunit demonstrated that it is structurally related to Cdks. It was originally identified as MO15 (Shuttleworth *et al.*, 1990) and then also known as Cdk7 (Fisher and Morgan, 1994). The CAK activity requires the association with two other proteins: cyclin H, the regulatory subunit (Fisher and Morgan, 1994) and MAT1. The 36 kDa MAT1 ring-finger protein was cloned in several organisms and was shown to stabilise CAK complex and to promote its activity *in vitro* (Devault *et al.*, 1995; Fisher *et al.*, 1995; Tassan *et al.*, 1995). Activation of the CAK complex may occur by two different mechanisms. Yeast two-hybrid system assays showed that interaction between cyclin H and CDK7 requires phosphorylation of the threonine-170 within the catalytic subunit. Alternatively, in the presence of MAT1, activation does no longer require phosphorylation (Fisher *et al.*, 1995). As a result, a T-loop phosphorylation

independent mechanism for the activation of the CDK7-cyclin H complex may be the initiating event of the following phosphorylation cascades. The complex MAT1-CDK7-cyclin H was also identified to be a subunit of the transcription factor IIH, a multisubunit protein complex involved not only in class II transcription events, but also in DNA repair mechanisms. This suggests that modulation of transcription along the cell cycle may be regulated if DNA needs to be repaired (Adamczewski *et al.,* 1996).

The Cdc2 kinase activity is regulated by the phosphorylation inhibitory state of two other residues (Fig. 4): threonine 14 and tyrosine 15 (numbers relative to the *S. pombe* Cdc2). These residues are part of the ATP-binding domain, thus their phosphorylation prevents binding of ATP due to electrostatic repulsions between the phosphates present in both molecules. Therefore, this ensures that the MPF complex remains inactive until the G2/M transition. *S. pombe* and animal cells exhibiting mutations in these residues, enter mitosis prematurely (Gould and Nurse, 1989; Krek and Nigg, 1991). Additionally, analysis of *S. pombe* cdc mutants suggested that proteins encoded by other genes, might influence the protein kinase activity of *S.pombe* MPF, by altering the phosphorylation state of the residues described above (Fig. 4). *Wee1*$^-$ mutants exhibit premature entry into mitosis indicated by their small size, whereas overproduction of the Wee1 protein increases the length of G2, thus also increasing cell size (Featherstone and Russel, 1991). Biochemical studies of the Wee1 protein identified it as a kinase that phosphorylates the inhibitory Tyr15 residue. Another gene, *mik1*$^+$ encodes a protein kinase very similar to Wee1, also capable of phosphorylating the inhibitory Tyr15 of Cdc2.

The Wee1 protein kinase that inhibits MPF is in turn inhibited through phosphorylation by another protein kinase encoded by the *nim1*$^+$ gene, thus promoting the entry to mitosis (Coleman TR *et al.,* 1993). This protein is known to respond to nutritional requirements, thus associating the regulation of MPF to environment conditions (Feilotter *et al.,* 1991).

Conversely, *cdc25*$^-$ yeast mutants did not enter mitosis at the non-permissive temperature, suggesting that this protein stimulates the activity of *S. pombe* MPF. This protein was shown to have a phosphatase activity, which removes the phosphate from the Tyr15 and Thr14, yielding an active MPF with a unique phosphorylated residue (Thr161). Cdc25 activity is increased by phosphorylation during the entry into mitosis and decreases as this phase comes to an end (Izumi *et al.,* 1992). Apparently, MPF complex is required for Cdc25 phosphorylation (Izumi and Maller, 1993), forming a positive feedback loop to amplify MPF activity. Other MPM-2 protein kinases may also play a role in Cdc25 phosphorylation (Kuang and Ashorn, 1993). MPM2 is a

monoclonal antibody raised against mitotic HeLa cells, which specifically recognises conserved phosphoepitopes present in mitotic proteins from a variety of species (Davis *et al.,* 1983). Increasing evidence suggests that polo-like proteins might act as MPM2 kinases. Studies in *Drosophila* suggested that polo protein is required for the phosphorylation of MPM2 reactive epitopes (Logarinho and Sunkel, 1998). A putative homologue from *Xenopus*, Plx1, was shown to phosphorylate Cdc25, thereby activating it and generating MPM2 reactive epitopes (Kumagai and Dunphy, 1996). Moreover, signals from DNA damage appear to be mediated via Cdc25 and prevent its phosphatase activity (Terada *et al.,* 1995). PP1 and PP2A phosphatases, however, were also demonstrated to have a role on Cdc25 activity as they can dephosphorylate Cdc25, therefore inhibiting entry into mitosis (reviewed by King *et al.,* 1994).

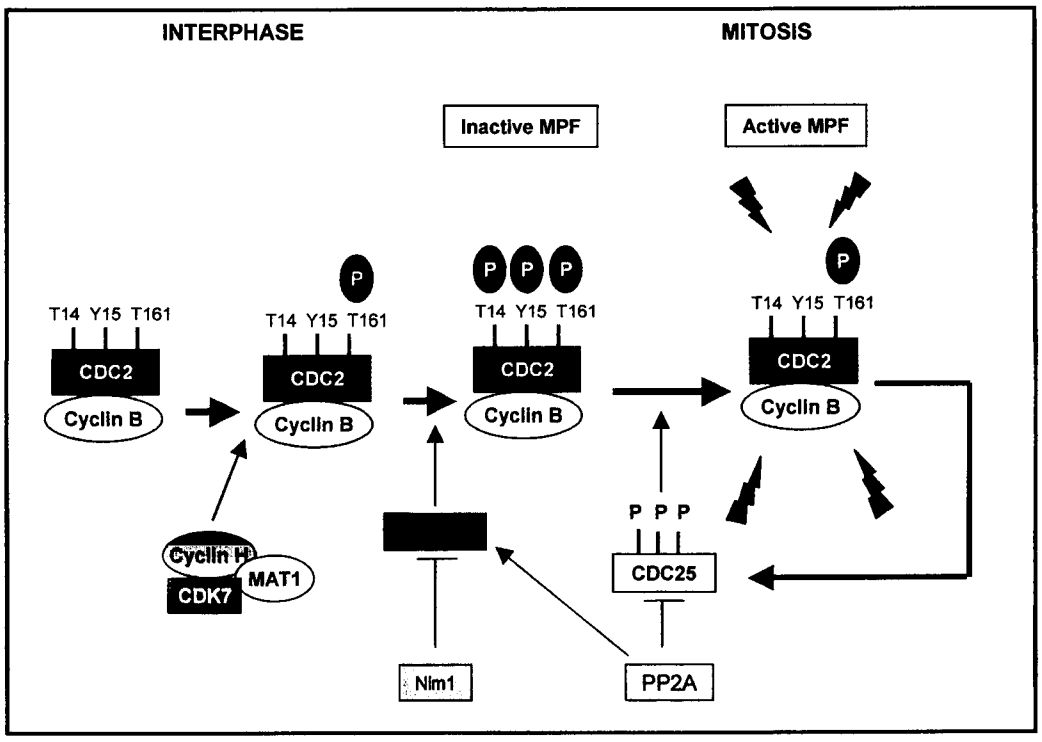

Figure 4: MPF regulation mechanisms (see detailed description in the text).

Activation of MPF is thus required for entry into mitosis. This is controlled by several factors including availability of the cyclin component, binding of Cdk inhibitors and Cdk phosphorylation. Ultimately, this complex is then responsible for phosphorylating several substrates. For example, phosphorylation of specific serine residues of nuclear lamins promotes depolymerization of the lamin-intermediate filaments contributing to the breakdown of the nuclear envelope into small vesicles. Phosphorylation of other proteins, such as histone H1, other chromatin proteins and

the components of the chromosome scaffold, may contribute to early mitotic events. Similarly, phosphorylation of microtubule-associated-proteins by MPF is required for the assembly of a dynamic mitotic spindle.

1.2.1.3. Exit from Mitosis

Studies performed in *Xenopus* egg cycling extracts showed that inactivation of MPF coincides with the late stages of mitosis (Gerhart *et al.,* 1984). It was demonstrated that proteolytic degradation of several proteins, including cyclin B, was necessary for exit from mitosis (Evans *et al.,* 1983). Molecular analysis of cyclin B, showed the existence of a destruction box at the NH_2-terminal, required for the proteolysis via the ubiquitin pathway (Glotzer *et al.,* 1991). The events of late mitosis such as sister chromatid separation and cyclin B degradation, are governed by the anaphase promoting complex (APC), that triggers the ubiquitin-dependent proteolysis.

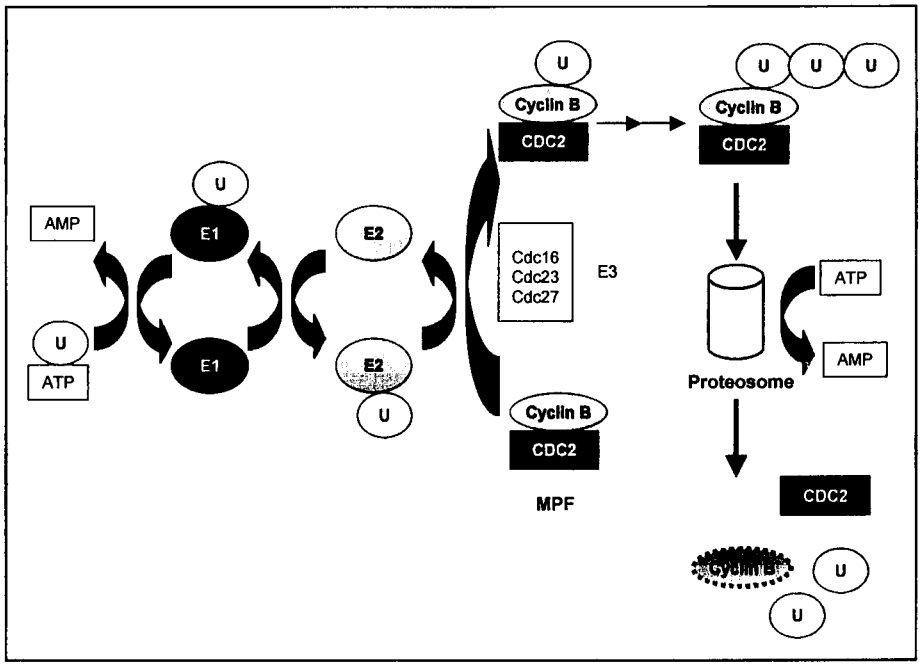

Figure 5: Proteolytic degradation via protein ubiquitination mechanisms. The first enzyme (E1) uses ATP hydrolysis to establish the association (phosphodiester binding) with an ubiquitin molecule. This complex transfers ubiquitin to another enzyme (E2). The final transfer of ubiquitin to target protein may be mediated by E2 alone or in association with an additional enzyme (E3) (adapted from Murray, 1995).

This occurs under highly controlled mechanisms, which ensure that events are properly ordered and coordinated. The APC is thought to be a ubiquitin ligase (E3 enzyme) which collaborates with a ubiquitin-activating enzyme (E1) and a ubiquitin-conjugating enzyme (E2) to catalyse the transfer of ubiquitin molecules to lysine side chains on target proteins (Fig. 5) (Hochstrasser, 1996).

The APC, a 20S-multisubunit complex, was demonstrated to be the only ubiquitination component whose levels oscillate throughout the cell cycle (King *et al.*, 1995). Several conserved APC subunits (CDC16, CDC23, and CDC27 in *S. cerevisiae*) contain tetratricopeptide repeats (TPR) that are thought to mediate protein-protein interactions. Additional subunits identified in several organisms are required to activate the APC complex: the budding yeast Cdc20 and Hct1/Cdh1 (Fizzy and Fizzy-related in *Drosophila* and *Xenopus*, p55Cdc/hCdc20 and hCdh1 in humans and Slp1 and Ste9/Srw1 in fission yeast) (reviewed in Morgan, 1999). Their mechanism of action is however not well clarified, but *in vitro* studies demonstrated that they are sub-stoichiometric APC activators whose binding to APC is a limiting determinant of its activity. There is evidence, primarily in budding yeast, that Cdc20 and Hct1 confer different substrate specificity on the APC and that they are regulated by different mechanisms.

Exit from mitosis requires sister chromatid separation, which is in part triggered by the APC-dependent destruction of anaphase inhibitors (securins). Securins include the Pds1 protein in budding yeast, the Cut2 protein in fission yeast and a recently identified Pds1 homologue in vertebrates (Zou *et al.*, 1999). Yeast expression of non-destructible mutant forms of Pds1 or Cut2 blocks sister chromatid separation, indicating that these proteins are required for maintaining sister chromatid cohesion. Conversely, *pds1* null strains are defective in anaphase checkpoint control. Before anaphase, Pds1 binds to Esp1 (or Cut1 - separin protein), inactivating the anaphase promoting activity of Esp1 (Ciosk *et al.*, 1998). During an unperturbed cell cycle, Pds1 becomes polyubiquinated at the metaphase to anaphase transition by the APC complex, and the modified forms are then recognised and degraded by the 26S proteosomes (Cohen-Fix *et al.*, 1996). Once released from Pds1, Esp1 becomes active and this activity induces cleavage of the cohesin Scc1, that is required to establish sister chromatid cohesion during S-phase (Uhlmann *et al.*, 1999) (Fig. 6). Cells completely lacking Pds1 at low temperatures do not undergo premature sister chromatid separation, suggesting that this protein is required but not sufficient to trigger the initiation of anaphase. That is, additional mechanisms not involving the APC must also restrain Esp1 activity (Ciosk *et al.*, 1998).

The highly ordered events occurring during the exit from mitosis require sequential changes in the APC substrate targeting (reviewed in Morgan, 1999). Thus, one possibility is that the APC could target anaphase inhibitors first, and then destroy inhibitors of late mitotic events (such as cyclins). In fact, it was shown in budding yeast that Cdc20 stimulates APC to start Pds1 destruction, whereas Hct1 targets the major cyclin (Clb2) for destruction (Visintin *et al.*, 1997). Some exceptions, however, should be noted. Frog early embryos do not express Hct1 protein, indicating that this protein is not required for cyclin degradation. Similarly, it is also not expressed in fly early embryos, where Cdc20 seems to be required for cyclin destruction. Hct1 appears later in the somatic cell cycles, when the G1 phase takes place during the cell cycle.

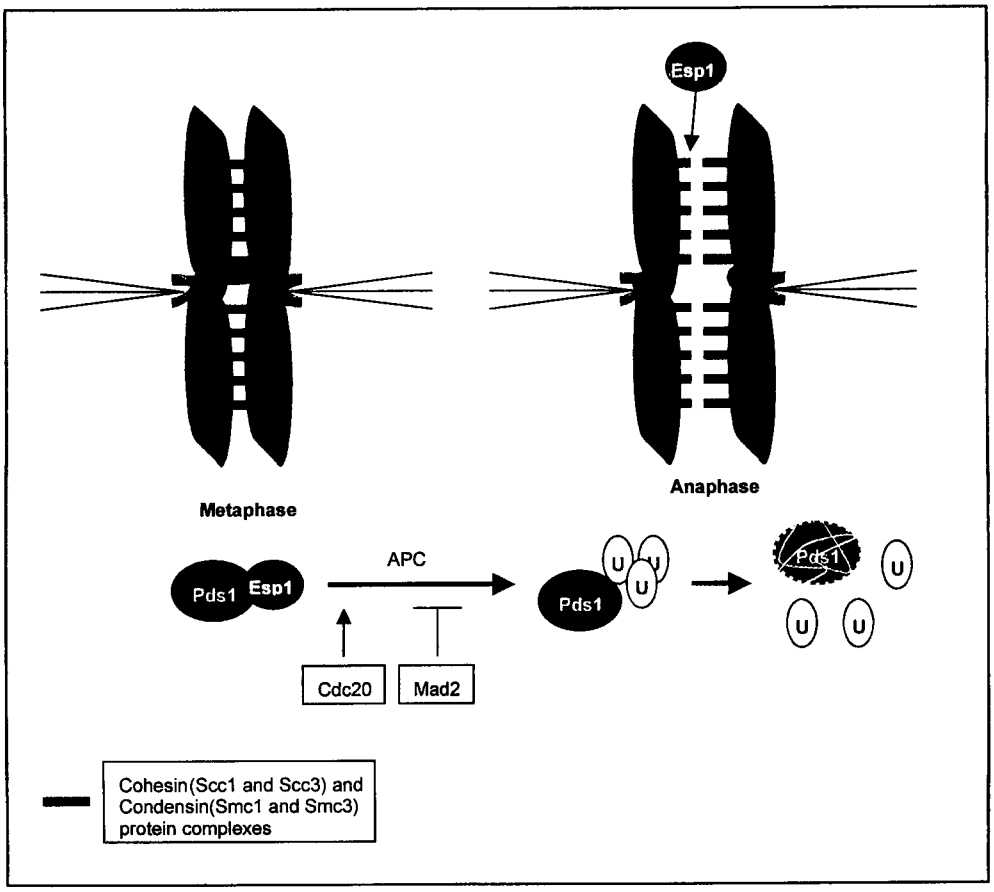

Figure 6: Regulation of anaphase in budding yeast. Sister chromatid cohesion is established during DNA replication in S phase. Loss of cohesion in anaphase depends on Esp1 activity. Before anaphase, Esp1 activity is inhibited by Pds1. At the onset of anaphase, APC ubiquitinates Pds1, which is degraded by the 26S proteosomes complexes (adapted from Clarke and Giménez-Abián, 2000).

Additionally, experiments in somatic vertebrate cells injected with a cyclin B-GFP (green fluorescent protein) fusion protein, showed that cyclin B destruction is initiated at the beginning of metaphase, and almost complete at anaphase onset (Clute and Pines, 1999). Since activation of Cdc20-APC also initiates at the same stage it is most unlikely that the order of late mitotic events in these cells is controlled simply by sequential changes of APC substrate specificity.

Cdc20 levels start to accumulate in S phase and continue through early mitosis, dropping in G1 via an APC-dependent destruction (Fang *et al.*, 1998). Post-translational mechanisms generate the abrupt Cdc20-APC activation required for initiation of anaphase, and include the phosphorylation of Cdc20 and of multiple subunits of the APC core. Previous work suggested that Cdc20 and several APC subunits undergo CDK-dependent mitotic phosphorylation in a variety of cell types (reviewed in Morgan, 1999). Thus, by promoting Cdc20-APC activity, CDKs initiate the process of their own destruction. Studies in embryonic cells suggest that additional mechanisms introduce a lag phase between CDK activation and APC activation.

Conversely, in budding yeast, phosphorylation of Hct1 by Cdk1 blocks the ability of Hct1 to activate the APC. Therefore Cdk1 blocks its own inactivation, via Hct1. It is reasonable to think that a drop in CDK activity to some threshold would lead to the sudden and complete activation of Hct1-APC complex necessary to degrade cyclin B. How the threshold is reached is not well understood. Studies in budding yeast revealed that Sic1 is a protein that binds and inhibits Cdk1-cyclin complexes in late mitosis and G1 (reviewed in Morgan, 1999).

In budding yeast the control of the cell cycle events ensure that Hct1 is activated after Cdc20. In fact, Cdc20 is able to promote the destruction of proteins that inhibit Hct1 activation. Pds1 may also be an inhibitor of cyclin destruction, since over-expression of a non degradable mutant form of Pds1 blocks not only sister chromatid separation but also prevents cyclin destruction and cytokinesis.

In vertebrate cells, APC subunits are concentrated at the kinetochores, spindle poles and along the spindle itself (Tugendreich *et al.*, 1995; Jorgensen *et al.*, 1998) whereas Cdc20 is found at the kinetochores throughout mitosis. There is also evidence that cyclin B destruction is initiated at the spindle poles (Clute and Pines, 1999).

In budding yeast mutations in several other genes cause a late mitotic arrest, in which anaphase has occurred but spindle disassembly and cytokinesis have not. These include, among others, several protein kinases (Cdc5, Cdc15, Dbf2, Dbf20) and a protein phosphatase (Cdc14) (reviewed in Morgan, 1999).

The phosphatase Cdc14 has been related to the direct control of cyclin destruction by catalysing dephosphorylation of Hct1 at the inhibitory CDK sites contributing to the Hct1-APC activation (Jaspersen *et al.*, 1999). Cdc14 is thus a potential key regulator of Cdk1 inactivation in late mitosis. Recent studies suggested that Cdc14 is under the control of a nucleolar protein Net1, which may sequester Cdc14 to the nucleolus and/or inhibit its phosphatase activity, before the onset of late mitosis events (Traverso *et al.*, 2001).

The highly conserved polo-like protein kinase is also involved in late mitotic events in the cell cycle, and was initially studied in *Drosophila* mutants (Sunkel and Glover, 1988). These proteins have been implicated in the control of mitosis in a wide range of eukaryotes (Nigg, 1998). In flies, mammals, frog and fission yeast (except in budding yeast), these kinases are required for normal centrosome maturation and mitotic spindle onset at mitosis (Sunkel and Glover, 1988; Ohkura *et al.*, 1995). Cdc5p, the budding yeast homologue of the polo kinase protein family, and the *Drosophila* polo kinase are required for cytokinesis (Ohkura *et al.*, 1995; Carmena *et al.*, 1998). Mutations of polo homologues in yeast and *Drosophila* also lead to abnormalities in the spindle apparatus in meiosis (Schild and Byer, 1980; Herrmann *et al.*, 1998). In *Xenopus*, polo is required for the activation of the cyclin destruction in egg extracts, similarly to the Cdc5p in budding yeast that promotes cyclin destruction, eventually by acting on the APC core rather than on Hct1 or Cdc20.

1.2.2. Checkpoint controls required for normal cell cycle progression

Although several checkpoint controls exist during cell cycle progression (Fig. 1), only the spindle assembly checkpoint and the DNA damage inducible checkpoint will be described in detail, considering the analysis performed in this thesis.

1.2.2.1. Spindle assembly checkpoint

Control of anaphase initiation is regulated by a complex mechanism identified as the spindle assembly checkpoint, responsible for blocking metaphase to anaphase transition in the presence of spindle damage, unattached kinetochores, spindle body defects, and kinetochore or centromere abnormalities.

Checkpoint signal emanates from unattached kinetochores (Rieder *et al.*, 1995), and in higher eukaryotes a phosphoepitope 3F3/2 is present specifically on these (Gorbsky and Ricketts, 1993). Thus, it is reasonable to admit that attachment of microtubules to a kinetochore induces dephosphorylation (or loss) of 3F3/2 phosphoepitopes. Once all epitopes are dephosphorylated the checkpoint becomes inactive and anaphase proceeds. The molecular mechanism underlying this process is still not well understood, though it was elegantly demonstrated by micro-needle manipulation of unattached kinetochores, that checkpoint sensors are tension-sensitive complexes localised within that region (Nicklas *et al.*, 1995). Consequently, lack of tension might generate the checkpoint signal.

The phosphorylated kinetochores are recognised by components of the checkpoint mechanism, leading to inhibition of anaphase onset. Experiments involving the fusion of cells that contain two functional and independent spindles revealed that the spindle assembly checkpoint signal is unlikely to be freely diffusible, but rather is probably associated with the spindle itself (Rieder *et al.*, 1997).

Yeast genetic studies have revealed molecular components of the spindle assembly checkpoint. Several groups of proteins have been identified in genetic screens for mutants sensitive to microtubule antagonists and include the Mad1, Mad2 and Mad3 (mitotic arrest defective) as well as Bub1, Bub2 and Bub3 (budding uninhibited by benzimidazole) (Li and Murray, 1991; Hoyt *et al.*, 1991). *In vitro* studies showed that vertebrate Mad2 binds phosphorylated kinetochores. In contrast, Mad2 binding to kinetochores is inhibited by microtubule attachments (reviewed in Clarke and Giménez-Abián, 2000). Therefore, it seems likely that first the attachment or tension-sensitive kinetochore components become phosphorylated, which are then recognised by Mad2 forming an active checkpoint complex. Mps1 kinase was shown to hyperphosphorylate Mad1 in the presence of spindle defects (Hardwick *et al.*, 1996). Phosphorylation of Mad1 is necessary to mediate metaphase arrest and also requires Bub1, Bub3 and Mad2 (Hardwick *et al.*, 1996; Hardwick and Murray, 1995). The association of Mad1 to Mad2, as a complex, was shown to improve phosphorylation of Mad1 by Mps1 kinase. These studies suggest that checkpoint activation relies in the kinetochore association with phosphorylated Mad1/Mad2 complex. Mad2 associates with Cdc20 in yeast and vertebrates and this association seems to be essential for spindle checkpoint activation to inhibit APC activation and anaphase onset. Over-expression of Cdc20 or expression of a Cdc20 mutant that cannot bind to Mad2, bypasses the spindle assembly checkpoint arrest (Hwang *et al.*, 1998).

1.2.2.2. DNA damage checkpoint

Failure to respond to DNA damage allows the cell to replicate and segregate damaged DNA molecules, resulting in increased genetic instability that in multicellular organisms, may lead to cancer (Hartwell and Kastan, 1994). In fact, if DNA damage is not repaired as soon as it arises, some options for repair may be lost when cells undergo the next cell cycle (Paulovich *et al.*, 1997b). The DNA damage checkpoint pathway is a complex signal transduction system, thought to have specialised sensors for DNA lesions, including DNA damage and incomplete DNA replication, and specific transducer proteins that transmit the signal to the cell cycle machinery. Some checkpoint proteins may also be involved in processing DNA lesions (Lyndall and Weinert, 1995) by inducing the expression of DNA repair genes apart from initiating checkpoint responses (Kiser and Weinert, 1996).

Since there are many different types of DNA damage, several sensors for specific DNA perturbations at distinct stages of the cell cycle are likely to take place. For example, in budding yeast, checkpoints sensing DNA damage or DNA replication depend on different factors. In fact, DNA replication proteins Polε, Rfc5p and Dpb11p are solely involved in sensing DNA damage and replication blocks during DNA synthesis, therefore linking entry into mitosis to proper completion of S phase (Araki *et al.*, 1995; Navas *et al.*, 1995; Sugimoto *et al.*, 1996). Conversely, Rad9p, Rad17p, Rad24p, Mec3p and Ddc1p are required for response to DNA damage, but not to incomplete DNA replication. Moreover, these proteins are proposed to act at an early step of DNA damage recognition at any stage of the cell cycle (Weinert and Hartwell, 1988; Siede *et al.*, 1993; Weinert *et al.*, 1994; Longhese *et al.*, 1996; Paulovich *et al* 1997a) (Fig.7). Putative sensor proteins in budding yeast may be subdivided into two classes, based on sensitivity of mutants to DNA damaging agents and the processing of DNA lesions: the Rad9 class and the Rad24 class (*rad24*, *rad17*, *mec3* and *ddc1*) (Lyndall and Weinert, 1995; Paciotti *et al.*, 1998). Ddc1p, Mec3p and Rad17p interact physically with each other, suggesting that they function in the same pathway (Paciotti *et al.*, 1998; Kondo *et al.*, 1999). Once DNA perturbations are sensed, the signalling process involves a protein phosphorylation cascade propagated through the two protein kinases, Mec1p and Rad53p (Weinert *et al.*, 1994; Sanchez *et al.*, 1999).

Rad53p is a protein kinase that becomes phosphorylated in response to DNA damage, in a Rad9p, Mec3p, and Mec1p dependent manner (Zheng *et al.*, 1993, Navas *et al.*, 1996; Sun *et al* 1996) (Fig.7). Rad53p has been proposed to account for delaying the G1-S transition after DNA damage in G1 (Sidorova and Breeden, 1997).

Mec1p is a member of the lipid kinase motif family, which includes *S. pombe* Rad3 (Bentley et at, 1996), mammalian ATM (Ataxia Telangiectasia Mutated) (Savitsky *et al.,* 1995), ATR (AT and Rad-related) (Bentley *et al.,* 1996) and the catalytic subunit of DNA protein kinase (DNA-PK) (Jeggo *et al.,* 1995). Mec1p, but not Rad53p, is required to phosphorylate the anaphase inhibitor Pds1p, and is probably the most upstream kinase of the transduction pathway (reviewed in Clarke and Giménez-Abián, 2000). Therefore, it may be a mediator between the sensor components and checkpoint targets in the G2/M transition.

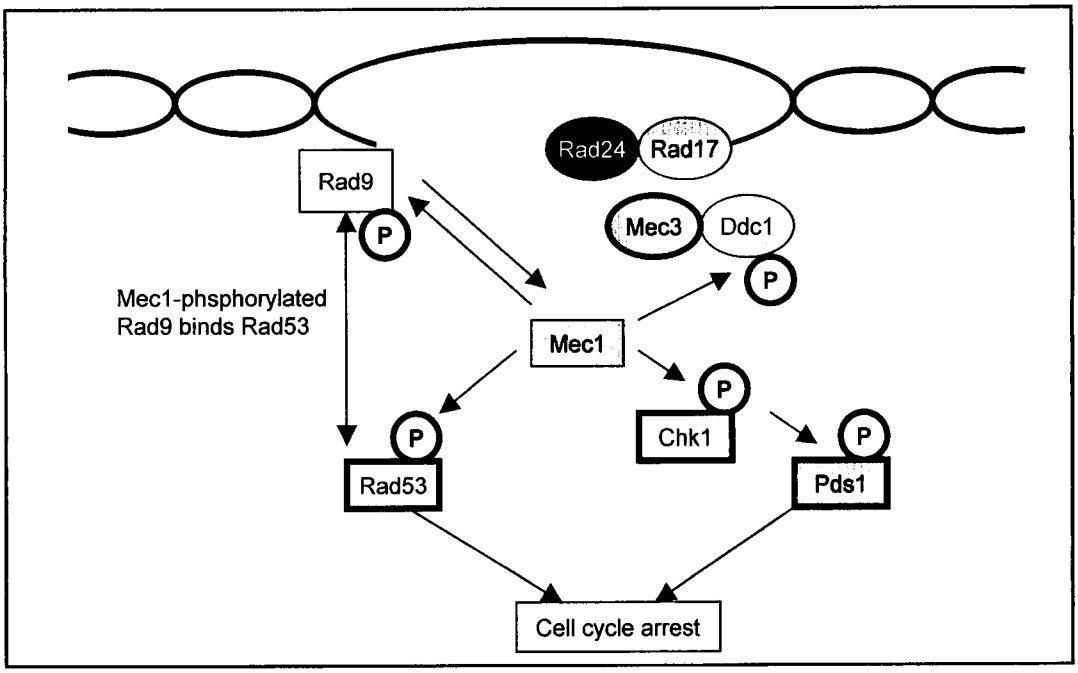

Figure 7: Proteins involved in the DNA damage inducible checkpoint (see details in the text)

Strong evidences for two parallel pathways acting downstream of Mec1 were provided: the Rad53 pathway and the Pds1 pathway (reviewed in Clarke and Giménez-Abián, 2000) (Fig. 7 and Fig. 8). Mec1p is also partially required for the phosphorylation of Rad9p and Ddc1p (Emili, 1998; Paciotti *et al.,* 1998; Vialard *et al.,* 1998).

Phosphorylated Rad9 is able to bind Rad53, and this complex is presumably the activating component of the Rad53 pathway (Vialard *et al.,* 1998). Rad53 phosphorylation requires not only Rad9 and Mec1 but also members of the Rad24 class. In contrast, phosphorylation of Pds1 requires Rad9 and Mec1p, but not members of the Rad24 group, indicating that distinct checkpoint activating complexes operate in a Mec1 dependent manner.

Ddc1, which is required for all known DNA damage checkpoints, probably acts together with Mec3, Rad17 and Rad24 at an early step of the DNA damage recognition process. Clearly, multiple protein interaction and phosphorylation events participate ultimately to activate the Mec1-Rad53 and the Mec1-Pds1 pathways. The mechanism of anaphase delay involving the Mec1-Pds1 pathway has been clarified to some extent. Dependent on Chk1 kinase activity, Pds1 degradation is blocked and thus Esp1 activity is inhibited.

It was previously demonstrated that Chk1 phosphorylation, induced by DNA damage is dependent on Mec1 and Rad9, but does not require Rad53. In contrast, anaphase delay by the Mec1-Rad53 pathway is less understood. The Dun1 protein kinase (damage inducible) was shown to act downstream of Mec1 and Rad53, and to induce transcription of genes involved in DNA repair (reviewed in Clarke and Giménez-Abián, 2000). Mammals have structural and functional homologues of the Mec1 and Rad53 proteins, the ATM (Ataxia Telangiectasia Mutated gene) and ATR (ATM and Rad3 related), and the Chk2 (checkpoint kinase) respectively. ATM is the gene mutated in ataxia telangiectasia patients whose cells exhibit checkpoint defects, which ultimately will lead to cancer. Chk2 becomes phosphorylated in an ATM-dependent manner after DNA damage has occurred, and thus can phosphorylate Cdc25C on serine 216 eventually preventing this phosphatase to activate the mitotic kinase. This phosphorylated residue seems to create a binding site for one of the 14-3-3 protein family members, resulting in Cdc25 inhibition.

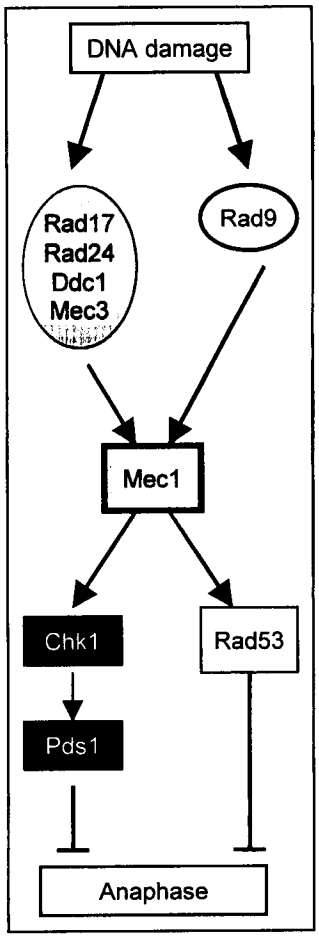

Figure 8: Simplified view of two DNA damage inducible checkpoint pathways (adapted from Clarke and Giménez-Abián, 2000).

Other ATM and ATR substrates have also been identified, including the p53 tumour suppressor protein, which in the presence of DNA damage becomes phosphorylated. p53 is a transcription factor that enhances the expression of specific genes that contain p53-binding sequences in the vicinity of the promoter regions, and is considered to be the most frequently mutated gene in human cancers. Previous studies demonstrated that in response to gamma rays p53 promotes the accumulation of p21 (WAF1, CIP1) known to be an inhibitor of several different Cdk-cyclin complexes (El-Deiry *et al.,* 1994). One

consequence of radiation-induced expression of p21 in G1 phase cells is inhibition of two Cdks (Cdk4/Cyclin D1 and Cdk2/Cyclin E) that appear to control the transition from G1 to S phase. p21 inhibits the PCNA-dependent DNA polymerase activity at DNA replication forks, whereas it causes little inhibition of PCNA-dependent DNA repair (Li *et al.*, 1994). Additionally, p53 is known to activate the transcription of a 14-3-3σ protein that was shown to sequester MPF, preventing the entry into mitosis. p53 also binds to the DNA binding motifs present in the *BCL2* and *BAX* genes which have opposite effects in inducing apoptosis (reviewed in Clarke and Giménez-Abián, 2000).

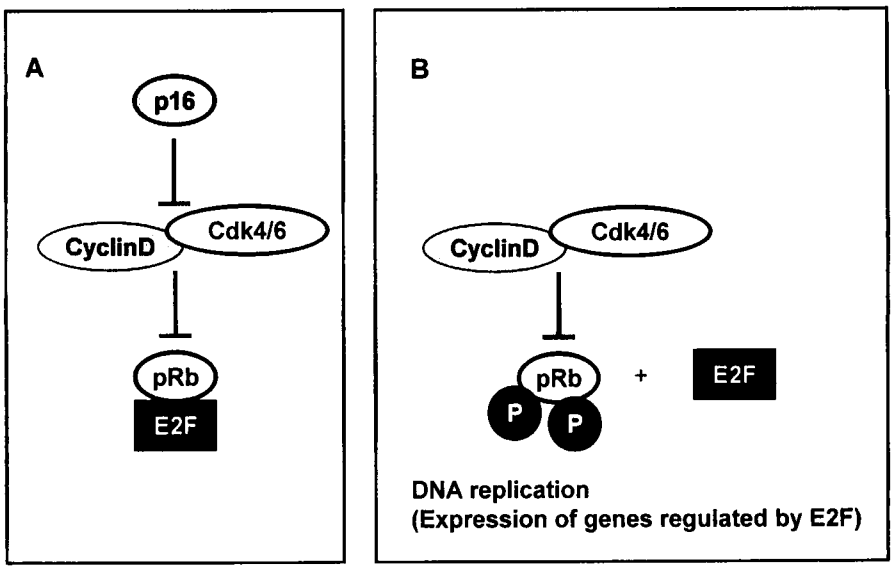

Figure 9: pRb DNA damage inducible-checkpoint. p16 accumulates in response to DNA damage and inhibits cyclinD-CDK4/6 complex activity. pRb remains dephosphorylated and attached to E2F transcription factors. Activation of cyclinD-CDK4/6 complexes leads to the phosphorylation of pRb and E2F factors are released.

A family of transcription factors – *E2F* - is also activated during the G1/S transition, and is responsible for inducing the expression of several genes involved in DNA synthesis (Fig. 9). Binding of two proteins – Rb and p107 – to E2F inhibits its transcriptional activity, thus controlling the entry into S phase. Mammalian G1 Cdk-cyclin complexes and Cdk2/cyclin A are able to phosphorylate Rb *in vitro*, which is then unable to bind E2F. The transcription factor is thus free to activate expression of specific genes. The kinase activities of Cdk4 or Cdk6 are inhibited by members of the INK4 gene family. The gene products, p16, p15, p18 and p19 accumulate in response to DNA damage. pRb remains hypophosphorylated in senescent cells (reviewed in Reddel, 1998) and this hypophosphorylation may be maintained by high p16 expression levels.

1.3. Chromosome Specific Structures Required For Faithful Transmission of Genetic Information

Faithful transmission of genetic information during cell division is essential for the survival of living organisms. To form a functional chromosome that is able to replicate and to segregate its chromatids during anaphase, specific sequences and structures are required: origins of DNA replication, centromeres and telomeres. These requirements were confirmed in experiments involving the construction of functional artificial chromosomes (Harrington JJ *et al.*, 1997).

A DNA replication origin is a specific nucleotide sequence localised in several sites along a chromosome that is required to initiate DNA replication during S phase. Specific proteins bind to these sites to initiate DNA replication. Homologues for many of these proteins have been identified in yeast, fungi, nematodes, frogs, flies and mammals. They include the Orc proteins that comprise the origin recognition complex (ORC), proteins encoded by cell division cycle genes, six minichromosome maintenance (Mcm) proteins, and the Cdc7 protein kinase and its cofactor Dbf4 (reviewed in DePamphilis, 2000).

The centromere is a specialised chromosomal region that forms the primary constriction of mitotic chromosomes. It plays an essential role in chromosome dynamics during mitosis and meiosis. Three structural and functional domains of mammalian centromeres were defined: the pairing domain, the central domain and the kinetochore domain (Pluta *et al.*, 1990). The region where sister chromatids interact and pair is called the pairing domain, where several proteins, such as INCENPs (Inner Centromeric Proteins) and CLiPs (Chromatids Ligating Proteins), localise (Pluta *et al.*, 1990). The central domain contains the CENP-B centromeric protein and constitutive heterochromatin necessary for kinetochore attachment. Detailed electron microscopic studies (Rieder, 1982) revealed a disc-like three-laminar structure localised at the surface of the centromere, called the kinetochore. The kinetochore is required to establish microtubule attachments during metaphase, through the external laminar structure (Rieder, 1982).

Telomeres are components of linear eukaryotic chromosomes required to maintain genomic stability (reviewed in Zakian, 1995; Biessmann and Mason, 1997; Pardue and DeBaryshe, 1999). These complex nucleic acid-protein structures are thought to counterbalance loss of terminal sequences during DNA replication and to protect the ends from fusion to other chromosomes. Presumably, the cell distinguishes a telomere from a broken chromosome end, at least in part, by the presence of telomere specific DNA-binding proteins. Telomeres might also play a role in the organisation of the interphase nucleus through interactions with the nuclear envelope

(Dernburg *et al.*, 1995). Loss of all or some of these functions has been suggested to be responsible for cancer and ageing in humans.

1.4. Telomeres

1.4.1 Origin of the telomere concept

Telomeres, word originated from the two Greek roots *telos* (end) and *meros* (part), were postulated to account for the observation that chromosome terminal deletions could not be recovered after X-irradiation (Muller, 1938; 1941). Thus it was proposed that the tip regions are required for the stability of linear chromosomes. Subsequently, the essential role of telomeres was demonstrated (McClintock 1941; 1942). While telomeres define stable natural chromosome ends, the introduction of a single chromosome break caused fusion after replication, leading to the formation of dicentrics that undergone breakage during mitosis. McClintock termed this event, a breakage-fusion-bridge cycle. Asymmetric breakage of the fused chromatids during division resulted in loss or gain of chromosomal material.

Although Muller's and McClintock´s studies provided the first analytical approaches for telomere investigation, purely cytological studies were performed in 1885 by Rabl (reviewed in Gall, 1995). He demonstrated that chromosome orientation in interphase nucleus reflected the poleward chromosome movement in anaphase of the previous cell cycle, with centromeres and telomeres at opposite sides. This configuration is referred to, ever since, as the Rabl orientation. Additionally, Rabl could sometimes see that chromosome ends attached directly to the nuclear envelope. The Rabl orientation was also demonstrated in the formation of polytene chromosomes in *Drosophila* salivary glands, where it presumably persists during several rounds of DNA replication (Hochstrasser *et al.*, 1986).

Telomere fusions have been reported in the first meiotic divisions of normal amphibian lampbrush chromosomes. Similar associations occur between the ends of polytene chromosomes of some fly species (reviewed in Gall, 1995).

In more recent years, chromosome fusion has also been reported in a variety of human tumours, ageing cells and several chromosome instability syndromes (Benn, 1976; Fitzgerald and Moris, 1984; Kovacs *et al.*, 1987; Mandahl *et al.*, 1988; Abruzzo *et al.*, 1991).

1.4.2. Telomeric repeat sequences

The first clues of telomere structure and replication were evidenced in ciliated protozoa, containing unusual chromosomes. The cells of these organisms contain two nuclei. A micronucleus, that undergoes typical mitotic divisions, and a large macronucleus, where DNA is divided into very small portions. These portions derive from fragmentation of the germ-line chromosomal DNA during the formation of the macronucleus after conjugation. These gene-sized chromosomes require the presence of telomeric sequences added *de novo* at their ends for genome stability. The numerous copies of telomeric DNA of macronuclei, make these organisms excellent biological systems to study chromosome end structures. Sequencing of the ends of *Tetrahymena* macronucleus rDNA molecules, isolated by CsCl gradient due to its high GC content, showed the existence of a simple and repetitive sequence (CCCCAA/GGGGTT) (Blackburn and Gall, 1978). A similar sequence of gene sized chromosome ends was then published in *Oxytricha* and *Stylonychia* (Oka *et al.*, 1980; Klobutcher *et al.*, 1981). Subsequently, similar repeats were also found in chromosome ends of many eukaryotes, suggesting strong conservation of telomeric DNA sequences (Table 1). Additionally, telomeric repeats of distinct species were shown to be functionally exchangeable (reviewed in Zakian, 1995).

Table 1: Examples of telomere repeat sequences. Detailed description in Henderson, 1995.

Organism	Sequence	Organism	Sequence
Ciliates		**Flagellates**	
Tetraymena	TTGGGG	*Trypanosoma*	TTAGGG
Oxytricha	TTTTGGGG		
Euplotes	TTTTGGGG	**Nematodes**	
		C. elegans	TTAGGC
Slime molds			
Physarum	TTAGGG	**Insects**	
Dictyostelium	AG_{1-8}	*Bombyx mori*	TTAGG
Sporozoans		**Algae**	
Plasmodium	TT(T/C)AGGG	*Chlamydomonas*	TTTTAGGG
Fungi		**Higher plants**	
Neurospora	TTAGGG	*Arabidopsis*	TTTAGGG
S. cerevisiae	$T(G)_{2-3}(TG)_{1-6}$	Tomato	TT(T/A)GGG
S. pombe	$TTAC(A)G_{2-5}$		
Candida albicans	ACGGATGTCTAACTTCTTGGTGT	**Vertebrates**	
Kluyveromyces lactis	ACGGATTTGATTAGGTATGTGGTGT	*Homo sapiens*	TTAGGG
		Mus spp	TTAGGG

Telomeres were shown to vary in length of the same organism within the same chromosome, thus telomeric restriction fragments have a fuzzy appearance in agarose gels. Nevertheless, exceptions have been reported in some hypotrichous ciliates and budding yeast, where restriction telomeric fragments appear as sharp bands in agarose gels (Klobutcher *et al.,* 1981; Pluta *et al* 1982; McEachern and Blackburn, 1994). These observations led to the conclusion that in these organisms telomeric length was tightly regulated.

Studies in *Tetrahymena* showed that telomeric sequences are polarised, in the sense that the TTGGGG repeat forms the 3' strand (G strand) and the CCCCAA repeat forms the 5' strand (C strand). This was also demonstrated for several other organisms suggesting a functional importance. Additionally, it was demonstrated that the G-strand protrudes at the 3' end as a single stranded overhang (12-16 nucleotides) (Klobutcher *et al.,* 1981).

Telomeres can be divided into different structural and functional domains, the telomere associated sequences and telomere repeat duplex (Fig. 10).

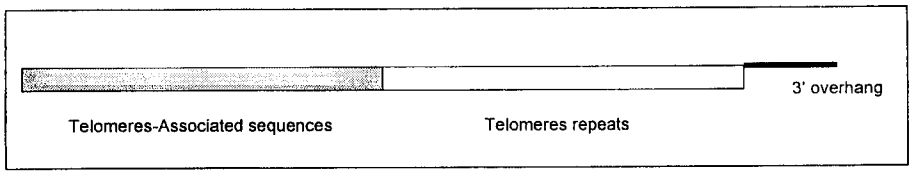

Figure 10: Schematic representation of telomeric DNA.

The telomere-associated sequences (TAS) are highly dynamic and variable among species. They are thought to act as a buffer zone between the distal chromosome sequences and the internal regions. In the ciliated protozoa, *Stylonychia*, TAS sequences were proposed to be involved in the excision of genes during macronuclear development, by recombination events between two 10 bp TAS palindromic sequences flanking a genomic region. The resulting loop structure would then be processed by a specific endonuclease, thereby releasing the gene in the loop domain (Maercker and Lipps, 1993). In yeast, there are two types of telomere associated sequences (Chan and Tye, 1983a,1983b): Y' is a highly conserved sequence that exists in a long (~6.7kb) and short (5.2kb) form, whereas X is less well conserved and ranges in size from 0.3-3.75 kb. The sequences can occur in tandem arrays separated from one another by tracts of (TG_{1-3}) 50-130 bp in length (Walmsley *et al.,* 1984). When X and Y' are present at the same telomere, X is centromere

proximal to Y'. Due to a weak sequence homology to mobile genetic elements it has been suggested that Y' elements arose from insertion into the ancestor yeast genome (Louis and Haber, 1992). Y' elements are sometimes absent in stable telomeres, suggesting that their presence is not required for telomere function. However, in telomere-length regulation yeast mutants (Lundblad and Szostak, 1989) only cells containing Y' elements survive. These elements became localised in all telomeres via a RAD52 recombination-dependent mechanism, suggesting a backup pathway for maintaining telomere length in the absence of telomerase (Lundblad and Blackburn, 1993). Subtelomeric repeats have also been identified in several other organisms, such as fungi (Coleman MJ *et al.,* 1993), *Plasmodium falciparum* (de Bruin *et al.,* 1994) and humans (Cooke *et al.,* 1985). The latter study demonstrated that TAS elements are involved in chromosomes pairing during pachytene in meiosis.

Another structural domain, the telomere repeat duplex (TR), present at the most distal chromosomal site (Allshire *et al.,* 1989), is usually composed of very closely related repeats that may vary in length among organisms, from <50 bp (eg. *Euplotes*) to >100 kb (eg. Mouse), ending as a single stranded overhang. The ability of telomere sequences to form unusual structures was initially suggested from experiments that showed that telomeres devoid of proteins were able to cohere (Lipps *et al.,* 1982, Oka and Thomas, 1987, Acevedo *et al.,* 1991). The G-overhang is thought to play a role in telomere-protein interactions, by establishing three-dimensional conformations, which result from intramolecular associations. The so-called G-quartet structure (Williamson *et al.,* 1989), consists of a planar arrangement of guanines by hydrogen bonding, stabilised by binding of cations. Sets of G-quartets can stack to form four stranded structures and hairpin conformations (Henderson *et al.,* 1987; Choi and Choi, 1994). These data suggested that triplex structures between the G-overhang and the duplex telomeric DNA could also be formed, eventually acting as a telomere-end protection mechanism (Frank-Kamenetskii, 1989). Intramolecular associations are thought to be dynamic events able to switch between telomere elongation and telomere-end protection. In fact, higher order structures formed by the G-G associations are not recognised by a telomeric protein, telomerase (referred below) (Zahler *et al.,* 1991). Associations between G-overhangs of distinct telomeres explains the chromosome end cohesion seen by Lipps *et al* (1982) and Oka and Thomas (1987) and make up a possible mechanism for telomere association *in vivo*.

More recent studies have demonstrated, by electron microscopy, that telomeres of mammalian cells end as large terminal loops. The telomere DNA loops back on itself, such that the 3' strand extension invades the duplex telomeric repeats (Griffith *et*

al., 1999). TRF2, a telomere-binding protein was shown to locate at the newly formed loop structures.

1.4.3. Telomeric duplex structure

The helical period of telomere sequences was shown to be identical as in the B-form DNA (Henderson *et al.*, 1988). Studies of telomere structures in several organisms suggested that long telomeres (>10kb, eg. mouse) appear to be packaged in nucleosomes (Makarov *et al.*, 1993), in contrast to tightly–regulated short telomeres (<100bp, eg. *Hypotrichs*). In this case, the terminal chromatin structure was identified as the telosome (Gottschling and Cech, 1984). In intermediate length telomeres (>300bp, eg. yeast and *Tetrahymena*) the packaging of DNA is non-nucleosomal, although a small percentage of telomeric DNA is packaged in closed nucleosome particles (Blackburn and Chiou, 1981), as are TAS sequences in yeast (Wright *et al.*, 1992).

1.4.4. Interstitial telomeric repeats

Interstitial telomeric repeats (ITRs) exist as copies inserted in several sites of the genome. They were shown to be quite stable in several species and usually present at the edges heterochromatic blocks (reviewed in Biessmann and Mason, 1994). ITRs are thought to be remnants of chromosome rearrangements that occurred throughout evolution. A possibility is that internal telomeres could result from the integration of telomere-bearing DNA elements into the genome. ITRs create hotspots for recombination events (Ashley and Ward, 1993; Katinka and Bourgain, 1992) and have already been associated with general genomic instability leading to neoplasia (Hastie and Allshire, 1989; Bouffler *et al.*, 1993).

1.4.5. Does telomere capping require telomeric DNA repeats?

Several studies have demonstrated that telomeric repeats are necessary for survival. In *Tetrahymena,* modification of telomeric-repeat sequences causes cell senescence (Yu *et al.*, 1990). The inability to extend telomere-repeats in yeast

telomerase mutants also leads to senescence (Lundblad and Szostak, 1989). Studies in yeast showed that a broken chromosomal site without telomeric repeats is enough to cause cell cycle arrest and loss of the broken chromosome after a few cell divisions, thus being recognised at the DNA damage checkpoint as uncapped (Bennett *et al.*, 1993; Sandell and Zakian, 1993). However, addition of new telomeric repeats, generally via a RAD52 dependent pathway or by *de novo* mechanisms, is enough to restore a fully functional chromosome end. Similar studies have been performed in several other organisms, showing that addition of telomeric repeats take place when a broken chromosome is produced artificially, or when linear DNA molecules are introduced into the nucleus (Matsumoto *et al.*, 1987; Pologe and Ravetch, 1988; Muller *et al.*, 1991; Yu and Blackburn, 1991).

It is however intriguing that broken chromosomes have been recovered in *Drosophila* that do not end in telomeric DNA sequences (Biessmann *et al.*, 1990a) and continuously lose DNA sequences from their ends (Biessmann and Mason, 1988; Levis, 1989). These chromosomes are stably transmitted through generations and do not cause cell cycle arrest, suggesting that capping of *Drosophila* chromosomes appears to act in a sequence independent manner. Thus, stability of telomeres is probably achieved via a protein binding mechanism to any sequence present at chromosome ends.

1.4.6. Telomere replication via the ribonucleoprotein enzyme telomerase

1.4.6.1. The Chromosome end replication problem

DNA replication studies performed by Watson in 1972 pointed out that the telomere replication standard model, consisting of a short RNA molecule necessary to initiate the extension of the new strand, posed no problem at one end of each template strand. However it would give rise to an unreplicated region at the other end due to posterior primer removal (Fig. 11). Watson demonstrated that this problem could be avoided by concatemerization, which would require repetitive sequences at the termini of chromosomal DNA. Another mechanism involving palindromic sequences at the ends of chromosomal DNA was also suggested by Cavalier-Smith in 1974, in such a way that the 3' end of a DNA strand could fold back to serve as a primer to fill in the gap of the opposite strand.

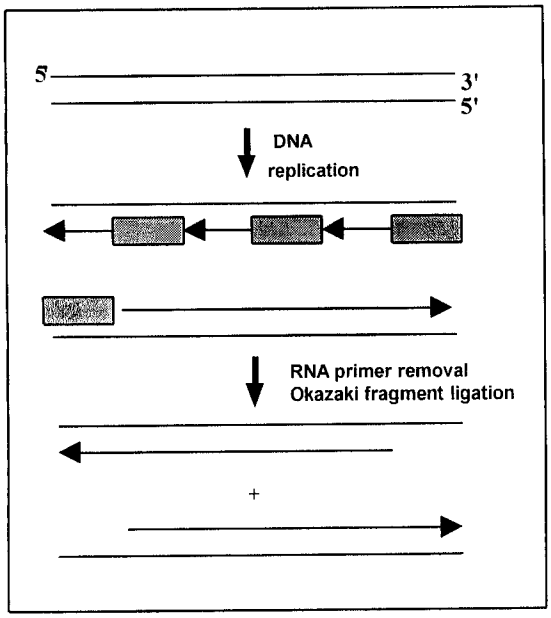

Figure 11: The chromosome end-replication problem. RNA primer removal in the lagging strand leaves an unreplicated region at one end of each daughter molecule.

1.4.6.2. Telomerase compensates the loss of telomeric repeats during DNA replication

The identification of a telomere specific DNA polymerase activity in *Tetrahymena* (Greider and Blackburn, 1985) and later in other species, suggested a *de novo* addition of telomere repeats to chromosome ends that would counterbalance for the loss of terminal DNA sequences during DNA replication. This enzyme, called telomerase, synthesises telomere repeats by adding nucleotides onto telomeric 3' ends. The complementary C-rich strand is thought to replicate by conventional DNA polymerases, although telomere specific proteins may regulate this process (Vermeesch and Price, 1994). *In vitro* experiments using RNase and micrococcal nuclease pre-treated extracts abolished telomerase activity, suggesting that telomerase contains an essential RNA component (Greider and Blackburn, 1989). Telomerase binds to the G-strand so that the TTGGGG repeat is base-paired with the 5' CAACCCCAA 3' template sequence in the RNA component, and the extension of the G-strand can take place. Mutations of the gene that codifies for the telomerase RNA component, showed that this enzyme is responsible for synthesising telomeres *in vivo* and that the RNA sequence provides the template, since telomeric incorporation of the predicted mutant repeats took place (Yu *et al.*, 1990). Cell viability varied with the type of telomere repeats added to chromosome ends, eventually due to distinct recognition capacities of telomere proteins to the different repeats. Disruption of the gene encoding the telomerase RNA led to telomere shortening (Lundblad and Szostak, 1989). Besides

adding telomere sequences to existing telomeres, telomerase also heals chromosomes by adding telomere sequences *de novo* onto fragmented chromosomes without telomeric repeats, as in the *hypotrichous* macronuclear development. Telomerase activity certainly competes with other telomere events, since several other proteins were demonstrated to bind telomeres *in vivo*. Additionally, *in vitro* experiments suggested that telomerase does not recognise the DNA telomeric repeats *per se*, but a chromosome substrate composed of both DNA and protein (Shippen *et al.*, 1994).

Telomerase has been identified in several other organisms, such as *Euplotes* and *Oxytricha*, as well as in human immortal cell lines, mouse tissues, rat and *Xenopus* (Zahler and Prescott, 1988; Morin, 1989; Shippen-Lentz and Blackburn, 1989; Prowse *et al.*, 1993; Mantell and Greider, 1994). The ribonucleoprotein activity was shown to be similar in these organisms, however with distinct RNA component sequence composition. Comparative sequence analysis of telomerase RNA sequences revealed that they are not highly conserved even between related species (reviewed in Greider, 1995). Nevertheless, computer predicted secondary structures were demonstrated to be similar among several species, suggesting a possible functional role. Telomerase RNA regions outside the template have been found to contribute to telomerase active site functions and to the assembly of the ribonucleoprotein complex (Roy *et al.*, 1998).

1.4.6.3. Telomerase protein components

Ten years after the identification of telomerase activity *in vitro* (Greider and Blackburn, 1985), protein components of *Tetrahymena* telomerase were identified using biochemical approaches (Collins *et al.*, 1995) (Fig. 12). Two polypeptides of 80 kDa and 95 kDa co-purified with telomerase activity and the telomerase RNA, and were shown to associate in a stable three-component configuration. Experiments involving nucleic acid cross-linking demonstrated that telomerase RNA binds to the p80 and that p95 specifically interacts with the telomeric primers, thus constituting the active site. Cloning of the p80 and p95 cDNAs revealed novel proteins. A weak homology has been found between the carboxyterminal region of p95 and a conserved active-site residue in the family of viral RNA dependent RNA polymerase.

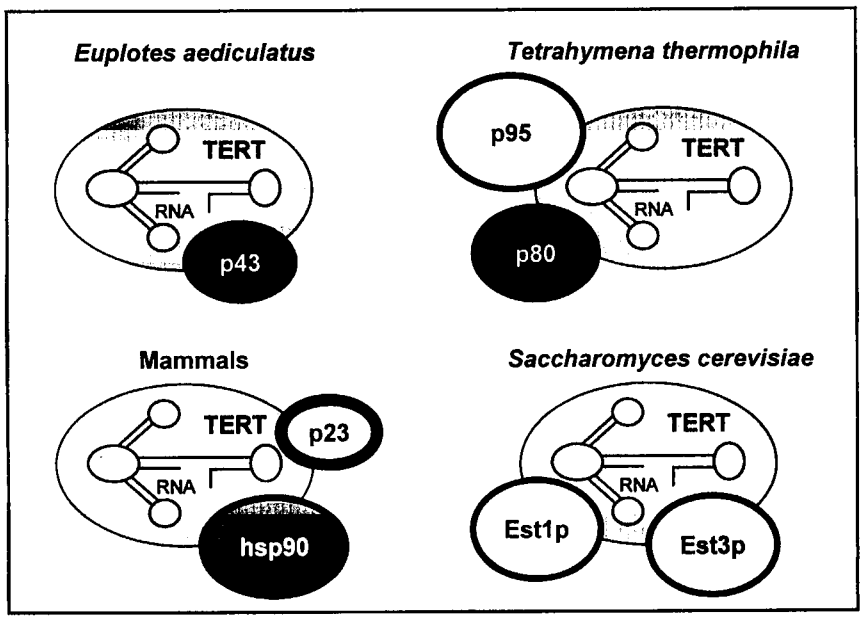

Figure 12: Telomerase, a conserved catalytic core TERT and species-specific accessory proteins. (adapted from Bryan and Cech, 1999).

Biochemical fractionation of cell extracts from the ciliate *Euplotes aediculatus* revealed the presence of two polypeptides that co-purified with telomerase activity (123 kDa and 43 kDa) (Lingner and Cech, 1996). The gene coding for p123 was found to be homologous to the *S. cerevisiae EST2* (Ever shorter telomeres) gene. Deletion of the gene that encodes for the template RNA of telomerase *TLC1* or the *EST2* gene, which encodes for the catalytic subunit of the enzyme, lead to shortened telomeres and senescence (Lundblad and Szostak, 1989; Lendvay *et al.,* 1996). The aminoacid sequence of p123 and Est2p revealed some homologous regions to reverse transcriptase (RT) proteins, consistent with the role of RNA-templated DNA polymerisation. Homologues of telomerase reverse transcriptase (TERT) have been identified in *Oxytricha*, yeast, *Tetrahymena*, mice and humans (Nakamura *et al.,* 1997; Greenberg *et al.,* 1998). Mutation of aminoacid residues conserved in all RTs abolished telomerase activity *in vitro* and *in vivo*, corroborating the importance of RT motifs to telomerase activity (Lingner *et al.,* 1997a; Harrington L *et al.,* 1997; Weinrich *et al.,* 1997).

In vitro experiments showed that the catalytic subunit TERT and the telomerase RNA was sufficient to reconstitute both human and *Tetrahymena* telomerase activity (Collins and Gandhi, 1998; Weinrich *et al.,* 1997). However, experiments in rabbit reticulocyte lysates demonstrated that human telomerase activity required two

chaperon proteins, p23 and hsp90 (Holt *et al.*, 1999). *Tetrahymena* p80 and p95, and the p80-related protein TEP1 (Telomerase-associated protein 1) in mammals are not required for *in vitro* telomerase activity (Collins and Gandhi, 1998; Weinrich *et al.*, 1997). In yeast, the catalytic subunit, Est2p, interacts with other telomerase components (Est1p, Est3p and Est4p also called Cdc13p) involved in telomere maintenance. However, similar studies as those performed in *Tetrahymena* and humans, demonstrated that Est1p and Est3p were not required for telomerase activity *in vitro*. Thus, yeast Est1p and Est3p, *Tetrahymena* p80 and p95 and mammalian TEP1 presumably act in the telomerase complex assembly and processivity.

1.4.7. Telomere proteins and telomere length regulation

The function of telomeres cannot be understood from their DNA sequence analysis alone, and requires knowledge of the protein components that bind specifically to chromosome ends. Telomeric proteins are thought to play a role in preventing nucleolytic degradation and end-to-end associations, and thus conferring stability to chromosomes. They also participate in chromosome organisation in nuclear architecture (Dernburg *et al.*, 1995) and in affecting expression of genes located nearby. Additionally, some of these proteins regulate telomerase accessibility to telomeres, thus playing a role in telomere-length regulation eventually also providing protection functions to telomere ends. Loss of some of these functions has been suggested to play a role in cancer and ageing in humans (Goldstein, 1990). Despite the homology of telomeric sequences present in distantly related species, proteins that act at telomeres are, surprisingly, not recognisable homologues of each other, even though they display functional similarity.

1.4.7.1. *Oxytricha*

Oxytricha telomeres have a length proximal to 20 bp and are maintained through a tightly regulated mechanism. The crystal structure of a two-subunit protein (α and β) that binds to single-stranded telomeric DNA in *Oxytricha nova* (Horvath *et al.*, 1998), revealed that the 3' end is buried in the protein, thus explaining how it caps telomeres and inhibits telomeric extension by telomerase (Froelich-Ammon *et al.*, 1998). The heterodimer protects DNA from digestion by BAL31 exonuclease, DNase I

and micrococcal nuclease (Price and Cech, 1987, 1989). The α and β subunits exist predominantly as monomers in the absence of telomeric DNA (Fang and Cech, 1993), and have been shown to have activities independent of each other. DNA-dependent dimerization allows the formation of a ternary complex. The α subunit is capable of binding every T_4G_4 repeat along a single stranded telomeric DNA *in vitro*, suggesting that this subunit may have a role in protecting a newly formed telomeric repeat *in vivo*. The α subunit is divided into two structurally separable domains: one is required for DNA binding and the other for α/β subunit interactions. The β subunit has regions of homology with histone H1 and DNA chaperone proteins, which explains its ability to promote the formation of G-quartet structures. *In vivo,* the β subunit chaperone activity may mediate telomere-telomere associations at a specific stage of macronuclear development when *de novo* telomere addition occurs in S-phase. Alternatively, it may promote the reverse reaction of unfolding G-quartet structure, enabling, for example the elongation of telomere length via telomerase, since G–quartets inhibit this enzyme activity (reviewed in Fang and Cech, 1995).

Immunostaining assays revealed that these proteins are localised throughout the *Oxytricha* macronucleus, and at specific foci that co-localise with the DNA replication band in S phase (Fang and Cech, 1995). Thus, the telomere protein may act to cap the newly synthesised telomere DNA and protect it from nucleolytic degradation. Nevertheless, *in situ* hybridisation using telomerase RNA demonstrated that its telomeric localisation is not cell cycle regulated, suggesting the existence of maturation sites where assembly of telomerase components takes place.

A telomere end binding protein such as the one found in *Oxytricha* has not been isolated from any other species, although a protein of similar properties has been characterised in *Xenopus* (Cardenas *et al.,* 1993).

1.4.7.2. Yeast

Yeast cells also exhibit short telomere lengths, although larger than *Euplotes*, and ranging in size from 300 bp to 400 bp. In yeast, mutations in three additional genes, *EST1*, *EST3* and *CDC13,* confer the same Est$^-$ phenotype (Lendvay *et al.,* 1996; Lundblad and Szostak 1989; Nugent *et al.,* 1996), although extracts prepared from these cells have telomerase catalytic activity (Cohn and Blackburn, 1995; Lingner *et al.,* 1997b). The apparent discrepancy between the *in vivo* and the *in vitro* study suggests that these three proteins act as positive regulators of telomerase.

Biochemical analysis demonstrated that Est1p and Est3p act in telomere replication as subunits of the telomerase holoenzyme, in contrast to Cdc13p, which is not tightly associated to telomerase although it specifically binds telomere chromatin. Est1p and Cdc13p bind single-stranded DNA and modulate telomerase activity (Lin and Zakian, 1996; Nugent *et al.,* 1996; Bourns *et al.,* 1998; Evans and Lundblad, 1999; Hughes *et al.,* 2000). However, unlike Cdc13p, Est1p requires free 3' terminus to bind telomeric substrates, suggesting that the primary function of this protein is to promote telomerase access to chromosome ends (Virta-Pearlman *et al.,* 1996). Analysis of *cdc13-2*^{est} missense mutated cells revealed a telomere replication defect, although telomerase catalytic activity was unaffected (Lingner *et al.,* 1997b). These results suggested that Cdc13p recruits telomerase to the telomere. This defect was bypassed if the high affinity DNA-binding domain of Cdc13p (DBD_{Cdc13}) was fused directly to either Est1p or Est3p (Evans and Lundblad, 1999). These observations suggested that DBD_{Cdc13}-telomerase does not require the recruitment function of Cdc13p to access the telomere. Moreover, a fusion between Cdc13p and the catalytic core of telomerase allows telomeres to be stably maintained in the absence of Est1p, supporting the idea that Esp1p acts as a binding molecule that associates the enzyme to chromosome termini (Evans and Lundblad, 1999; reviewed in Evans and Lundblad, 2000).

Telomerase is not able to extend blunt-ended DNA *in vitro* (Lingner and Cech, 1996). Therefore, following conventional DNA replication the blunt-ended chromosome ends created on the leading strand must be processed to create single strand extension prior to Cdc13p binding and telomerase extension. This mechanism is however poorly understood.

Several studies showed that the coordination between C strand and G strand synthesis is required for proper telomere maintenance. *S. cerevisiae* cells carrying mutations in DNA polymerase α at the semi-permissive temperature show a telomerase–dependent increase in telomere length, exhibiting an increase in the G strand relative to the C strand (Adams Martin *et al.,* 2000).

This suggests that extended elongation by telomerase may actually be inhibited by C strand synthesis. Mutations of *CDC13* have been shown to promote elongation of the G strand in a telomerase-dependent manner, similar to what happens in cells carrying mutated forms of DNA polymerase α (Grandin *et al.,* 1997; Qi and Zakian, 2000). Moreover, it was demonstrated that Cdc13p is physically associated with DNA polymerase α (Qi and Zakian, 2000). These results point to a dual role of Cdc13p in telomere regulation: it may first recruit telomerase to telomeres, and subsequently act

to limit the extension of the G strand by telomerase, in response to synthesis of the C strand by DNA polymerase α primase complex (Fig.13).

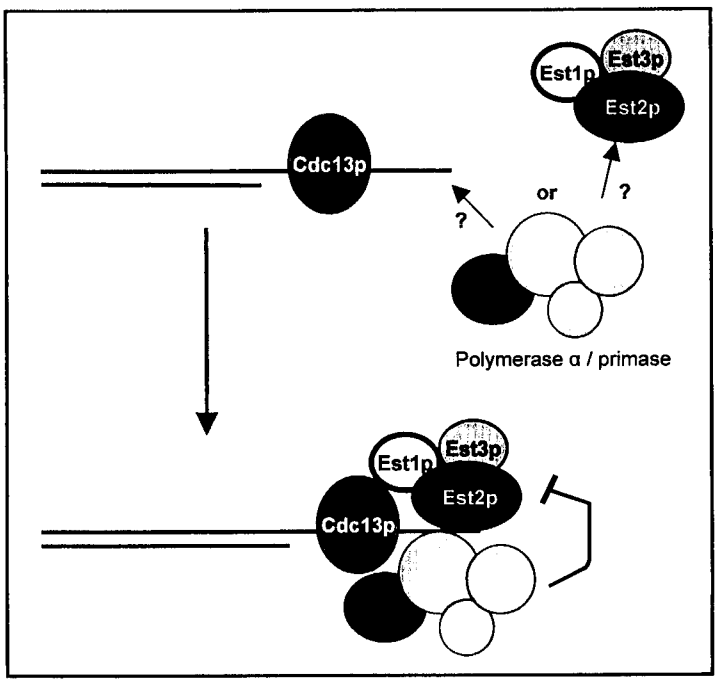

Figure 13: Regulation of telomere length in *S. cerevisiae*. Recruitment of telomerase to the chromosome terminus requires the presence of Cdc13p and the DNA polymerase α/primase complex. Further extension of the telomeres by telomerase is eventually inhibited by those proteins (adapted from Evans and Lunblad, 2000).

However, further studies involving *de novo* telomere synthesis of induced double strand DNA breaks have implicated the synthesis of the C strand in telomere replication (Diede and Gottschling, 1999), since elimination of DNA polymerase α and δ also abolishes elongation of the G strand. These results suggested that the telomere holoenzyme must interact with one or more components of the lagging strand synthesis machinery to elongate chromosome termini. A model was proposed which suggests that recruitment of the C strand synthesis machinery could be essential for telomerase enzymatic activity. Subsequently, the extent of the G strand might be negatively regulated by C strand synthesis.

The 5´to 3' DNA helicase protein, Pif1p, has been described to inhibit the catalytic activity of telomerase. Mutations in the yeast *S. cerevisiae* of the *PIF1* gene cause telomere lengthening and a large increase in the formation rate of new telomeres (Zhou *et al.*, 2000).

A double-stranded DNA-binding protein Rap1p (Repressor/Activator Protein 1) identified in yeast (Conrad *et al.,* 1990) plays two essential roles at telomeres. It is involved in transcriptional silencing and it controls telomere length (reviewed in Shore, 1997). Deletion mutations in the Rap1p carboxyl terminus lead to an increase in telomere length, suggesting that Rap1p plays a negative regulatory role by inhibiting telomere lengthening via telomerase enzyme (Kyrion *et al.,* 1992; reviewed in Greider, 1996). Conversely, the Rap1p carboxyl terminus may also play a positive role in telomere elongation, most likely involving other proteins that bind to Rap1p (Ray and Runge, 1998). Several proteins interact with Rap1p C-terminus and regulate telomere length and transcriptional silencing, such as Rif1p, Rif2p and Sir3p (Hardy *et al.,* 1992; Moretti *et al.,* 1994; Wotton and Shore, 1997). Sir3p associates as a complex with Sir2p, Sir4p and chromatin to silence transcription of nearby genes, an event known as telomere position effect (TPE) (Hecht *et al.,* 1996). The *rif1 rif2* double mutant phenotype is identical to that of *rap1^t* mutants, which lack the Rap1p C-terminus (Kyrion *et al.,* 1992). Later studies, in which a hybrid Rap1p-Gal4 fusion protein was targeted to Gal4 binding sites placed adjacent to telomeres, demonstrated that telomere length decreased by an amount proportional to the number of Rap1p molecules targeted. Thus, the number of Rap1p molecules provides a feedback mechanism for telomere length control, and Rif1p and Rif2p probably play a role during this process (Marcand *et al.,* 1997). Yeast telomeres contain high affinity Rap1p-binding sites at a periodicity of approximately 18 bp (Gilson *et al.,* 1993).

It was proposed that telomere length measurement involves the assembly of a folded chromatin structure dependent on the presence of a threshold number of telomeric Rap1p molecules (Fig. 14). This folded structure links the chromosome terminus and the telomere/non-telomere junction and inhibits telomere lengthening (Ray and Runge, 1999). The folded structure might be stabilised through Rif-Rif protein interactions. Rap1p also binds to the upstream regions of many genes, including ribosomal protein and glycolytic enzyme genes, where it seems to act as a transcriptional activator (reviewed in Shore, 1994).

Another double-stranded telomere-binding protein with a Myb-like domain, Taz1p, isolated from *S. pombe* (Cooper *et al.,* 1997), plays a role in the modulation of telomerase activity and regulates the access of telomere structures to recombination processes during meiosis (Cooper *et al.,* 1998; Nimmo *et al.,* 1998). Moreover Taz1p has been associated to telomere capping functions in the absence of telomerase activity (Cooper *et al.,* 1997).

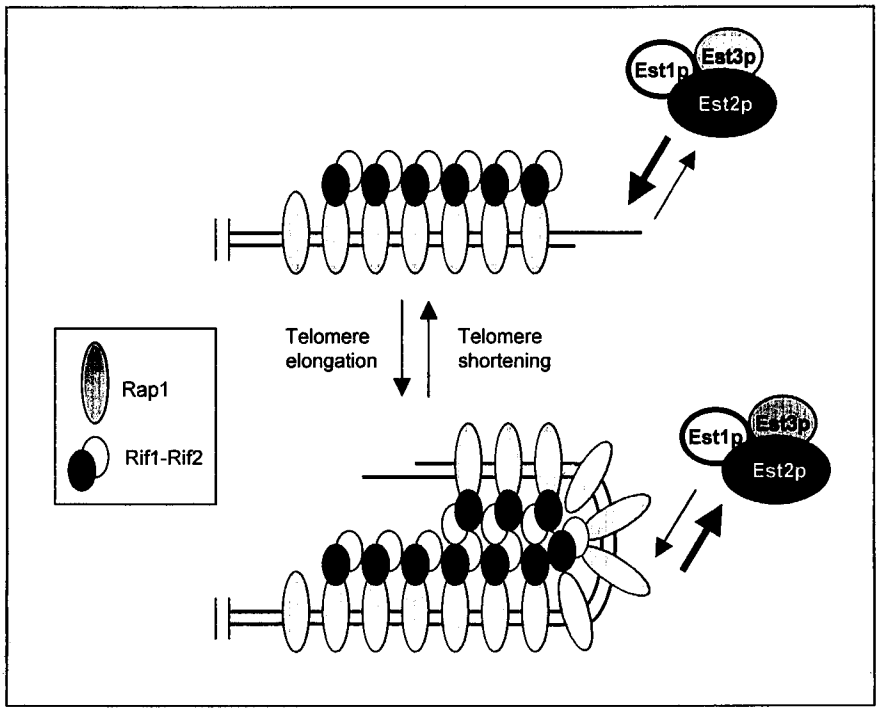

Figure 14: Rap1p modulates access of telomerase to the chromosome terminus. See detailed description in the text (adapted from Evans and Lundblad, 2000)

1.4.7.3. Mammals

In mammalian cells, double-stranded telomeric repeats are bound directly by two proteins, TRF1 (Telomeric Repeat-binding Factor 1) and TRF2. These proteins, as Rap1p itself, have a DNA-binding domain similar to that of the Myb oncoprotein. The mechanisms of DNA-binding by TRF1 and Rap1p are quite similar given the fact that both require two Myb domains for binding and inducing shallow bends in the DNA (Bianchi *et al.,* 1997).

Over-expression of wild-type TRF1 in a telomerase-expressing immortal cell line reduced telomere length, whereas over-expression of dominant-negative TRF1 increased telomere length (van Steensel and de Lange, 1997). These results suggest that, like Rap1p in yeast, the amount of protein in the cell can affect telomere elongation. Thus, increasing TRF1 molecules leads to the inhibition of telomere elongation mechanisms. Additionally, TRF1 was shown to induce parallel pairing of telomeric tracts *in vitro* (Griffith *et al.,* 1998).

The identification of tankyrase protein (Smith *et al.,* 1998) provided a clue of how TRF1 might modulate telomerase activity, since both localise to telomeres and associate with one another. Tankyrase has a domain, which is homologous to the

enzyme poly (adenosine diphosphate-ribose) polymerase, that catalyses the addition of ADP-ribose groups to proteins. *In vitro* assays revealed that tankyrase was able to ribosylate TRF1, and that this process inhibited the binding of TRF1 to telomeric DNA. Therefore, it is possible that the removal of TRF1 from telomeres via tankyrase will allow telomerase to access chromosome ends. However, *in vivo* assays still need to be performed. Another TRF1-interacting nuclear protein (TIN2) has been identified (Kim *et al.,* 1999), using the two-hybrid interaction assay in yeast. Over-expression of wild-type TIN2 has the same effect as in TRF1 studies, in the sense that causes telomeres to decrease in length. Over-expression of TIN2 mutant forms increased telomere length. In contrast to what happens with tankyrase, *in vitro* studies revealed that association of TRF1 with TIN2 did not block binding of TRF1 to telomeric DNA. Moreover, it was demonstrated that mutant TIN2 forms continued to associate to TRF1-DNA complexes although it did not allow the arrangement of higher order structures of the complex as wild-type TIN2 did. Therefore, TIN2 may act as a promoter of TRF1-dependent pairing of telomeric repeats.

Experiments, inducing over-expression of the wild-type form of another double-strand DNA binding protein TFR2, also reduced telomere length (Griffith *et al.,* 1999; Smorgorzewska *et al.,* 2000). Yet, over-expression assays of dominant negative TRF2 induces unique phenotypes, such as loss of single-stranded telomeric repeats, end-to-end fusions and ATM/p53-dependent apoptosis (van Steensel *et al.,* 1998; Karlseder *et al.,* 1999), and may even lead to senescence. Loss of the single-stranded G-overhangs appears to be sufficient to activate a DNA damage response and to produce end-to-end fusions. These results suggest that TRF2 protects telomeres from non-homologous end joining, thus contributing to chromosome stability, and that this protein is involved in DNA damage response pathways. Detailed analysis demonstrated that fused chromosomes possessed telomeric DNA repeats, but both fused and nonfused chromosomes had lost their G-tails. Therefore, TRF2 appears to prevent end-to-end associations by maintaining single stranded G strands, although, surprisingly, it only binds double stranded DNA *in vitro*.

Electron microscopy of mammalian telomeres showed how telomere proteins act, particularly how TRF2, which binds double-stranded telomere repeats, might affect the single stranded tail *in vivo*. These experiments revealed that at least half of the mammalian telomeres form loops of duplex DNA called t-loops (Griffith *et al.,* 1999). *In vitro* t-loop formation requires double stranded repeats, single-stranded repeats in a 3' end overhang and TRF2. The 3' end G-strand over-hang folds back inside the double stranded DNA at the loop junction. TRF2 eventually localises at the base of the site

where the G-strand probably establishes base pairs with the complementary strand of the invaded duplex (D-loop) (Fig. 15). Purified cellular t-loops were de-proteinized before visualisation, so the *in vivo* distribution of TRF2 is unknown. However, TRF2 bound the D-loop junction *in vitro*, and the lack of TRF2 resulted in a substantial reduction in the number of molecules found as loops. *In vivo* t-loops are larger than predicted by energetic constraints, thus suggesting the existence of other factors that regulate t-loop dimensions. The functional consequence of the loop formation has not been demonstrated so far. However, one can speculate that it plays a role in protecting the vulnerable single-stranded G-strand. This hypothesis is supported by over-expression studies of a TRF2 dominant-negative form that resulted in the loss of the G-strand over-hang (van Steensel *et al.,* 1998).

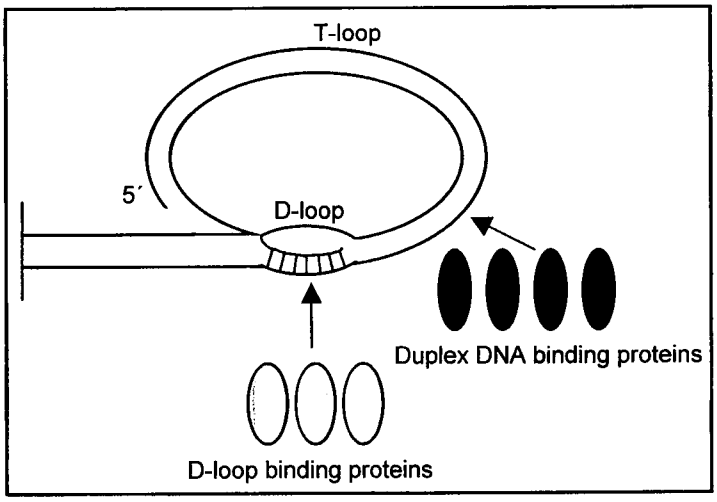

Figure 15: The new view of telomere structure (adapted from Greider, 1999).

T-loops may explain the ability of cells to distinguish chromosome ends and DNA breaks, given the fact that sequestration of the G-strand may prevent a DNA damage response. Since TRF1 was shown to promote parallel pairing of telomeric tracts eventually stimulated or stabilised by TIN2, this protein complex could promote the TRF2-dependent t-loop formation *in vivo*. Additionally, one would expect these t-loops to be dynamic structures, forming and unwinding, in order to inhibit or enable telomerase elongation respectively. The observation that many types of cells do not contain telomerase activity and progressively shorten their telomeres, suggests that t-loops are not always present and that eventually a minimal telomere length is required for its formation. Nevertheless, more experimental assays in several organisms and cell lines are needed to confirm this hypothesis. If telomere function mediated by t-

loops is conserved, the existing models of telomere binding proteins in telomere function will need to be examined. For example, single stranded DNA binding proteins could have a regulatory role inhibiting t-loop formation and thus promoting telomere elongation. Alternatively, they could interact with free 3' ends and enhance t-loop formation, eventually stabilising the displaced strand of the D-loo

Telomere structures are dynamic nucleoprotein complexes that can switch stochastically between two states: capped and uncapped. Capping preserves telomere integrity allowing cell division to proceed, and regulated uncapping also occurs normally in dividing cells. Telomerase activity regulation is a complex mechanism, including several different controlling pathways, which affect its activity and/or expression as function of the cell cycle, growth, development and cell type (reviewed in Lundblad and Wright, 1996). Regulation of telomerase is executed primarily through the transcriptional control of the gene encoding the catalytic subunit TERT, by alternative splicing processes (Kilian *et al.*, 1997). Thus cells with catalytically inactive TERT isoforms can lack telomerase activity (Ulaner *et al.*, 1998). Inactive TERT molecules would compete with residual functional isoforms in the assembly with telomerase protein subunits. Telomerase RNA (TR) is expressed ubiquitously and is taken up during protein complex assembly. Additionally, there is evidence that post-translational control of telomerase activity also takes place (Liu *et al.*, 1999; Li *et al.*, 1998; Kang *et al.*, 1999). The 3' end telomerase RNA was shown to have structural and functional similarities with H/ACA family of small nucleolar RNAs (Mitchell *et al.*, 1999a). These motifs were shown to be required for telomerase activity, since they enabled telomerase RNA accumulation and 3' end processing *in vivo*. Recently, a protein component called dyskerin, of both, H/ACA small nucleolar ribonucleoproteins (snRNPs) and the human telomerase ribonucleoprotein (RNP), has been identified (Mitchell *et al.*, 1999b), suggesting that the human telomerase RNP incorporates an entire H/ACA RNP and not just a H/ACA RNA. Initial assembly of H/ACA sub-domain RNP may facilitate subsequent association with TERT. In fact, mutations in dyskerin, causes the disease dyskeratosis congenita that exhibits reduced accumulation of telomerase RNP and abnormally short telomeres (Mitchell *et al.*, 1999b).

1.4.8 Telomere remodelling in response to DNA damage

A link between telomere structure and proteins involved in DNA repair and DNA damage checkpoints has been demonstrated in yeast and other organisms. Ku was

originally identified as a protein required for targeting and activating the catalytic subunit of DNA-dependent protein kinases of the PI3K family required for non-homologous end-joining (NHEJ) of double strand breaks during DNA repair and V(D)J recombination (Leiber *et al.*, 1997). Ku protein was shown to localise at telomeres (Boulton and Jackson, 1998) and yeast cells deficient for this protein have shortened telomeres (Gravel *et al.*, 1998). Ku is also involved in proper processing of single stranded G-rich overhangs, and seems to play a role in protecting telomeres from nucleolytic degradation and recombination (Gravel *et al.*, 1998; Polotnianka *et al.*, 1998). Mutations in other NHEJ-associated proteins namely those comprising the Mre11/Rad50/Xrs2 complex also lead to abnormally short telomeres (Haber, 1998). Moreover, it was demonstrated that Ku and other proteins (Sir3, Sir4 and Rap1p) involved in transcriptional silencing of genes near the telomeres are released from telomeres in a RAD9, DDC1 or MEC1-dependent response to DNA damage (Martin *et al.*, 1999; McAinsh, 1999; Mills *et al.*, 1999). It was suggested that telomere proteins might contribute to NHEJ by creating specialised chromatin domains near double strand breaks, allowing proper alignment and re-joining while preventing access to transcription factors or nucleases.

Moreover, *RAD53*, *MEC1*, *DDC1* and *RAD17* genes, which are involved in different aspects of DNA repair, are necessary for telomere length maintenance, since mutations in all of these genes cause a decrease in telomere size. The telomeric shortening in *RAD53* and *MEC1* mutants is further enhanced in the absence of *SIR* genes, suggesting that Rad53/Mec1 and Sir proteins contribute to chromosome end protection by different pathways (Longhese *et al.*, 2000).

Furthermore, *TEL1* initially isolated in a screen for genes involved in telomere regulation, was later shown to be related to the ATM human gene, which is involved in DNA damage checkpoint responses (reviewed by Freidberg *et al.*, 1995). *S. cerevisiae* strains mutations in both yeast ATM homologues, *TEL1* and *MEC1*, show gradual telomere loss and lead to senescence. Thus, checkpoint proteins may also regulate the access of telomerase to chromosome ends and play a role in telomere length maintenance.

1.4.9 Telomeres and meiosis

The pairing of homologous regions is an essential pathway in meiosis that promotes the exchange of genetic material by recombination and facilitates

chromosome segregation. Cytological studies have suggested that telomeres are involved in homologous chromosome alignment since the relocation of telomeres to a small region of the nuclear envelope in early stages of meiosis has been observed in a wide range of eukaryotes. In the so called "bouquet" configuration, telomeres become associated to the spindle pole body in *S. pombe*, and chromosomes start to move back and forwards within the cell, with the telomeres and the spindle pole body leading the movement. This "horse tail" movement is thought to facilitate homologue alignment (reviewed in Cooper, 2000).

Deletion of Taz1p in *S. pombe* prevents the telomeres from becoming associated with the spindle pole body during meiotic prophase so both telomeres and centromeres remain dispersed in the nucleus (Cooper *et al.*, 1998; Nimmo *et al.*, 1998). Analysis of these mutants revealed a reduction in meiotic recombination and an increase in chromosome missegregation, suggesting that Taz1p is required for proper homologue alignment. This protein shares regions of homology with the human TRF1 (Chong *et al.*, 1995). Genetic experiences in budding yeast have shown that telomeres participate in homologous recognition prior to synapsis, and implicate the meiotic telomere-localising protein Ndj1 (Rockmill and Roeder, 1998). *NDJ1* deletion is known to cause meiotic defects, including chromosome missegregation (Chua and Roeder, 1997; Conrad *et al.*, 1997).

1.4.10. Telomeres, senescence and carcinogenesis

It has been suggested that telomere shortening constitutes the "molecular clock" that leads to senescence (the cessation of cell division). Senescence is characterised by a permanent growth arrest where cells enter G0/G1 phase of the cell cycle, assume an altered morphology and exhibit modified gene expression, though they remain metabolically active. The point where cells enter this senescence program was initially identified as the Hayflick limit (Hayflick, 1965), where short telomeres can no longer prevent chromosome ends from being recognised as DNA double strand breaks.

Several studies have revealed the correlation between replication-dependent loss of telomeric sequences and limited proliferative capacity (reviewed in Harley, 1995). The finite replicative potential is linked not to the chronological age of a culture but to the number of cell divisions and to telomeres (Cristofalo *et al.*, 1998). Figure 16

shows the classical model of the relationship between telomere length and the replicative life span of human cells.

Progressive telomere shortening and loss of function can activate two cellular responses, which depend on the genetic context: senescence and crisis. During the initial pathways of carcinogenesis, potential cancer cells bypass the proliferative barrier checkpoint of replicative senescence, via tumour suppressor loss, and enter telomere crisis, characterised by chromosomal instability such as chromosome fusions and aneuploidy (Fig. 14). Only rare immortalised clones will emerge from crisis and form tumours after an essential activation of telomere length maintenance mechanisms (either via telomerase or alternative lengthening of telomeres). In fact, it was demonstrated that over-expression of *c-Myc* oncogene induces expression of telomerase in fibroblasts and epithelial cells, which suggests that the activation of telomerase is a carcinogenic event (Wang *et al.,* 1998). The specific events that take place in tumour formation remain to be proven, but chromosomal loss or gain will certainly lead to important changes in gene dosage that could also contribute to transformation. Telomere shortening could also alter the expression of genes located nearby and fuel further development of cancer progression.

It was demonstrated that, unlike the germ line, embryonic and stem cells, normal human somatic cells usually lack significant telomerase activity, and continuously lose DNA from chromosome ends eventually leading to cellular senescence (reviewed in Ostler *et al.,* 2000). In general, cells that exhibit finite proliferative capacity and shortening telomeres lack telomerase activity, whereas cells with indefinite proliferative capacity and stable telomere length possess active telomerase enzyme. Exceptions, however, will be pointed out and discussed later on.

Several data support the "molecular clock" hypothesis. Experimentally disrupting telomerase activity in telomerase-positive cells, by over-expressing dominant-negative TERT forms (Zhang *et al.,* 1999; Hahn *et al.,* 1999) or using telomerase RNA anti-sense oligonucleotides (Herbert *et al.,* 1999), caused telomere shortening and apoptosis. Previous experiments in yeast lacking telomerase RNA or expressing Est2p (RT catalytic subunit) mutant inactive forms led to cell senescence (Singer and Gottschling, 1994). Knockout mice lacking active telomerase displayed progressive telomere shortening, both as animals age and over successive generations (Blasco *et al.,* 1997; Rudolph *et al.,* 1999).

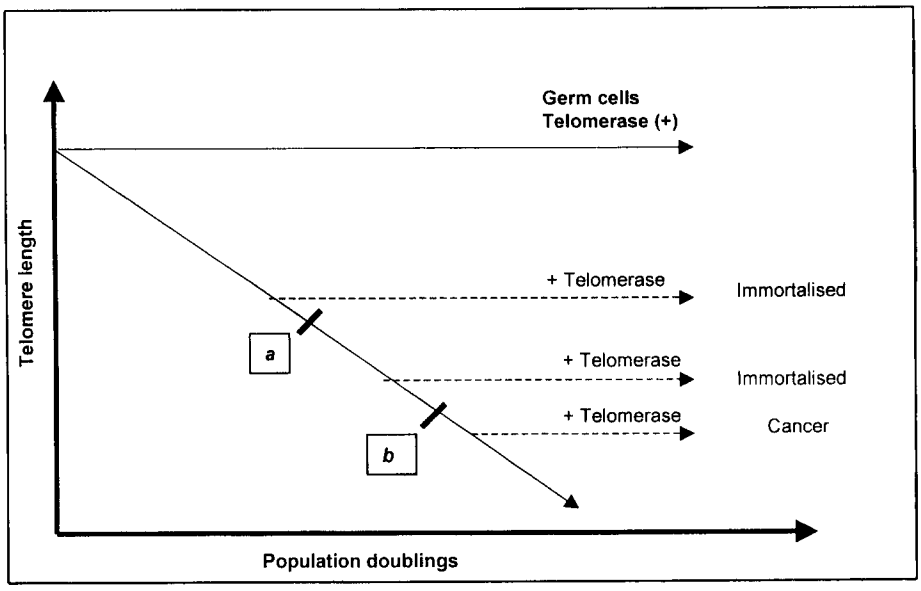

Figure 16: Telomere hypothesis. Relationship between telomere length and the replicative life span of human cells. (a) Replicative senescence checkpoint and p53/Rb inactivation. (b) Crisis; genetic catastrophe (adapted from Artandi and DePinho, 2000).

Conversely, in some experiments, ectopic expression of hTERT alone in certain human somatic cells, which lack telomerase activity, when grown in primary cultures led to an increase of telomere length and life span, sometimes leading to immortalisation (Counter *et al.*, 1992; Bodnar *et al.*, 1998; Vaziri and Benchimol, 1998; Wang *et al.*, 1998; Jiang *et al.*, 1999; Morales *et al.*, 1999). Most somatic cells contain all the other components of the telomerase enzyme so that the expression of TERT component led to the assembly of the enzyme activity. It is somehow surprising that hTERT alone is able to immortalise these cells, since it was previously well demonstrated that immortalisation of human cells by SV40 or other tumour viruses is a multistep process that requires the inactivation of p53 and Rb/p16 checkpoint pathways in association to telomere length maintenance mechanisms (Shay *et al.*, 1991). In fact, SV40-immortalised cells that have activated telomerase still require SV40 for continued proliferation (Holt *et al.*, 1996). Additionally, it was demonstrated that primary human fibroblasts undergo carcinogenesis in the presence of defined genetic elements (T-antigen, which inhibits Rb and p53 pathways, *ras* and hTERT). This apparent incongruity may depend on the existing telomere length previous to immortalisation. Thus, post crisis SV40-immortalised cells with active telomerase display very short but stable telomeres. If functional p53 and Rb/p16 are re-supplied to the cells, a DNA damage inducible checkpoint may be triggered and cease cell proliferation. In contrast, hTERT-immortalised normal cells, eventually maintain telomere length at a sufficient

length such that DNA damage-sensing pathways are never activated even in the presence of active p53 and Rb/p16 proteins. To conclude, although TERT itself is immortalising, it does not seem to be oncogenic, at least *in vitro*. In human cells that express T antigen and which have bypassed replicative senescence but not yet entered crisis, transfection of TERT prevents crisis and confers immortalisation (Counter *et al.,* 1998; Zhu *et al.,* 1999). Primary human cells have been transfected with TERT and did not show evidences of genetic instability (Morales *et al.,* 1999; Jiang *et al.,* 1999). However, studies reported so far suggest that the ability of hTERT alone to immortalise cells is probably also cell-type dependent (reviewed in Bryan and Cech, 1999). Furthermore, it should be noticed that upregulation of the TERT subunit by Myc oncoprotein suggests that it plays an essential role during carcinogenesis (reviewed in Greider, 1999).

To test the hypothesis that short telomeres may trigger a DNA damage-inducible response, the relation between telomere dysfunction and p53 activation was demonstrated (Chin *et al.,* 1999). The number of apoptotic cells in late-generation knockout mice, both for telomerase RNA and for p53 genes (*mTR-/-*; *p53-/-*), was found to be much lower than that observed in *mTR-/-*; *p53+/+* mice, demonstrating that telomere shortening induces a cellular response via p53 pathway. Additionally, transformation was enhanced in a *p53-/-* background, providing surprising evidence that telomere crisis is not a tumour suppressor mechanism and instead constitutes a period of genetic instability that results in either cell death or cellular transformation. Similarly, loss of telomere function in human cells by TRF2 removal from telomere sites causes chromosome fusions and an ATM- and p53-dependent cell death takes place (Karlseder *et al.,* 1999).

Several experiments suggested that telomere length *per se* does not state the fate of a cell (reviewed in Blackburn, 2000). In fact, experiments in yeast cells expressing an hypomorphic but fully active telomerase showed that they continuously lost telomere sequences but did not cease cell division even when telomeres became shorter than the control telomerase lacking cells which had stopped dividing (Prescott and Blackburn, 1997). These results suggest that telomere shortness may not alone determine cell fate and that the presence or absence of active telomerase may play a critical role. This was also supported by studies in human cells (Zhu *et al.,* 1999). Remarkably, active telomerase does not appear to be required when telomere length is sufficiently large. Only when it falls to a critical value, telomerase plays a critical role.

The discovery of immortal human cell lines that did not express telomerase (Lundblad and Blackburn, 1993; Bryan *et al.,* 1995, 1997), suggested the existence of

alternative pathways for telomere length maintenance. Additionally, cells from the sixth generation telomerase RNA knockout mice (*mTR-/-*) that did not contain detectable telomeric sequences, could form immortal cell lines and initiate tumour formation in nude mice despite the presence of an inactive telomerase enzyme (Blasco *et al.*, 1997). Initially mutant mice appeared quite normal and possessed long telomeres, but in later generations effect of telomere shortening finally led to decreased proliferation and increased apoptosis in multiple tissue compartments (Lee *et al.*, 1998).

1.4.10.1. Telomerase and cancer therapy: future perspectives?

Inactivation of telomerase has been proposed as a potential therapy for human cancers. The studies performed so far concerning the regulation of telomerase and its relationship with carcinogenesis suggest that the response to such inhibitors would also depend in other factors such as the p53 status. Thus, cells with defective p53 would be more resistant to this type of cancer therapy. The success of such approach would also depend on how promptly alternative-lengthening mechanisms would arise after telomerase inhibition *in vivo*. The potential impact of telomerase inhibitors on several host cell types should also be considered, since some somatic cells, such as stem cells, do possess telomerase activity. Undesirable secondary biological consequences could therefore take place.

New studies in telomerase RNA deficient mice will allow us to understand why tumour formation in these organisms continues to proliferate despite the absence of telomerase. This implies either the existence of alternative lengthening mechanisms or an eventual adaptive mechanism that allows the cell to minimise severe telomere dysfunctions. However, the higher transformation rate in *mTR-/-*; *p53-/-* mice and the increased incidence of spontaneous tumours in *mTR-/-* mice, suggest that short telomeres can in fact enhance early steps in tumour formation. Furthermore, studies involving the restoration of telomerase activity in *mTR-/-*; *p53-/-* cells resulted in a decrease in tumour formation, eventually because telomerase deficiency was acting as stimulatory factor, presumably by lowering the threshold to additional mutations that cooperate with *myc* and *ras* in transformation mechanisms (reviewed in de Lange and Jacks, 1999). Thus, the use of telomerase inhibitors at least in some contexts could eventually result in the opposite effect.

1.4.11. Telomere maintenance without telomerase

Telomere elongation by the telomerase ribonucleoprotein is not universal. At least two other chromosome elongation mechanisms exist that do not require telomerase. It has been demonstrated in *Saccharomyces* that recombination occurs, under some circumstances in cells containing linear plasmids with short stretches of telomeric repeats (Wang and Zakian, 1990). Telomerase defective *est1*$^-$ strains gradually lose telomere sequences from chromosome ends and eventually die. However, a small fraction of yeast cells are able to survive due to telomere elongation via RAD52-dependent recombination events. In fact, this alternative process is able to add Y' subtelomeric repeats and $C_{1-3}A$ sequences to most of the chromosome ends (Lundblad and Blackburn, 1993; McEachern and Blackburn, 1996). Similar results were obtained in experiments with *K. lactis*, which involved inactivation of telomerase via deletion of the telomerase RNA.

Drosophila telomeres do not contain the highly conserved telomerase elongated repeats. Instead they are maintained by repeated transposition of two non-LTR (Long Terminal Repeats) retrotransposons, Het-A and TART. These elements belong to the evolutionary conserved family of LINEs (Long Interspersed Elements) (reviewed in Mason and Biessmann, 1995; Pardue, 1995).

The *Chironomus* insect also contains unusual telomeres, since they are composed of large sized repeats (340-350bp) (Kamnert *et al.*, 1998). Unequal recombination and reverse transcription have been suggested in maintaining telomere length in *Chironomus* (Kamnert *et al.*, 1997). However, possibilities of telomere maintenance by telomerase, retrotransposition, gene conversion or recombination need still to be confirmed.

1.4.11.1. *Drosophila melanogaster*

1.4.11.1.1. *Drosophila* unusual telomeres

The telomeres of *Drosophila melanogaster* are different in that they are composed of multiple copies of two telomere specific LINE-like retrotransposons (LTRs), namely Het-A and TART (reviewed in Mason and Biessmann, 1995; Pardue, 1995; Pardue and DeBaryshe, 1999) arranged in a head-to-tail configuration. Both retrotransposons exist as a mixture in chromosome ends, although Het-A elements are

more abundant. Het-A and TART elements transpose as truncated forms at telomeres and are approximately 6 kb and 10 kb in size, respectively. Thus each telomere repeat in *Drosophila* is much longer and complex than the repeats added via the telomerase enzyme. However, *Drosophila* telomere sequences are also added to chromosome ends via an RNA-templated mechanism, such as in telomerase elongation processes. The most obvious difference between telomerase and the *Drosophila* reverse transcriptase relies in the fact that telomerase uses a small portion of its RNA template, while the *Drosophila* enzyme appears to use the entire RNA sequence. An interesting feature that suggests that *Drosophila* telomere elongation mechanisms and telomerase evolved from a common ancestor element, is the similarity in size and complexity between Het-A sequences and telomere-associated sequences (TAS). In fact, Y' elements from yeast can serve as an alternative mechanism for maintaining telomeres (Lundblad and Blackburn, 1993) and were characterised as being capable for retrotransposition (Louis and Harber, 1992).

Het-A and TART attach themselves to chromosomes by an oligo (A) tail (Fig. 17), a common feature to non-LTRs retrotransposons, and all copies are in the same orientation. This class of transposons associates to chromosomes by the 3' end of the RNA intermediate molecule and the chromosome break before reverse transcription takes place (Luan *et al.*, 1993). An expected RNA intermediate of ~6 kb has been identified in *Drosophila* (Danilevskaya *et al.*, 1994). Previous studies demonstrated that Het-A sequences are added to terminal deleted chromosomes at a frequency of 1% *per* generation. Additionally, 5' truncated Het-A sequences were also observed.

The entire sequence of the Het-A element was deduced by comparing two incomplete transposons localised in *Drosophila* telomeres (Biessmann *et al.*, 1994). The Het-A element has a 5' non-coding region (~800 bp) with A-rich repetitive sequences that may eventually be involved in three-dimensional conformations required for protein binding. The coding region is usually composed by over-lapping open reading frames (ORF), requiring a –1 frameshift to produce a full-length polypeptide. Retrotransposons usually encode gag-like proteins in the most 5' ORF and a reverse transcriptase enzyme in the second ORF. Het-A elements contain zinc-finger motifs, a general feature of gag-like polypeptides (Biessmann *et al.*, 1992a; Danilevskaya *et al.*, 1992) of several retroposons, but no sequence homology to any reverse transcriptase (RT). Consequently, the transposition of the Het-A element appears to require a RT from some other source within the genome (Biessmann *et al.*, 1992a).

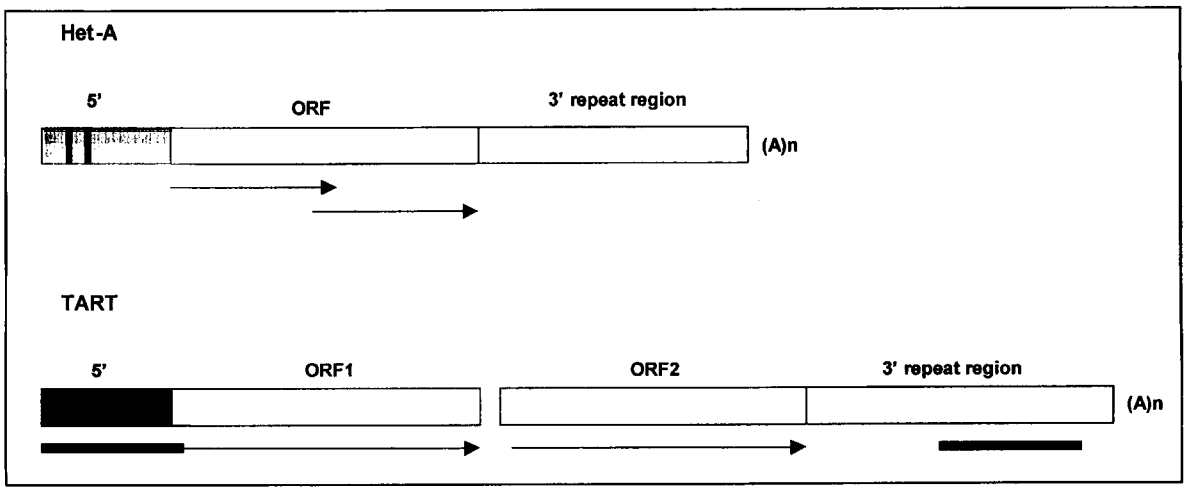

Figure 17: Schematic representation of *Drosophila* telomeric retrotransposons. The two black bars in Het-A 5' region indicate the A-rich repeat regions. The black bars shown below the TART element indicate two repeat regions.

The lack of its own enzyme seems to be part of the cellular control of Het-A transpositions. Almost half of a Het-A element is a 3' non-coding region composed of imperfect repetitive sequence arrays dispersed in a regular manner among species (Biessmann *et al.*, 1992a). Since Het-A elements are usually truncated in the 5' region, the 3' regions are highly enriched and are thought to play a role in chromatin structure (Danilevskaya *et al.*, 1993). Later studies revealed that the Het-A promoter activity is located in the 3' end of the element (Danilevskaya *et al.*, 1997), unlike the 5' end seen for other non-LTR retroposons. It was demonstrated that the 3' sequence of a Het-A element promotes the activity of its down stream neighbour.

The TART element was identified using a chromosome walk strategy from a P-element insertion located at the tip of the 3R chromosome arm (Levis *et al.*, 1993). Subsequently, terminal deleted chromosomes were shown to acquire TART elements demonstrating that these sequences were able to transpose to chromosome ends (Sheen and Levis, 1994). The 5' non-coding region of TART elements is approximately 960 bp. These 960 bp plus 85 bp of the adjacent ORF is identical to a sequence present in the 3'non-coding region. The TART-coding region is composed of two non-overlapped ORFs. One ORF produces a polypeptide with three zinc finger-like motifs and the second ORF codifies a LINE-like reverse transcriptase enzyme (Sheen and Levis, 1994). TART transposition is, therefore, independent of an external genomic reverse transcriptase. As Het-A elements, TART transposons exhibit an unusually long 3' non-coding region, however more heterogeneous within the same species. Despite

the strong sequence similarities of gag-proteins produced by Het-A and TART elements, further studies revealed that both have very different types of transcription.

Although *Drosophila* telomeric sequences are considered to be an exception, studies have demonstrated that Het-A elements are capable of forming G-quadruplex DNA. These results suggested that the 3' repeat region of Het-A may structurally behave as the telomeric repeats common to a majority of eukaryotes (Abad and Villasante, 1999)

In *Drosophila*, two genes have been identified that are required for maintaining telomere stability. The ubiquitin-conjugating enzyme 1 (UbcD1) was found to be required for proper telomere behaviour, since strains carrying mutations in this gene exhibit telomere attachments during mitosis and male meiosis (Cenci *et al.*, 1997). It is thought that in *UbcD1* mutants, the telomere associations observed in metaphase and anaphase chromosomes could be the consequence of the failure to degrade protein targets of the ubiquitin pathway. More recently, it was shown that heterochromatin protein 1 (HP1) is also required to protect telomeres in a sequence independent manner (Fanti *et al.*, 1998). Mutations in this gene cause end-to-end fusions. A protein-based mechanism involved in protecting telomere ends is also likely to exist in mammalian cells: TRF2 acts upon telomeres by preventing end-to-end fusions (Steensel *et al.*, 1998).

1.4.11.1.2. Terminal deletions in *Drosophila melanogaster*

In *Drosophila melanogaster*, early experiments failed in recovering terminal deletions after irradiation (Muller 1938,1941), leading to the conclusion that chromosomes lacking their telomeres were lost during cell divisions. However, subsequent studies showed that terminal deficiencies could be recovered when homozygous *mu-2* (*mutator-2*) females were irradiated. Male progeny with chromosomal breaks at the tip of the X chromosome (where the yellow gene is localised) were obtained. The broken chromosome was then introduced in a stock containing an attached-X so that terminal deletions could be transmitted through males. The terminally deleted chromosomes were found to be stable through many generations (Biessmann *et al.*, 1990a, 1990b) but to continually loose sequences from their broken ends at a rate of 75 bp *per* generation, presumably due to the end replication problem (Biessmann and Mason, 1988). Since no telomeric sequences were detected at broken ends, it was suggested that in *Drosophila* the end replication

and capping functions are separable. This also led to the hypothesis that protective telomeric proteins and terminal DNA interact via a sequence independent mechanism, which may involve the *mu-2* gene product. The *mu-2* mutation was suggested to promote the recovery of terminal deletions, enabling a newly broken chromosome to bypass DNA repair checkpoint mechanisms. However, *mu-2* mutation was not required for maintaining terminal deficiencies, since deleted X chromosomes were subsequently introduced and stably transmitted in strains which do not carry the mutation.

Later two X chromosomes bearing different terminal deletions were shown to acquire Het-A and TART sequences (Biessmann *et al.,* 1990b, 1992b), via a homologous recombination independent mechanism. It was subsequently demonstrated that those chromosomes stopped loosing DNA from their termini and the authors concluded that occasional acquisition of retrotransposons on broken ends plays a healing and protective role.

Terminal deficiencies were also recovered in strains that did not carry the *mu-2* mutation by Flip site-specific recombinase (Ahmad and Golic, 1998), in small stable derivatives of the X chromosome (Karpen and Spradling, 1992) and after destabilisation by P transposase (Levis, 1989).

1.4.12 Chromosome fate following DNA breakage in *Drosophila* and in yeast

Chromosome breaks are thought to activate DNA damage checkpoints leading to cell cycle arrest. To test this hypothesis in *Drosophila,* the fate of *Drosophila melanogaster* dicentric chromosomes was monitored in male germ-line mitotic cells, by constructing a dispensable chromosome containing P-elements with FLP recombinase target inverted repeats. The acentric fragment produced after FLP recombination did not segregate at mitosis and was lost, while the dicentric chromosome broke and was transmitted to daughter cells (Ahmad and Golic, 1998).

Several data support the idea that, in *Drosophila*, DNA damage responses result from detrimental effects of aneuploidy and not a cell cycle checkpoint. In fact, terminal deletions have been recovered after the expression of P transposase and after dicentric chromosome breakage. Additionally, irradiated eye imaginal disc cells died only after cell division. In all these cases, cells did not seem to be subjected to a DNA damage checkpoint and arrest.

However, there is also some evidence that supports the existence of DNA damage checkpoints in *Drosophila* cell cycle. Hari *et al.* (1995) showed that *mei-41*$^{+}$ is required for cell cycle arrest after X-irradiation. Evidence of a checkpoint response to radiation was found in early embryos (Fogarty *et al.* 1994). It has also been demonstrated that *Drosophila* somatic cells do detect or respond to a single broken chromosome, by arresting the cell cycle and undergoing apoptosis. The ultimate cellular consequence of that checkpoint response was shown to vary according to the developmental context of the cell (Ahmad and Golic, 1999). Early eye imaginal discs showed cell cycle arrest after the activation of the checkpoint induced by a single broken chromosome, while late eye imaginal discs undergo apoptosis. This event coincides with the two waves of mitosis driven by extrinsic signals. In fact, it has already been demonstrated in mammals that cell cycle arrest or apoptosis occur depending on the cell type and environmental conditions. One model proposed is that p53 always induces a cell cycle arrest, but in some cells this conflicts with extrinsic signals to divide, and the conflict provokes apoptosis. *mei-41* gene products have been shown to be required for cell cycle arrest after X-irradiation, but not in the response of a single broken chromosome. X rays produce extensive DNA damage, creating several broken ends and possibly single stranded breaks. Perhaps other type of damage or a minimal threshold of damage is required for activating the checkpoint in a *mei-41* dependent manner or may be this gene is not involved in inducing apoptosis, like it has been reported with the homologue in mammals (Barlow *et al.* 1997).

Ahmad and Golic (1999) demonstrated that after dicentric chromosome breakage, occasionally cells were able to divide at least once. In fact, terminal deletions without telomeric sequences have been recovered in *Drosophila* suggesting that telomeres can eventually be established *de novo* in a sequence independent manner, and that once established they are maintained. Nevertheless, it is certainly possible that some sequences are not compatible for telomere formation (Ahmad and Golic, 1998).

The fate of a dispensable chromosome lacking a single telomere was monitored during cell division in yeast (Sandell and Zakian 1993). In wild-type, elimination of a telomere caused a RAD9 mediated cell cycle arrest, indicating that telomeres help cells to distinguish intact chromosome ends from damaged DNA. However, many cells recovered from this arrest without repairing the damaged DNA and managed to replicate it and segregate it for as many as ten cell cycle divisions prior to its eventual loss. The authors speculated that one possible explanation for the recovery from the arrest is that the broken chromosome is eventually altered in a way that masks it from

the arrest system (e.g. by binding of a protein that is induced by DNA damage) but does not stabilise the chromosome. In fact, yeast DNA repair proteins such as Ku were found to bind to telomeres. Alternatively, the RAD9 pathway after an initial arrest may be turned off during a limited number of cell cycles.

1.5. P element-mediated insertional mutagenesis in *Drosophila melanogaster*

One of the best-characterised forms of mobile DNA in *Drosophila* are the P family of transposable elements. They were identified and shown to be responsible for the genetic phenomena known as hybrid dysgenesis. This is characterised by high frequencies of mutations and chromosomal rearrangements, sterility, male intrachromosomal recombination, and chromosomal missegregation. Mutant phenotypes are observed in the progeny of crosses between males, which harbour P-elements (P cytotype), and females without these transposable elements (M cytotype). Abnormal phenotypes are limited to the progeny of a dysgenic cross, and result from the high frequency of P-element transposition in the germ cells.

Complete P-elements are 2907 bp in length, contain short inverted repeats and transpose by a non-conservative mechanism (Engels *et al.*, 1990). P-elements harbour terminal inverted repeats of 31 bp in length and may be classified in two categories: (1) complete P-elements, 2,9 kb average sized, which contain two genes that codify two proteins by differential processing, an 87 kDa transposase and a repressor protein of 66 kDa; and (2) a heterogeneous class of defective P-elements, some of which are thought to codify truncated proteins with distinct biological activities.

Transposition of complete or defective P-elements depends on the 87 kDa transposase activity codified by the complete P-element, whose production is generally restricted to the germ line cells due to a specific RNA processing mechanism present in those cells. Transposase acts in *trans* by recognising target P-element DNA sequences adjacent to the inverted repeats. Although incomplete P-elements do not usually produce this enzyme, they can be mobilised by adding an exogenous transposase since they harbour the inverted repeats necessary in *cis* for transposition events. In typical P-stocks (containing 10-15 complete P-elements and 30-40 defective P-elements) transposition is repressed by a cytoplasmic state known as P cytotype. The molecular basis of the P cytotype is not completely understood but it is known that repressor molecules are produced by certain defective P-elements. A maternally

expressed 66 kDa repressor protein, produced by differential RNA processing of the complete P-element in somatic cells, also plays an important role. The lack of repressor activity in stocks that do not contain P-elements represents the M cytotype. P-elements have been widely used for genetic and molecular analysis in *Drosophila*.

This thesis reports the study of a new late larval lethal mutation in *Drosophila* that causes high frequency of end-to-end fusions between homologous and heterologous chromosomes during all stages of mitosis and meiosis. This strain was obtained through a P-element mobilisation assay. The mutation in the *locus* that we have called *telomere fusion* (*tef*), causes chromosome fusions that do not resolve, leading to cycles of chromosome breakage and rejoining and severe genome rearrangements. Chromosome ends appear to be essential for end-to-end fusions. Results suggest that the *tef* locus encodes a protein whose function may be required to protect chromosome ends.

2. MATERIALS AND METHODS

2. MATERIALS AND METHODS

2.1 *Drosophila* Stocks

Cultures were maintained at 24ºC on standard cornmeal-sucrose-yeast-agar medium:

5 g agar, 28 g yeast, 60 ml honey, 70 g cornmeal and 60 ml Nipagin solution (10 % in absolute ethanol) to 1L of water

The Oregon-R wild-type *Drosophila melanogaster* strain was obtained from the *Bloomington Stock Centre*.

The P-element and the deficiency *Drosophila* strains (see *Results* section) were either obtained from the *Bloomington Stock Centre (USA)* or the *Department of Jozsef Attila University, Szeged (Hungary).*

The *tef* mutant is part of the collection produced by mutagenesis using P-element mobilisation described in Karpen and Spradling (1992), and was kindly provided by Dr. Margaret Heck, John Hopkins University, Baltimore, USA.

The ring R(1)2 chromosome was obtained from the *Umea Drosophila Stock Centre (Sweden)*, and has the following genotype: *In(1)w[vC]/y[1]w[1]/Dp(1;Y)y[+]*

2.2 Bacterial Strains

Escherichia coli strain was used to transform and amplify plasmid DNA. Table 1 shows genotypes of several *E. coli* strains used during this work.

Table 1 - Genotypes of the *Escherichia coli* strains

***Escherichia coli* strains**	**Genotype**
C600	*e14⁻ (mcrA) supE44 thi-1 leuB6 lacY1 tonA21*
P2392	*HfrH argE(am) rpoB galT:: (intFII)P2*
XL1-Blue	*RecA1 endA1 gyrA96 thi-1 hsdR17 supE44 relA1 lac (F´proAB lacI^{q}ZΔM15 Tn10* (tet)r)
XL1-Blue MRF´	*Δ(mcrA)183 Δ(mcrCB-hsdSMR-mrr)173 endA1 supE44 thi-1 recA1 gyrA96 relA1 lac (F´proAB lacI^{q}ZΔM15 Tn10* (tet)r)
SOLR ™	*e14⁻ (mcrA) Δ(mcrCB-hsdSMR-mrr)171 sbcC recB recJ umuC:: Tn5(kanr) uvrC lac gyrA96 relA1 thi-1 endA1 λ^R(F´proAB lacI^{q}ZΔM15) Su⁻*

2.3 Vectors

2.3.1 λdash phage vector

A useful vector for constructing genomic libraries is the λdash phage substitution vector since it is able to accommodate 9-23 kb DNA fragments (Fig.1).

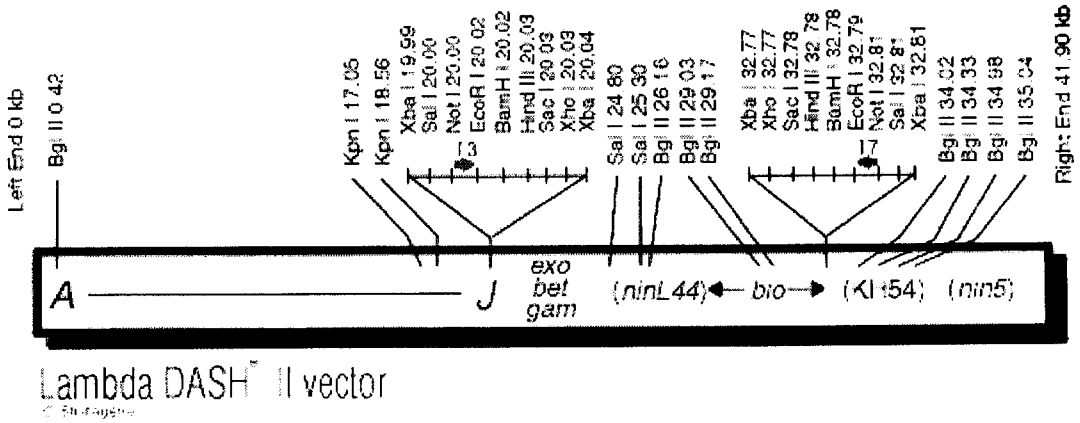

Figure 1: λdash phage vector. Restriction sites and primers are represented. (*in* Stratagene, USA)

2.3.2 UNIZAP phage vector

The UNIZAP phage vector (Fig. 2) is double digested with *Eco*RI and *Xho*I and will accommodate cDNA inserts up to 10 kb. This system allows rapid *in vivo* excision of the pBluescript SK(-) phagemid, allowing the insert to be analysed in a plasmid system. This method overcomes the need to clone the DNA insert after phage clone isolation.

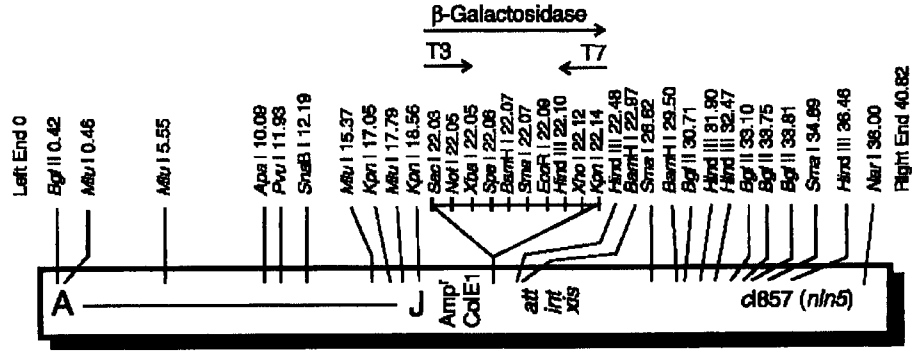

Figure 2: λdash phage vector. Restriction sites and primers are represented. (*in* Stratagene, USA)

2.3.3 λ gt10 phage vector

The λ gt10 phage is a substitution vector (Fig. 3) and is able to accommodate small cDNA fragments (~6 kb) in a single *Eco*RI restriction site localised to the immunity region. The *E. coli* bacterial strain C_{600} was used to amplify the phage

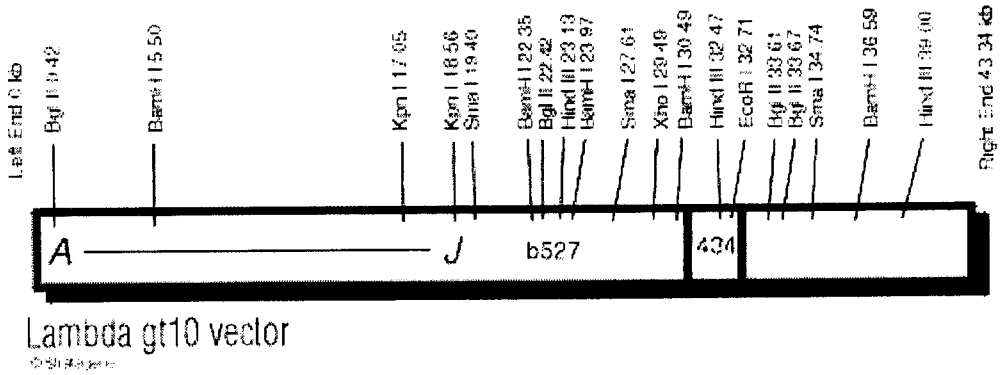

Figure 3: λgt10 phage vector. Restriction sites are represented. (*in* Stratagene, USA)

2.3.4 pBluescript SK(+) plasmid

The pBluescript SK(+) Plasmid is a cloning vector with 2961bp derived from the pUC19 vector. The SK designation indicates that the polylinker is orientated in such a way that the *lacZ* transcription is processed from the *Sac*I to the *Kpn*I restriction sites (Fig. 4)

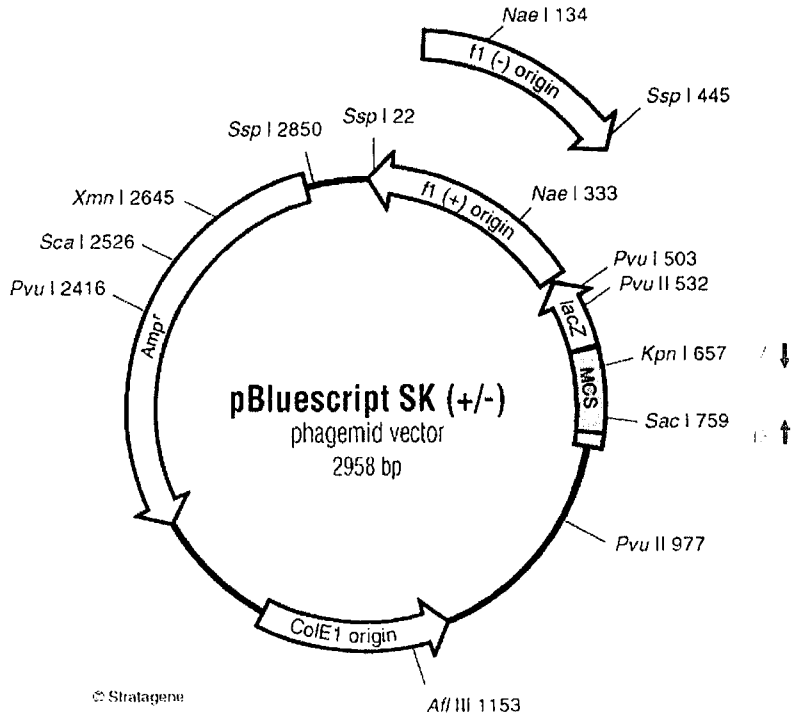

Figure 4: pBluescript vector. Restriction sites are represented. (*in* Stratagene, USA))

2.3.5 P1 bacteriophage vector

P1 cloning vectors are able to harbour inserts of 75-100 kb. They contain a P1 packaging site (*pac*) that allows the recombinant vector to be packaged into infectious particles, a pair of *loxP* recombination sites that serve as targets for the *Cre* recombinase to circularise the DNA once it has been injected into suitable host cells, and a kanamycin resistance gene to enable selection of transformed cells. Although the vector is normally maintained at 1 copy per cell by the plasmid replicon, it can be amplified 20-30 copies per cell by means of a P1 lytic replicon, under the control of a *lac* promoter (Sternberg, 1990) (Fig. 5)

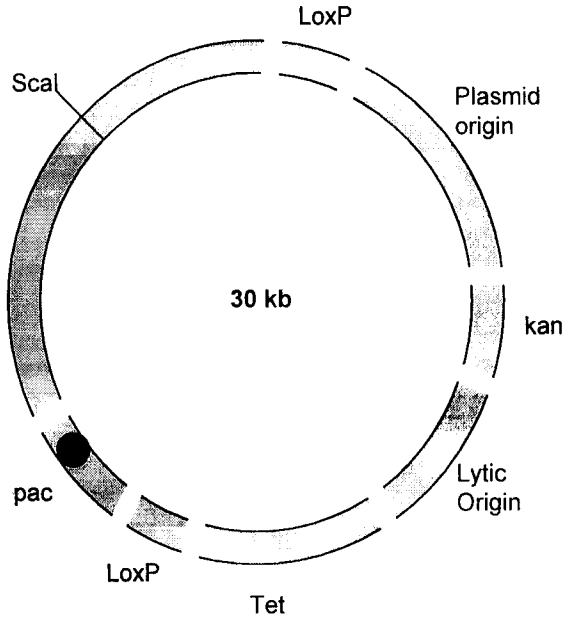

Figure 5: Bacteriophage P1 vector.

2.3.6 PZ vector

PZ vector is used as a transformation vector in *Drosophila*. It contains a wild type *rosy* gene (~7,2 kb) as a dominant marker that allows the selection of transformed flies, a kanamycin resistance gene which enables the selection of transformed bacterial cells after plasmid rescue, and a *lac* gene (Fig. 6).

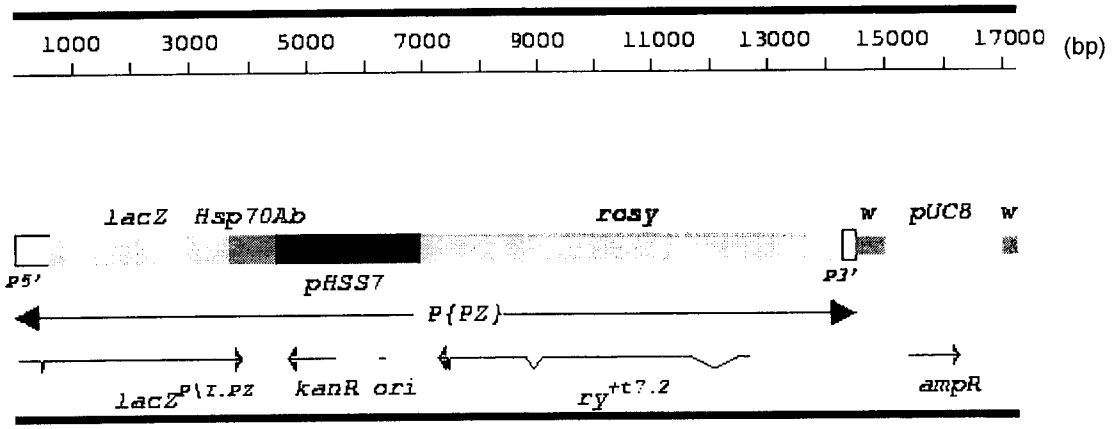

Figure 6: PZ transformation vector

2.4 Mitotic Chromosome Preparation from *Drosophila melanogaster* Neuroblasts for Fluorescence Microscopy Analysis

Mitotic chromosomes were prepared from late larval neuroblasts dissected in an isotonic 0.7% NaCl solution. Neuroblasts were transferred to an hypotonic solution 0.5% of sodium citrate, during 2 minutes. Brains were then fixed in 45% acetic acid (in water) and in 60% acetic acid for 1 minute. The fixed brains were spread, the cover slip removed after immersion of the slide in liquid nitrogen and then mounted in Vectashield (Vector Laboratories, UK) containing propidium iodide (5 μg/ml).

For metaphase chromosomes studies, neuroblasts were treated in a 0.5% sodium citrate hypotonic solution during 5-10 minutes, immediately before the 45% acetic acid fixation.

Colchicine treatment was performed by incubating dissected neuroblasts in 0.05 mM colchicine solution during 30 minutes followed by a hypotonic shock for 10 minutes, before fixation.

2.5 *In situ* Hybridisation to Mitotic Chromosomes

DNA probes (~1μg) were labelled with biotin-14-dUTP using the Bionick Translation system (Gibco, BRL). This reaction was performed by adding 5μl of a 10x dNTP mixture (0.2 mM of each dCTP, dGTP, dTTP; 0.1 mM dATP; 0.1mM biotin-14-dATP; 500 mM Tris-HCl pH 7.8; 50 mM MgCl2; 100 mM β-mercaptoethanol; 100 μg/ml

nuclease free BSA), 5 μl of a 10x Enzyme mixture (0.5 units/μl DNA polymerase I; 0.0075 units/μl DNase I; 50 mM Tris-HCl pH 7.5; 5 mM magnesium acetate; 1 mM β-mercaptoethanol; 0.1 mM phenylmethylsulfonyl fluoride; 50% v/v glycerol; 100 μg/ml nuclease free BSA) and water to a final volume of 45 μl. Labelling reaction was incubated at 16ºC for 1 hour and finally 5μl of stop buffer were added. One volume of 2x hybridisation solution was added to the labelled probe.

When two different probes were used simultaneously an additional labelling reaction was performed directly with Cy5-dCTP using the Fluorolink Cy5 nick translation kit (Amersham Life Science). This reaction was performed by adding to ~1μg of DNA probe, 5 μl of dNTP mixture (0.5 mM of each dATP, dGTP and dTTP and 0.001 mM dCTP), 0.5μl Cy5-dCTP (1 nmol/μl Cy5-dCTP in 10 mM phosphate buffer pH7), water until 15μl of the final volume, and 5 μl enzyme mixture (DNA polymerase I and DNase I in optimised proportions in 0.05 M Tris buffer, 0.01 M $MgCl_2$ and 0.001 M DTT). Reaction was incubated at 16ºC for 1 hour and stopped by adding 5 μl of stopping solution (0.2 M EDTA).

Mitotic chromosomes were prepared as described above. After cover slip removal, slides were immersed in 70% ethanol solution for 5 minutes and in 100% ethanol for another 5 minutes. Slides were air dried and incubated at 58ºC for 1 hour. Chromosomes were denatured in a 70% formamide, 2xSSC solution at 70ºC for 2 minutes. Slides were immediately dehydrated in 70% ethanol for 5 minutes and in 100% ethanol for other 5 minutes, and finally air-dried. 100 ng of denatured probe (at 95ºC for 5 minutes) were applied to denatured chromosomes. Incubation was performed overnight at 58ºC in a humid chamber.

Excess of probe was washed away in a 2xSSC solution at 53ºC for 2 minutes, followed by 5 minutes successive washes in 4xSSC, 4xSSC with 0.1% Triton X-100, and 4xSSC solutions.

Slides were incubated in a dark humid chamber for 30 minutes with a 2% avidin-Fluorescein conjugate (Vector Laboratories, #A-2001) in 4xSSC. Washes were performed as described above, and finally chromosomes were stained with propidium iodide in an anti-fading mounting medium (Vector laboratories).

Slides were analysed in fluorescence and/or Confocal microscopy.

In situ hybridisation to wild-type and *tef* mitotic chromosomes was performed with the subtelomeric P1 clones (Table 2).

Table 2 - Subtelomeric probes used for *in situ* hybridisation

Chromosome	P1 clone	Hybridisation site
X	26-92	1D1-2
2L	37-40	21E3-F
2R	42-48	60A1-A2
3L	73-50	61F3-F4
3R	3-95	100A1-A2

Dodecasatellite (Abade *et al.*, 1992) and RSP (Wu *et al.*, 1988) were used as centromeric probes for chromosome 3 and 2, respectively.

2.6 *In situ* Hybridisation to *Drosophila melanogaster* Polytene Chromosomes

Chromosomes were prepared by dissecting salivary glands from third instar larvae in 0.7% NaCl isotonic solution. Glands were fixed in 45% acetic acid solution for 1 minute and mounted in 8µl 1:2:3 solution (1 volume of lactic acid, 2 volumes of water and 3 volumes of glacial acetic acid). Gentle tapping on the cover slip using the top of a pencil was performed, in order to spread polytene chromosomes. Slides were then gently squashed, immersed in liquid nitrogen and cover slip was immediately removed with a razor blade. Chromosomes were dehydrated in a 100% ethanol solution for 30 minutes.

After air drying, slides were incubated in a 2xSSC solution at 65ºC during 30 minutes, followed by 5 minutes successive dehydrations in 70% ethanol solution and 100% ethanol. After air drying slides were denatured in a 70mM NaOH solution for 2 minutes at room temperature and immediately dehydrated in 70% ethanol solution for 5 minutes and in 100% ethanol for 5 minutes. The denatured probe mixed with 2x hybridisation solution was applied on chromosome preparations and then incubated in a humid chamber at 58ºC overnight.

Excess of probe was washed as described for *in situ* hybridisation to mitotic chromosomes.

20xSSC – 3 M NaCl, 0.3 M sodium citrate

2x Hybridisation solution - 8x SSC, 20% Dextran sulfate, 2x Denhardt's, 0.4% salmon sperm DNA

2.7 Immunostaining of Neuroblasts and Male Meiotic Cells

Third instar larvae neuroblasts were dissected in 0.7% NaCl solution. Fixation was performed for 1 minute in a 2% formaldehyde, 2% Triton X-100, 1x PBS solution, and neuroblasts were mounted in a fixation solution containing 2% formaldehyde and 45% acetic acid. Brains were squashed and slides were immersed in liquid nitrogen. The cover slips were removed and slides were immersed in a TBST solution. Neuroblasts were then blocked in a 10% fetal calf serum (FCS) in TBST during 30 minutes. The 1st antibody was added in appropriate dilution in 5% FCS and 2.5 μg/ml of RNase solution, and slides were incubated overnight at 4°C in a humid chamber. Slides were washed three times in TBST during 5 minutes. Second antibody was added in appropriate dilution in a 5% FCS TBST solution. Slides were incubated for 1 hour at room temperature in a humid chamber and then washed 5 minutes in TBST three times. Finally, chromosomes were mounted in Vectashield containing 5 μg/ml of propidium iodide.

Microtubules were labelled with an anti-α-tubulin (Amersham, UK) antibody in a 1/1000 dilution and anti-centrosomine (REF) was used in a 1/500 dilution. Second antibodies were anti-mouse conjugated with fluorescein (Vector Laboratories, UK) and anti-rabbit conjugated with Cy5 (Vector Laboratories, UK). Peanut antibody was used in a dilution of 1/1000 (REF).

Preparation and immunostaining of male meiotic cells was performed by dissecting testis in B1 solution on a clean slide. A siliconized cover slip was placed over a drop of B1 solution containing the dissected testis, which were squashed by drawing the liquid with a filter paper. Slide was immersed in liquid nitrogen and cover slip was removed. The slide was immersed in methanol previously cooled at –20°C for 5 minutes and then in acetone at –20°C for 2 minutes. The slide was transferred to a B2 solution containing 0.5% Acetic Acid and 1% Triton X-100 for 10 minutes at room temperature. Washing procedures were performed three times 10 minutes in B2 solution. Testis were then incubated in 10% FCS, 0.3% Tween-20 and 2μg/ml RNase in PBS for 1 hour in a humid chamber at room temperature. Testis were then incubated with primary antibody in 10% FCS, 0.1% Tween-20 in PBS overnight at 4°C in a humid chamber. Slides were washed in 0.1% Tween-20 in PBS from 1 to several hours. The second antibody was added in the appropriate dilution in a 10% FCS PBS solution and incubated for 1 hour at room temperature. Slides were washed in 0.1% Tween-20 in

PBS as before, and mounted in Vectashield (Vector Laboratories, UK) containing 5 μg/ml of propidium iodide.

Microtubules were labelled with an anti-α-tubulin antibody (1:1000 dilution, Amersham, UK). All observations were done using a confocal laser microscope MRC-600 (BioRad, USA) and the images processed using the COMOS software (BioRad, USA).

TBST - 50 ml Tris 1 M (pH 7.5), 30 ml NaCl 5 M, 5 ml Tween 10% in 1 litre of ddH20

B1 solution – 183 mM KCl, 47 mM NaCl, 10 mM Tris pH6.8, 1 mM PMSF, 1 mM EDTA

B2 solution – 1 mM $CaCl_2$, 2.6 mM KCl, 1.5 mM KH_2PO_4, 0.5 mM $MgCl_2$, 137 mM NaCl, 8.1 mM Na_2HPO_4

1x PBS – dissolve 8g of NaCl, 0.2g KCl, 1.44g Na_2HPO_4, 0.24gKH_2PO_4 in 1 litre of water. Adjust pH to 7.2

2.8 Irradiation Experiments

Analysis of a DNA damage checkpoint was performed by irradiating third instar larvae with several doses, using a Gammacell 1000 Elite research irradiator. Neuroblast dissection and preparation of mitotic chromosomes were performed at several times after irradiation to quantify mitotic parameters.

Survival of homozygous mutant individuals was analysed by irradiating embryos laid from the *tef /TM6B* stock. Several doses were tested and the *mus 101[D2]* mutation was used as a control.

2.9 Apoptosis Assay

Apoptotic cells in wild-type and *tef* neuroblasts were detected using the Oncor Apoptag Plus *in situ* Apoptosis detection Kit-Fluorescein and performed as described previously (Basu *et al.*, 1999).

2.10 HP1 Immunostaining to Polytene Chromosomes

Salivary glands were dissected in Cohen and Gotchel medium G with 0.5% NP-40, and incubated in this medium for 8-10 minutes. Glands were transferred to

formaldehyde fixative solution and incubated for 25 minutes. Glands were fixed in a drop of 45% acetic acid solution in a cover slip, mounted with a slide, and gently spread by moving the cover slip back and forth. Spreading was monitored under the microscope. The preparation was gently pressed with the thumb and immersed immediately in liquid nitrogen. Cover slip was removed with a razor blade and slide was transferred to TBS immediately. Washes were performed three times for 5 minutes in TBS/0.05% Tween-20 at room temperature. The first antibody (anti-HP1-antibody) diluted 1:50 in TBST was added to polytene chromosomes. Slides were incubated overnight at 4°C in a humid chamber. Slides were washed in TBST three times for 5 minutes. The second antibody (anti-mouse-fluorescein, Amersham, UK) was added to the polytene chromosomes, and slides were incubated for 1 hour at room temperature. Washing procedures were performed as described previously. DNA was stained with DAPI solution and slides were mounted in antifading solution. Preparations were observed under a Nikon microscope associated to a CCD Coolsnap RS photometrics camera.

Cohen and Gotchel (1971) medium G – 25 mM di-Na glycerolphosphate, 10 mM KH_2PO_4, 30 mM KCl, 10 mM $MgCl_2$, 3 mM $CaCl_2$, 160 mM sucrose

Formaldehyde fixative solution – 5% formaldehyde, 100mM NaCl, 2 mM KCl and 10 mM Na phosphate (pH 7), 2,5% NP-40

2.11 Genomic DNA Isolation from Adult Flies

Flies were collected and frozen in liquid nitrogen. ~100 individuals were homogenised in 1 ml of solution A. The resulting suspension was centrifuged at 8000 rpm for 5 minutes. Supernatant was removed and the sediment was re-suspended in 1 ml of solution A. A new centrifugation was performed. This procedure was repeated until the supernatant appeared sufficiently clean. The last re-suspension was done in 500 µl of solution A, followed by addition of proteinase K to a final concentration of 100 µg/ml and 50µl of 10% SDS solution. Eppendorfs were inverted several times and then incubated at 37°C for several hours. A phenol extraction was performed twice, followed by a chloroform extraction. DNA was precipitated by adding 2 volumes of ethanol. Genomic DNA was observed and isolated using a toothpick, transferred briefly to a 70% ethanol solution and finally to ~50 µl of water.

Solution A - 10mM Tris-HCl (pH 7.5), 60 mM NaCl, 10 mM EDTA, 0.15 mM spermin, 0.15 mM spermidin

2.12 DNA Extraction from P1 Clones

Frozen cells were inoculated in 5 ml of L-Broth with 50 μg/ml of kanamycine and grown at 37°C overnight. A 1/100 dilution was performed with the overnight culture in fresh L-Broth with 50 mg/ml of kanamycine and IPTG at a final concentration of 100mM. Culture was grown for more 5 hours approximately. Cells (~50 ml) were centrifuged for 5 minutes at 4000 rpm, and re-suspended in 100 μl of solution I. Cell lysis was performed by adding 300 μl of solution II and incubating for 5 minutes at room temperature. 150 μl of solution III were added and the lysate was incubated on ice for 15 minutes. The supernatant was transferred to a new eppendorf and 5 μl of 10 mg/ml RNase were added followed by an incubation at 37 °C for 15 minutes. Chloroform extraction was performed, followed by DNA precipitation with 0.6 volumes of isopropanol. DNA was washed with 70% ethanol, dried and re-suspended in 20 μl of water.

Solution I – 50 mM Glucose, 25 mM Tris-HCl (pH 8.0), 10 mM EDTA (pH 8.0)
Solution II – 0.2 M NaOH, 1%SDS
Solution III – 3 M potassium acetate (pH 4.8)

2.13 Southern Blot of *Drosophila melanogaster* Genomic DNA

Genomic DNAs (5-10 μg) were digested with several restriction enzymes in 40μl final volume during 6 hours using appropriate buffers and incubation temperatures. Loading buffer was added (~5μl) to digested DNA and to ~2 μg of lambda DNA digested with *Hind*III. Samples were applied in a 0.8% agarose gel (20x20cm) in 1xTAE buffer, and electrophoresis was performed at 25 volts during 12 hours. The gel was photographed and the standard molecular weight bands were registered.

10xTAE – 0.4 M Tris-acetate (pH 8.0), 0.01 M EDTA
6x Loading buffer – 0.25% bromophenol blue, 15% Ficoll in water

The gel was incubated in a depurinating solution for 15 minutes and in a denaturing solution for 30 minutes. Southern blotting was performed during at least 4 hours using an alkaline transfer solution. After blotting the N+ membrane was treated in a neutralising solution for 10 minutes. DNA cross-link to the membrane was performed at 80°C for 2 hours in an oven.

Depurinating solution – 0.25 M HCl
Denaturing solution – 1.5 M NaCl, 0.5 M NaOH
Transferring solution – 1.5 M NaCl, 0.25 M NaOH
Neutralising solution – 0.5 M Tris-HCl (pH 7.2), 1.5 M NaCl, 1 mM EDTA

The membranes were incubated for 1 hour at 65°C in pre-hybridisation solution. Labelled probe was added to the membrane and hybridisation was performed overnight at the same temperature.

Pre-hybridisation solution – 6.25 ml 20xSSC, 1.25 ml 10% SDS, 1.25 ml 100% Denhardt's, 50 µl denatured salmon sperm DNA, in a final volume of 25 ml.

Membranes were washed in 2xSSC, 0.1% SDS for 20 minutes at room temperature, and with 1xSSC, 0.1% SDS for 15 minutes at 65°C. Background radioactive signal was monitored with a Geiger Counter and if significant, a higher stringent wash was performed using 0.1xSSC, 0.1% SDS solution.

Membranes were exposed to autoradiographic films (Agfa) at –70°C for at least 1 day.

2.14 DNA Labelling Using the "Multiprime DNA labelling system" (Amersham).

Probes were labelled using the "Multiprime DNA labelling system" (Amersham). 10 µl of labelling buffer (dATP, dGTP, dTTP in Tris-HCl pH7.8, MgCl2 and 2-mercaptoethanol) and 5 µl of primer mixture were added to 50 ng of denatured probe. Water was added until a final volume of 47 µl. 1µl of α(32-P)-dCTP (10 µCi/ml) and 2U of Klenow enzyme were finally added, and the reaction was incubated at 37°C for 1 hour. Free nucleotides were eliminated by filtration of the labelled probe using a Sephadex G-50 column equilibrated with TNE (10 mM Tris-HCl pH 7.5, 20 mM NaCl, 2 mM EDTA, 0.1% SDS). 20 µl of loading buffer were added to the probe before applying to the column. Filtered probe was recovered in an eppendorf, denatured at 95°C for 5 minutes and kept on ice until used for hybridisation.

6x Loading buffer – 0.25% bromophenol blue, 15% Ficoll in TNE

2.15 Isolation of Genomic DNA from Single Flies Followed by Southern Hybridisation

A single fly was homogenised in 100 μl of solution HM, and incubated at 65°C for 20 minutes. 15 μl of potassium acetate 8M was added and the tube was mixed thoroughly and incubated on ice for 30 minutes. Tube was centrifuged for 20 minutes at 8000 rpm and the supernatant was transferred to a new tube. 200 μl of cold ethanol was added and tube was left on ice for 1 hour. DNA was precipitated by centrifugation at 8000 rpm for 5 minutes, washed with 70% ethanol, and dried for 10 minutes at 65°C. Restriction enzyme buffer (10x) was added for a total volume 50 μl followed by 5 μl of restriction enzyme. Digestion was incubated at appropriate temperature and applied in a 0.8% agarose gel used for electrophoresis.

Solution HM – 200 mM Sucrose; 100 mM Tris Base pH 7,5; 50 mM EDTA pH 8,2; 500 mM SDS; 100 mM NaCl

2.16 Screening Phage Libraries

The *Drosophila* embryo (2-14 hour) cDNA Uni-ZAP^{TM}XR library was cloned at *Eco*RI and *Xho*I sites of the Uni-ZAP^{TM}XR vector, in a way that the 5′end of the mRNA localises to the *Eco*RI site. The *E. coli* XL1-Blue MRF′ was used as the host strain. pBluescript SK plasmid excision containing cDNA fragments was performed by co-infection of the XL1-Blue MRF′ with a helper phage Exassist and infection of SOLR^{TM} cells. Plating and *in vivo* excision procedures were performed as described in the instruction manual of the Uni-ZAP^{TM}XR library. Phage λgt10 screenings were performed using the *E. coli* bacterial strain C_{600} as a host strain. Experimental procedures were performed as described for the Uni-Zap^{TM}XR library. The λ gt10 phage is a substitution vector (fig) and is able to accommodate small cDNA fragments (~6 kb) in a single *Eco*RI restriction site localised to the immunity region. The λgt10 vector harbours non-oriented cDNA fragments. Extraction of phage DNA is performed as described in Maniatis *et al.* (1989).

The genomic DNA library initially screened with the 94-46 P1 clone was constructed in the λdash vector. P2392 *E.coli* strains were used as host cells. Screening of membrane replicas were performed by immersing them in denaturing solution for 5 minutes, neutralising solution for other 5 minutes and finally in 5xSSC for

2 minutes. Membranes were fixed, pre-hybridised and hybridised as described for the southern blot analysis.

Denaturing solution – 1.5 M NaCl, 0.5 M NaOH
Neutralising solution – 0.5 M Tris-HCl (pH 7.2), 1.5 M NaCl, 1 mM EDTA

2.17 Phage DNA Isolation

Phage DNA of λgt10 and λdash isolated clones was prepared as described in Maniatis *et al.* (1989).

2.18 Alkaline Lysis Mini-Preparation of Plasmid DNA

A single colony was isolated and inoculated in a 5 ml L-Broth medium with 50 μg/ml of ampicillin. The culture was grown over night at 37°C. 3 ml of the cell culture were centrifuged for 5 minutes at 4000 rpm. Cells were re-suspended in 100 μl of solution I. Cell lysis was performed by adding 200μl of solution II and incubating for 5 minutes at room temperature. Proteins were precipitated by adding 150 μl of solution III, and incubating on ice for 15 minutes. Eppendorfs were centrifuged for 15 minutes at 12000 rpm. Supernatant was recovered for a subsequent chloroform extraction. DNA was then precipitated by adding 2 volumes of ethanol and centrifuged for 30 minutes at 12000 rpm. DNA was washed with a 70% ethanol solution, dried and re-suspended in 20 μl of water.

Solution I – 50 mM Glucose, 25 mM Tris-HCl (pH 8.0), 10 mM EDTA (pH 8.0)
Solution II – 0.2 M NaOH, 1% SDS
Solution III – 3 M potassium acetate (pH 4.8)

2.19 Boiling Method for Isolation of Plasmid DNA

A single colony was inoculated in 10 ml LB with 50 μg/ml of ampicillin, and grown overnight at 37°C in a shaking incubator. The bacterial culture was centrifuged at 4000 rpm for 5 minutes and the pellet was re-suspended in 200 μl of STET buffer. 4 μl of lyzosyme (50 mg/ml) were added and the suspension was incubated for 5 minutes. The samples were then boiled for 45 seconds and centrifuged at 12000 rpm

for 10 minutes. The resulting sediment was removed using a toothpick. Nucleic acid precipitation was performed by adding 8µl of 5% CTAB solution and a 10 minute centrifugation at 12000 rpm. The pellet was re-suspended in 300 µl NaCl 1.2 M. DNA precipitation was performed by adding 750 µl of absolute ethanol, followed by centrifugation during 10 minutes. DNA was washed with 70% ethanol, dried and re-suspended in 20 µl TE.

STET buffer – 8% sacharose, 0.1% v/v TritonX-100, 50 mM EDTA, 50 mM Tris-HCl pH8
CTAB solution- 5% cetylmetyl ammonium bromide

2.20 Preparation of Competent Cells

A single colony was grown overnight in 10 ml of LB in a shaking incubator at 37°C. This culture was then diluted in 400 ml LB and grown at 37°C until an optical density of 0.6 at 600nm.

After rapid cooling the culture was centrifuged at 4000 rpm for 15 minutes. The pellet was re-suspended in 100 ml of cold solution A and centrifuged at 4000 rpm during 8 minutes. The pellet was resuspended in 20 ml of cold solution B and frozen as 200 µl aliquots at –70°C.

LB – 1% tryptone, 0.5% yeast extract, and 0.5% NaCl
Solution A – 30 mM KCH_3COO, 50 mM $MnCl_2$, 10 mM $CaCl_2$, 100 mM KCl, 15% glycerol
Solution B – 10 mM Na Mops (pH 7), 75 mM $CaCl_2$, 10 mM KCl, 15% glycerol

2.21. "Freeze-squeeze" Method for DNA Fragment Isolation from Agarose Gel

λgt10 phage DNA (~2µg) was digested with *Eco*RI restriction enzyme and then used in gel electrophoresis. cDNA inserts were cut from the agarose gel with a razor blade and incubated in sodium acetate 0.3 M pH 4.8, for 30 minutes. Gel slice was placed in a small eppendorf prepared with a small amount of siliconized glass wool and two holes, one on top and the other at the bottom, made with a needle. Small eppendorf was frozen in liquid nitrogen and placed in a larger eppendorf. Tubes were centrifuged for 10 minutes at 12000 rpm. 2.5 volumes of absolute ethanol were added to the centrifuged solution present in the large eppendorf. DNA was precipitated by

centrifugation at 12000 rpm for 10 minutes, washed with 70% ethanol, dried and resuspended in water.

2.22 Subcloning of DNA Fragments in pBluescript SK vector

λgt10 cDNA inserts were ligated to pKS vector using the following equation, for a total 1 μg DNA:

Insert (ng)= [Vector (ng) x insert size (kb)]/ Vector size (kb) x ratio insert/vector (~5)

Ligation was performed in a 20 μl reaction containing 4 μl ligase reaction buffer and 0.1 units of ligase enzyme (GibcoBRL) at 14 °C overnight.

2.23 Plasmid DNA Transformation of Competent Cells

Approximately 100 ng of DNA (or the total volume of a ligation reaction) was added to 200 μl of competent cells. This mixture was incubated on ice for 20 minutes. Cells were then incubated at 42 °C for 45 seconds and immediately incubated on ice for 2 minutes. 800 ml of LB was added and cells were incubated at 37°C for 1 hour. Cells were centrifuged at 3000 rpm for 5 minutes. 100 μl supernatant were used to re-suspend cells. This suspension was plated in a solid LB- agar medium containing 50 μg/ml of ampicillin, 0.1 mM of IPTG and 40 μg/ml of X-gal. Petri dishes were incubated overnight at 37°C.

2.24 Double stranded DNA Sequencing

DNA sequencing was performed with the "Sequenase 2.0 version" (USB). Plasmid DNA was isolated using the boiling method. Approximately 3 μg of DNA were denatured by the addition of 4 μl of a 1 M NaOH, 1 mM EDTA solution, in the presence of ~50 ng of primer in a 20 μl final volume. DNA was incubated at 37°C for 30 minutes, and precipitated with 2 μl of 2 M Ammonium acetate and 66 μl ethanol. The tube was incubated at –70°C for 10 minutes and centrifuged for 15 minutes at 13000 rpm. Supernatant was removed and the pellet was re-suspended in 9.6μl of water. 5.9μl of a sequencing mixture was added to each reaction (2 μl sequencing buffer, 0.4 μl labelling mixture, 1 μl 0.1 M DTT, 1.75 μl enzyme dilution buffer, 0.5 μl 10 μCi/μl (35S)-dATP

and 0.25 µl 13 U/µl sequenase enzyme). Tubes were incubated for 15 minutes at room temperature. To 2.5 µl of each termination mixture pipetted to different eppendorfs (ddATP, ddTTP, ddGTP, ddCTP) 3.5 µl of the reaction mixture were added and incubated at 37°C for 5 minutes. The sequencing reaction was stopped by adding 4µl of a stop dye. Probes were denatured at 95 °C for 5 minutes before loading the acrylamide gel.

Sequencing buffer – 200 mM Tris-HCl pH 7.5, 100 mM MgCl2, 250 mM NaCl
Labelling mixture – 7.5 mM of each dGTP, dCTP and dTTP)
Enzyme dilution buffer – 10 mM Tris-HCl pH 7.5, 5 mM DTT, 0.5 mg/ml BSA
Termination solutions :
ddGTP – 80 mM of each dATP, dTTP and dCTP; 8 mM ddGTP; 50 mM NaCl
ddCTP- 80 mM of each dGTP, dTTP and dATP; 8 mM ddCTP; 50 mM NaCl
ddTTP – 80 mM of each dGTP, dATP and dCTP; 8 mM ddTTP; 50 mM NaCl
ddATP – 80 mM of each dGTP, dTTP and dCTP; 8 mM ddATP; 50 mM NaCl
Stop solution – 95% formamide, 20 mM EDTA, 0.05% bromophenol blue, 0.05% xylene cyanol FF)

Sequencing gel was prepared with a solution containing 21g urea, 7.2 ml 10xTBE, 6 ml 50% Acrylamide Long Ranger (HydroLink, AT Biochem, Inc., USA), 30 µl TEMED, 300 µl 10%APS. After polymerisation, pre-running was performed at 60 Watts in 0.6 TBE. The gel sequencing reactions were loaded on the gel. The gel was dried in a vacuum system at 80°C and exposed to an autoradiografic film for at least 16 hours.

2.25 Northern Blot

Exceptional care must be taken while extracting RNA (described in Maniatis *et al*, 1989).

Homozygous *tef/tef* and wild-type larvae (~100mg) were isolated and homogenised in 1 ml of Trizol reagent (GibcoBRL). Suspension was centrifuged at 12000 g for 10 minutes at 4°C. Supernatant was incubated 5 minutes at room temperature to allow the complete dissociation of nucleoprotein complexes. A purification assay was performed by adding 0.2 µl followed by vigorous shaking. Tubes were centrifuged at 12000 g for 15 minutes at 4°C. the aqueous phase was collected and RNA was precipitated by adding 0.5 ml of isopropyl alcohol. Samples were incubated 10 minutes at room temperature and centrifuged at 12000 g for 10 minutes at 4°C. Total RNA was then resuspended in water and used for isolating mRNA by the

Quick prep Micro mRNA purification kit (Amersham), as described in the instruction manual.

Northern Blotting was performed in a denaturing formaldehyde gel prepared by autoclaving 160 ml of deionised water containing 3g of agarose, followed by the addition of 32 ml of 37% formaldehyde and 20 ml of gel buffer. Running buffer was prepared by adding 75 ml of 20x gel buffer and 120 ml of 37% formaldehyde in a total volume of 1.5 litres. Precipitated RNAs were resuspended in 20 µl of sample buffer at 65°C for 5 minutes followed by the addition of 20 µl of dye buffer. Samples were loaded on the gel. Gel ran overnight at 40-50 volts and 100-125 mA. Gel was soaked in 10xSSC for 20 minutes. Blotting was performed overnight in 10xSSC. Membrane was dried at room temperature for 30 minutes and then exposed on the ultraviolet light for 5 minutes. Pre-hybridisation was performed in a solution containing 50% formamide, 5xSET, 5x Denhardt's, 200 µg/ml salmon sperm DNA and 2x gel buffer, at 42°C for 2 hours. The $\alpha(^{32}P)$-dCTP labelled denatured cDNA probe was added to the membrane and hybridisation was performed overnight. Membrane was washed at room temperature in 0.5xSET, 0.5% SDS solution.

20x gel buffer – 0.36 M Na_2HPO_4, 0.04 M NaH_2PO_4
20x SET – 3 M NaCl, 0.6 M Tris-HCl pH8, 40 mM EDTA
Sample buffer – 50% formamide, 6% formaldehyde, 1x gel buffer
Dye buffer – 50% formamide, 50% glycerol, 1x gel buffer
100 x Denhardt's – 2% BSA, 2% polyvinylpyrolidone, 2% ficoll, 20 mM EDTA

3. RESULTS

3.1. Isolation and characterisation of the *tef* mutant

3. RESULTS

3.1 Isolation and characterisation of the *tef* mutant

3.1.1 Analysis of the mitotic phenotype in *tef* mutant neuroblasts

The *tef* mutant strain was originally isolated from a collection of P element-induced recessive late larval lethal mutations. However genetic analysis indicated that the P-element was not associated with the lethality or the mitotic phenotype. Accordingly, a number of isogenic recombinant lines that did not contain the P-element, but retained the lethality and mitotic phenotype were produced (described below). The recombinant line *ru h th st cu tef* was used throughout this study.

Homozygous mutant cells display severe mitotic abnormalities that are characterised by the fusion of chromosome arms (Fig.1). Cytological analysis suggests that chromosome arms establish these attachments through their telomeres (Fig.1E-F, Fig.2). Mitotic chromosomes display end-to-end fusion behaviour from early stages of mitosis since associations are already observed during prophase (Fig.1B-C). Most metaphase cells exhibit fusion between one or more chromosomes (Fig. 1E-F, Fig. 2). These associations may involve single chromatid attachment (SCA) or double chromatid attachment (DCA) (Fig.1E-F, Fig.2). Even with hypotonic shock treatment, chromosome arms remain associated, indicating that those attachments are solid and not easily resolved. These attachments persist during anaphase (Fig.1H-I) and cells may contain one or multiple DNA bridges, even after chromatin decondensation in telophase (Fig.1K-L). Accordingly, we have named the locus *tef* (*te*lomere *f*usion).

Other types of abnormal chromosome structures were also observed. *In situ* hybridisation, using chromosome specific pericentromeric and subtelomeric probes, was performed in order to determine the type of chromosome rearrangements (Fig.3). Chromosomal rearrangements included the exchange of subtelomeric sequences from one chromosome to heterologous chromosomes (Fig.3B-C), unusual sized euchromatic arms (Fig.3D-E), duplication of subtelomeric sequences (Fig.3F-G) and evidence of DNA breakage in subtelomeric regions (Fig.3F). Polyploid cells with highly rearranged chromosomes were also observed at low frequencies (Fig.3H-I). As shown above (Fig.1), mutant cells still display chromatin bridges during anaphase and telophase.

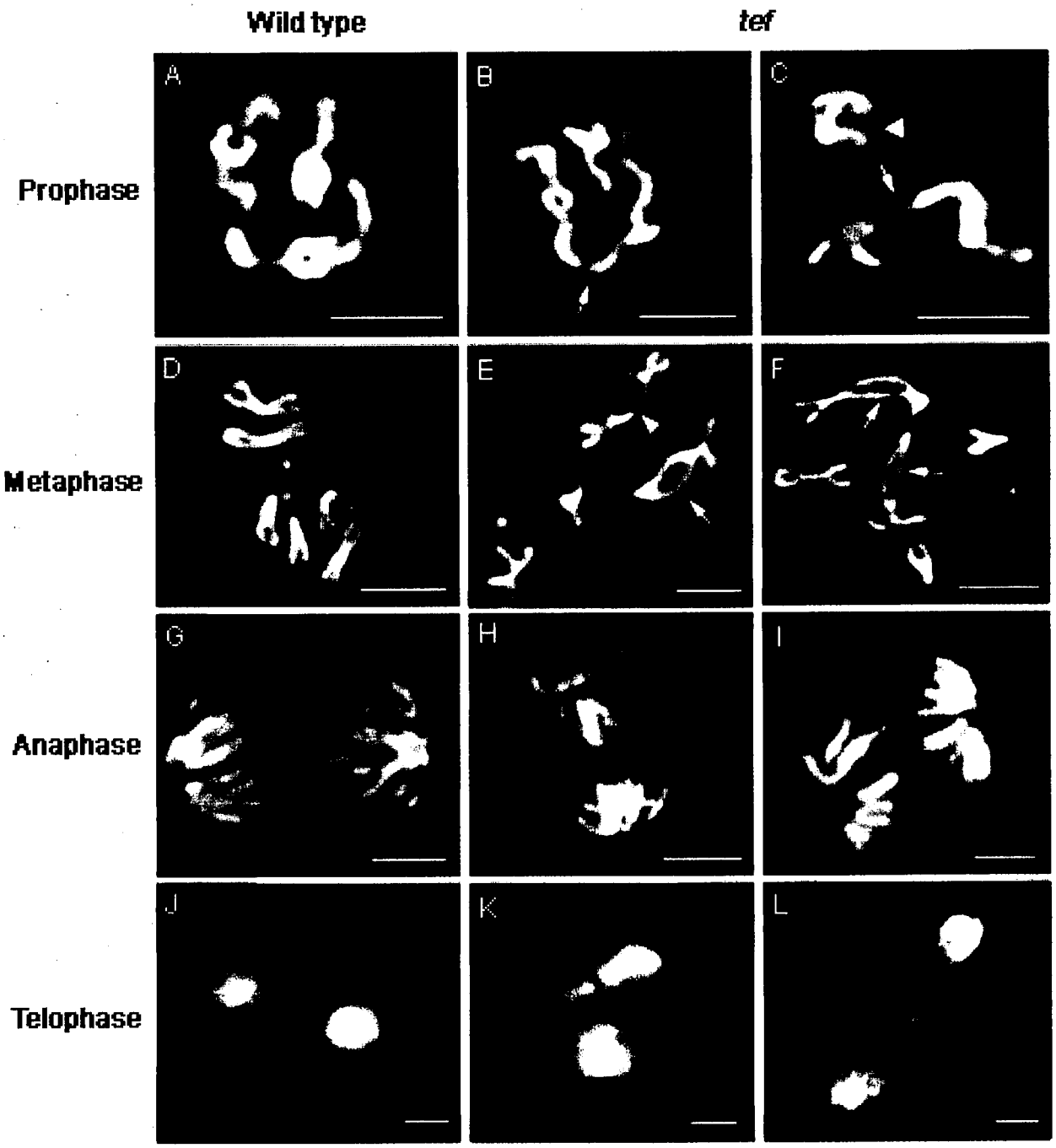

Figure 1: Mitotic alterations in *tef* homozygous neuroblasts. Wild-type (A,D,G and J) or *tef* mutant cells (B,C,E,F,H,I,K and L) are shown at different stages of mitosis. (A) Wild-type female cells in prophase. (B) Mutant cell in prophase with both autosomes fused by their termini (arrow). (C) Mutant cell in prophase showing an association between the X chromosome and one of the autosomes (arrow) and a ring conformation resulting from fusion of opposite arms of an autosome (arrowhead). (D) Wild-type cell at metaphase. (E) Mutant cell at metaphase showing a DCA between an autosome and an X chromosome (arrow), and a SCA between 2 autosomes (arrow head). (F) Mutant cells at metaphase showing a DCA linear attachment involving 3 autosomes. (G) Wild-type cell during anaphase. (H) Mutant cell at anaphase with multiple and (I) with a double DNA bridge. (J) Wild-type cell at telophase. (K and L) Mutant cells at telophases with unresolved DNA bridges. Bar is 10 μm.

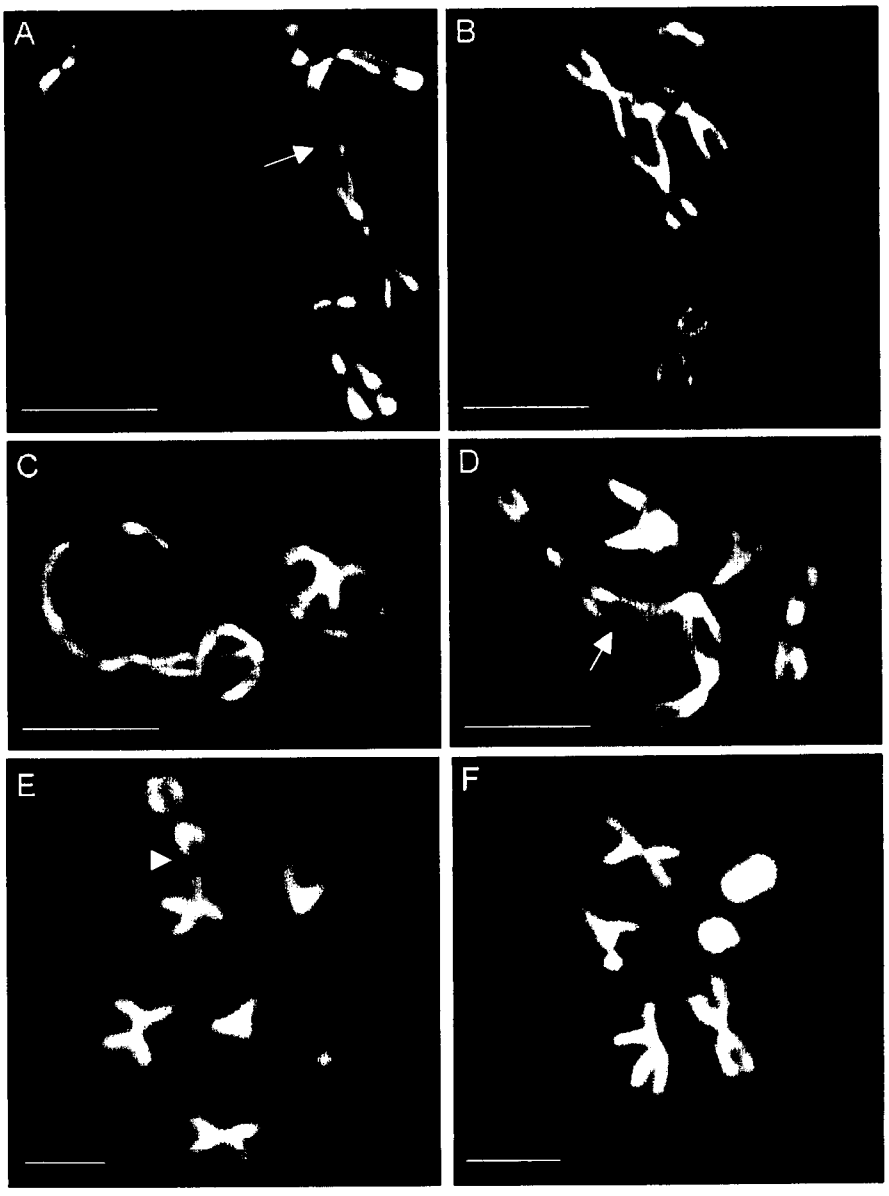

Figure 2: Examples of abnormal metaphase chromosomes in *tef* neuroblasts. Arrows in figures (A) and (D) refer to DCAs. Arrow head in (E) shows a SCA. Note that in (C) almost all metaphase chromosomes associate in a continues thread-like structure. X Chromosomes in (E) and (F) are fused to the fourth chromosome at the XL and XR arm respectively. (F) shows abnormal ring-like chromosomes. Bar is 10μm.

Evidence of DNA breakage in non-subtelomeric regions could occasionally be observed in anaphase (Fig.4), which could explain the exchange of chromosomal material between heterologous chromosomes. To determine the chromosome regions associated with DNA bridges, *in situ* hybridisation using subtelomeric regions of the autosomes and the X chromosome was performed (Fig.5). The results indicate that in most of these cells, subtelomeric sequences are present in chromatin bridges.

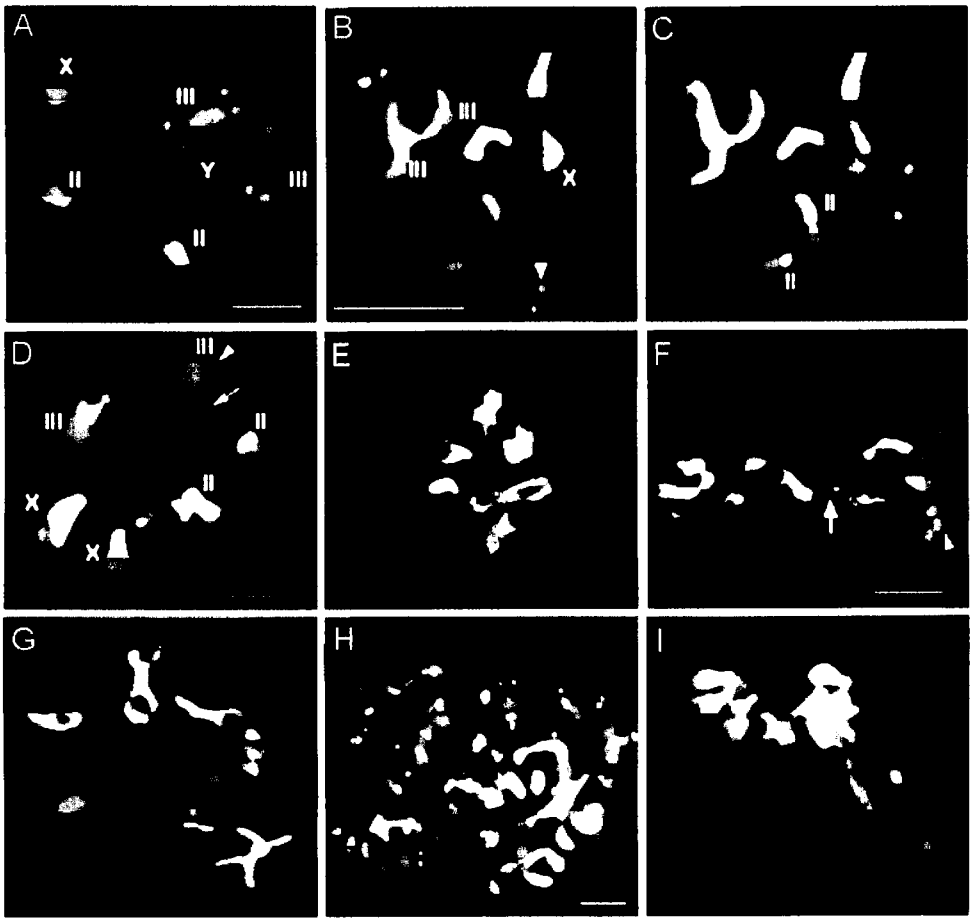

Figure 3: Chromosomal rearrangements present in *tef* mutant neuroblasts. DNA was stained with propidium iodide (red). (A) Wild-type cell at metaphase hybridised with subtelomeric probes of the third chromosome (green) and the *dodecasatellite* centromeric probe (blue). (B) Cell at metaphase hybridised with *dodecasatellite* specific for the pericentromeric region of chromosome 3 (blue) and subtelomeric sequences specific for 3L and 3R (green). Subtelomeric probes hybridise to chromosome 2 (arrow head) identified using a RSP centromeric probe (green) following washes and rehybridisation (C). (D) Metaphase cell hybridised with *dodecasatellite* (blue) showing an abnormal chromosome 3 with unusual short euchromatic arms (arrow head) and a chromosome 2 identified by the RSP (green) signal with an abnormal long euchromatic arm (arrow). (E) Metaphase cell hybridised with the centromeric probes RSP (green) and dodecasatellite (blue). Note that one of the third chromosomes exhibits an unusual large arm. (F) Metaphase cell hybridised with subtelomeric probes for chromosome 3. Note that two pairs of subtelomeric sequences are detected in one arm of a single chromosome (arrow head). Also note that this metaphase cell contains at least 10 sites of hybridisation instead of 8, as expected, and breakage in a subtelomeric region (arrow). (G) Metaphase cell hybridised with subtelomeric probes for 3R. More hybridisation signals were detected than those expected. (H) Highly polyploid metaphase cell hybridised with *RSP* (blue) and subtelomeric sequences specific for the left and right arm of the second chromosome (green). (I) Polyploid cell with chromosomes arranged at the metaphase plate. Note three X chromosomes and a misalignment of chromosomes. Bar is 10 μm.

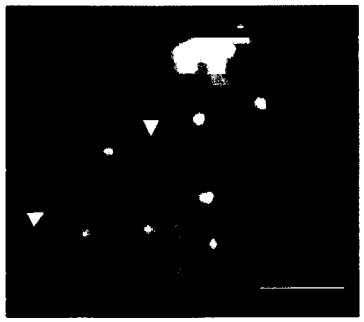

Figure 4: Non telomeric chromosome breakage in *tef* mutant anaphases. Subtelomeric DNA from the third chromosome (green) and dodecasatellite DNA (blue) were used as probes. Chromosomes were stained with propidium iodide (red). Bar is 10 µm.

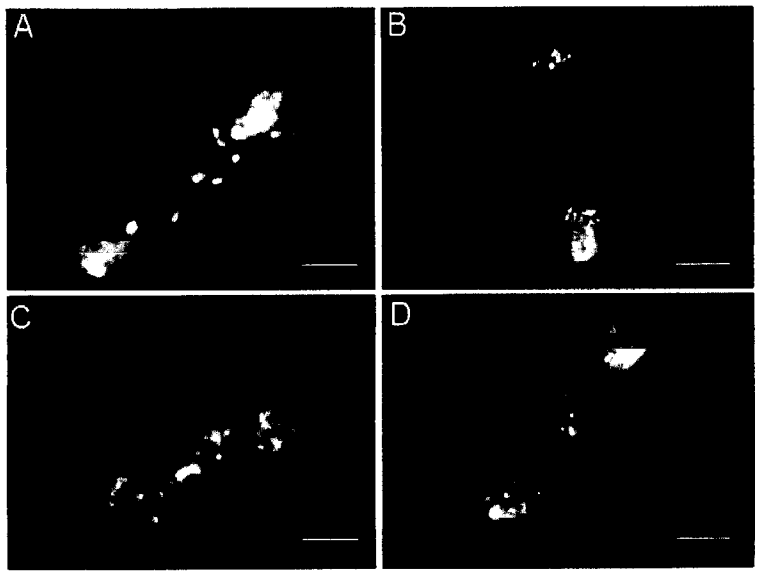

Figure 5: Characterisation of chromatin bridges present in *tef* mutant telophases. Telophase cells hybridised with a mixture of subtelomeric probes to visualize all chromosomes except the fourth. The images show that the unresolved chromatin bridges normally contain subtelomeric sequences. Chromosomes were stained with propidium iodide. Bar is 10 µm.

3.1.2 Types of chromosomal associations in *tef* neuroblasts

The *tef* mutation causes a high frequency of chromosome association during metaphase that can be classified as those involving homologous chromosomes, heterologous chromosomes, and those involving sister chromatids of the same chromosome.

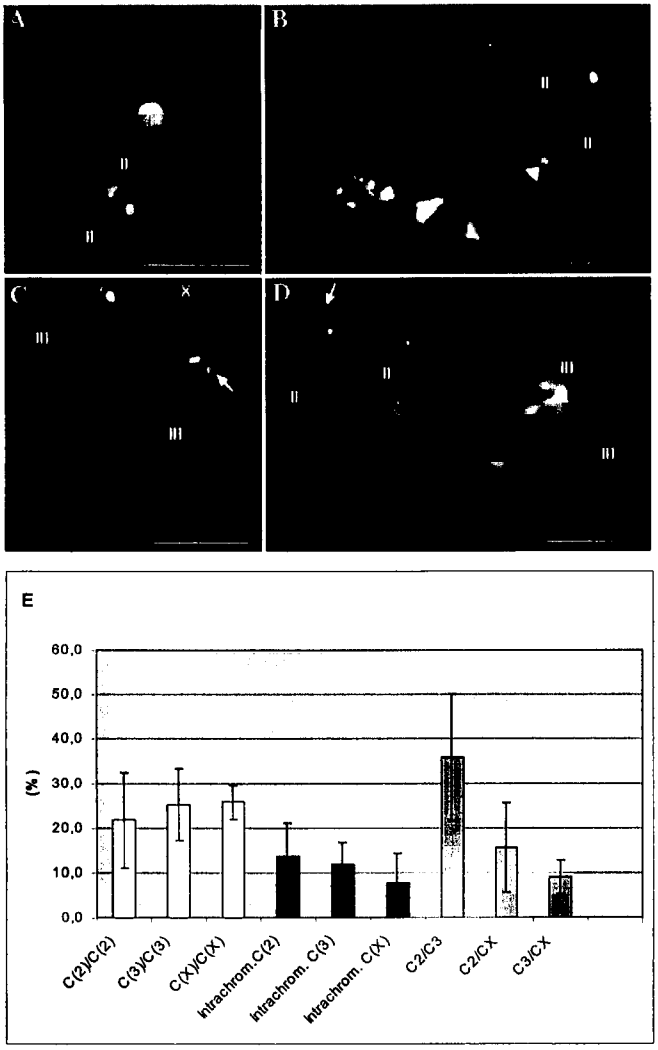

Figure 6: Identification and quantification of different types of chromosomal interactions in *tef* mutant cells. In order to determine specific chromosome interactions, *tef* neuroblasts were isolated, incubated in colchicine followed by hypotonic shock and then hybridised with pericentromeric and/or subtelomeric probes. (A) The cell at metaphase was hybridised with a probe for chromosome 2 (RSP in blue) and subtelomeric sequences specific for 2L and 2R (green). This cell shows homologous associations between the two second chromosomes and heterologous associations between the two autosomes. (B) Metaphase cell hybridised with probes as for A, showing intrachromosomal association (arrow head). Note the presence of extra subtelomeric hybridisation signals of chromosome 2 in other chromosomes. (C) Metaphase cell hybridised with subtelomeric sequences specific for the right arm of chromosome 3 (green) showing heterologous association. The arrow indicates a subtelomeric probe (green) that hybridises in a more proximal region of the chromosome. (D) Metaphase cell hybridised with the *dodecasatellite* DNA (blue) and subtelomeric probes for both arms of chromosome 2 (green). The arrow indicates an intrachromosomal association that resulted in a ring conformation. In all figures DNA was stained with propidium iodide. Bar is 10 μm. (E) Quantification of different types of chromosome interactions in *tef* neuroblasts. Homologous interactions between chromosome 2, 3 and X are designated by C(2)/C(2), C(3)/C(3) and C(X)/C(X), respectively. Intrachromosomal associations involving chromosomes 2, 3 and X and different types of heterologous associations between them are also quantified. A total of 263 metaphases were analysed and obtained from 8 brain squashes. The sum of frequencies is never equal to 100% because one metaphase usually exhibits more than one type of fusion.

In order to determine the frequency of each individual type of chromosomal association, *in situ* hybridisation with specific subtelomeric and pericentromeric probes was performed (Fig.6). Intrachromosomal associations occur in two different ways. Those that take place between the same arm of one chromosome (Fig.6B), or those involving opposite arms of a chromosome, originating ring conformations (Fig.6D). We

have also quantified interchromosomal associations involving one or more sister chromatids (Fig.6A, C). The results (Fig.6E) indicate that all chromosomes that were analysed (X, 2 and 3) are capable of forming different types of associations. Analysis of their frequencies indicates that in general intrachromosomal associations are less frequent than homologous or heterologous interactions. The most frequent interactions are observed between chromosomes 2 and 3.

Two different types of interactions were also quantified in more detail. Single chromatid attachments (SCA) are those where sister chromatids behave independently, forming sister unions (Fig.6B, arrow head) or dicentric chromosomes (Fig.1E, arrow head). Double chromatid attachments (DCA) occur when both sister chromatids behave in the same way, originating chromosomes with ring conformations (Fig.6D, arrow), or linear attachments with other chromosomes (Fig.1E-F, arrow). The results (Table 1) show that overall, DCAs are far more frequent (86%) than SCA (36%) and that linear attachments (72%) are more frequent than ring (14%) conformations.

Table 1 -Types of chromatid association

		SCA		DCA	
	N° Metaphases	**SU**	**Dicent.**	**ring**	**linear attach.**
Total	**253**	**40**	**51**	**36**	**181**
Freq.		**16%**	**20%**	**14%**	**72%**

7 neuroblasts were scored
SCA-single chromatid attachment
su-sister union
Dicent.- dicentric or polycentric chromosomes
DCA-double chromatid attachments
linear attach.-linear attachments also forming dicentric or multicentric chromosomes

We have also analysed whether there is any significant difference in the frequency of association of the long or short arm of the X telocentric chromosome. We observed that, out of approximately 80 metaphase figures from 7 neuroblasts analysed, the long arm of the X chromosome is much more likely to undergo association (83%) than the short arm (21%). This data is in good agreement with previous results (Cenci *et al.*, 1997) and fully supports the idea that mitotic chromosomes in *D. melanogaster* display a Rabl orientation within the nucleus, with telomeres and centromeres segregated to opposite sides.

3.1.3 Analysis of the mitotic spindle organisation and the midbody structure in *tef* mutant neuroblasts

Mitotic spindle organisation and centrosomes were also analysed in detail by performing immunostaining assays using specific antibodies against α-tubulin or centrosomine. Immunostaining assays (Fig.7) revealed that both, the mitotic spindle and the centrosomes were similar in *tef* mutant and wild-type neuroblasts, even when *tef* mutant cells contained chromatin bridges. These results suggest that the assembly of the mitotic apparatus is not affected by the *tef* mutation.

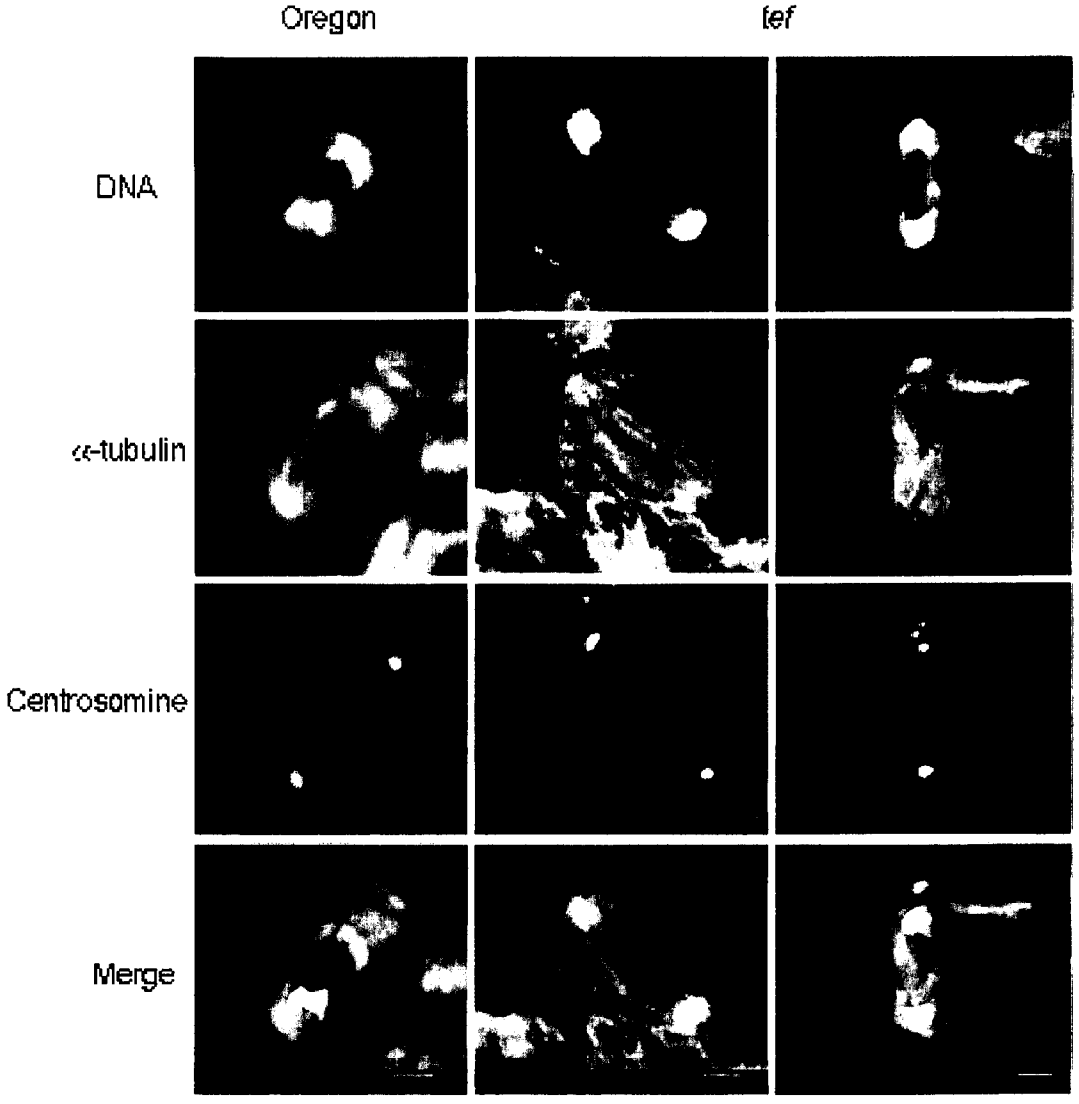

Figure 7: Organisation of the mitotic apparatus in *tef* mutant neuroblasts. Immunostaining assays performed in neuroblast squashes using the α –tubulin (green) and centrosomine (blue) antibodies. DNA was stained with propidium iodide (red). Spindle and centrosome abnormal structures were not detected in *tef* mutant when compared with the wild-type control

In order to determine whether the formation of the cleavage furrow in telophase was compromised in the presence of DNA bridges, immunostaining assays using antibodies against the peanut protein were performed (Fig. 8). The peanut protein localises to the cleavage furrow of dividing cells during cytokinesis and to the intercellular bridge connecting post-mitotic daughter cells (Neufeld and Rubin, 1994). DNA bridges of telophase cells in the *tef* mutant did not seem to interfere with the distribution of peanut at the cleavage furrow. Resolution of DNA bridges due to breakage or chromatin separation was also observed within the cleavage furrow.

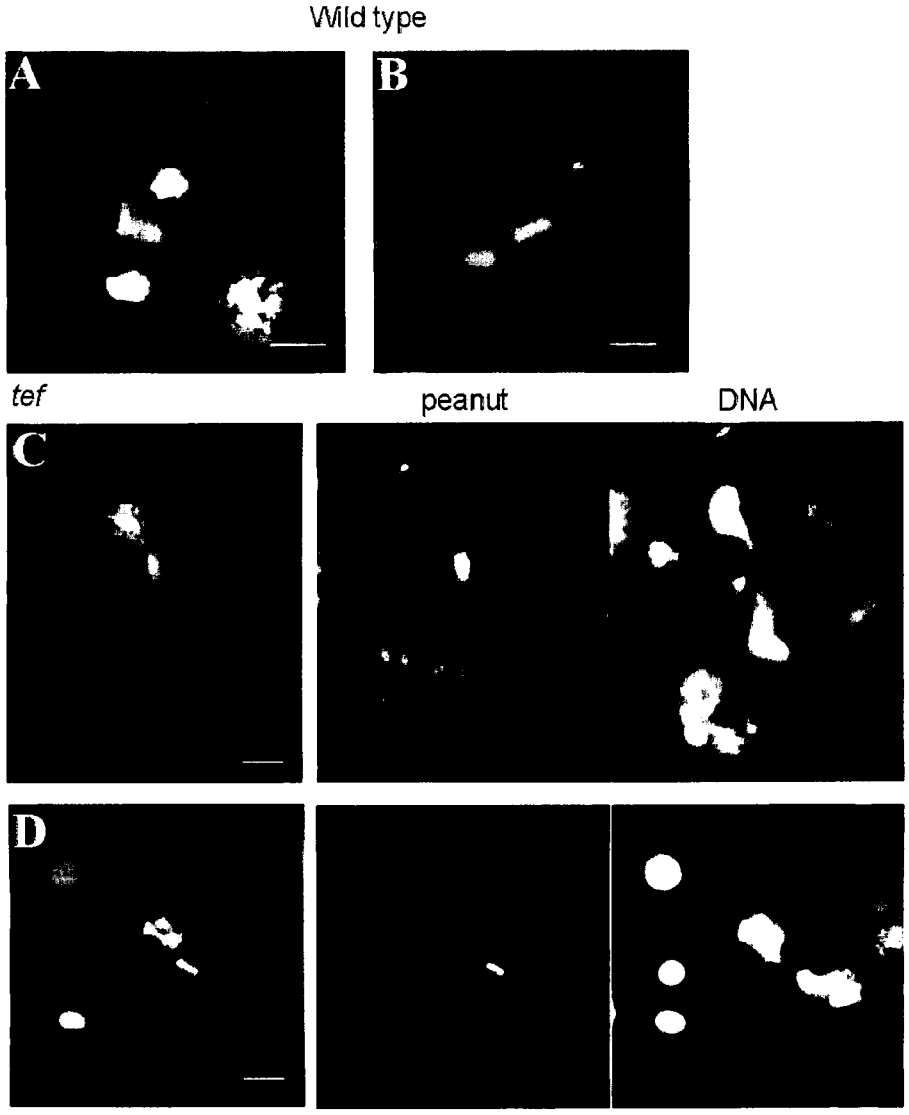

Figure 8: Organisation of the cleavage furrow in *tef* mutant neuroblasts. Immunostaining assays performed in neuroblast squashes using antibodies against the peanut protein. The peanut protein is present at the midbody during cytokinesis. Bar is 10 μm.

3.1.4 Mapping the *tef* locus

3.1.4.1 Meiotic recombination mapping

The *tef* mutant was originally identified in a P element induced mutagenesis screen. *In situ* hybridisation on polytene chromosomes of the mutant strain, showed a single P-element localised at 84A4-5. To determine if this insertion was responsible for the abnormal mitotic phenotype and the late larval lethality, genetic complementation over *Df(3R)Scr* was performed. *tef/Df(3R)Scr* individuals die as pharate adults, and show a similar phenotype as mutants for the proboscepedia (*pb*) gene. The complementation of the mitotic phenotype by the deficiency suggested that the mitotic abnormalities are not associated with the P element insertion.

In order to map the mitotic phenotype and late larval lethality, genetic recombination was performed using a multiple marked chromosome (Fig. 9).

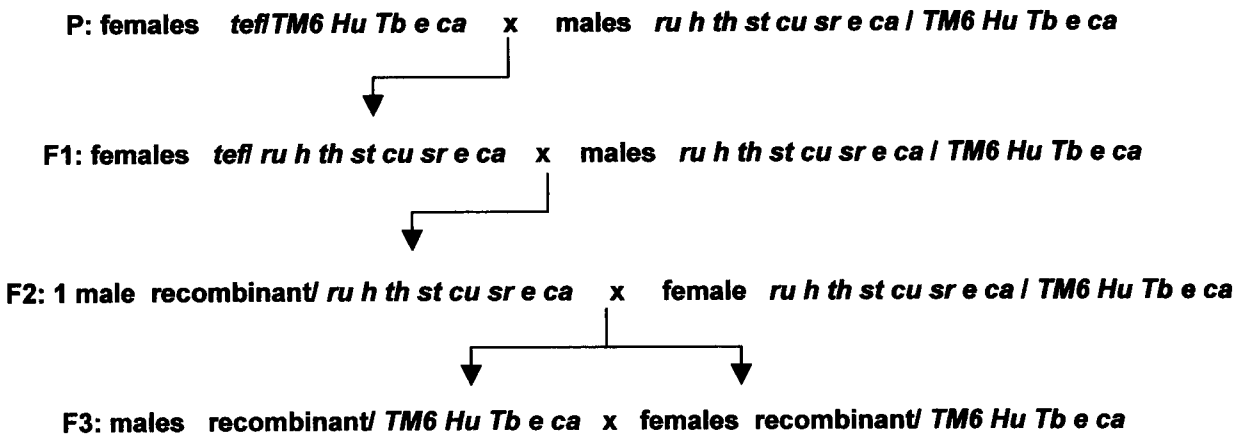

Figure 9: Genetic crosses performed to map the *tef* mutation based on meiotic recombination. In F2, recombinant males harbouring different regions of the *tef* chromosome were selected according to the recessive phenotypes of the *rucuca* chromosome. Stocks were established in F3 (in Joana Perdigão PhD thesis, 1997).

Analysis of different recombinant lines (Fig.10), allowed mapping of the mitotic phenotype and lethality between *cu* and *sr* (86D1-4 to 90D2-F7). The phenotypic analysis reported in this thesis was performed in homozygous individuals of the recombinant line *ru h th st cu tef*. This line displayed the abnormal mitotic phenotype and was associated with third instar larval lethality and did not contain P-element insertions.

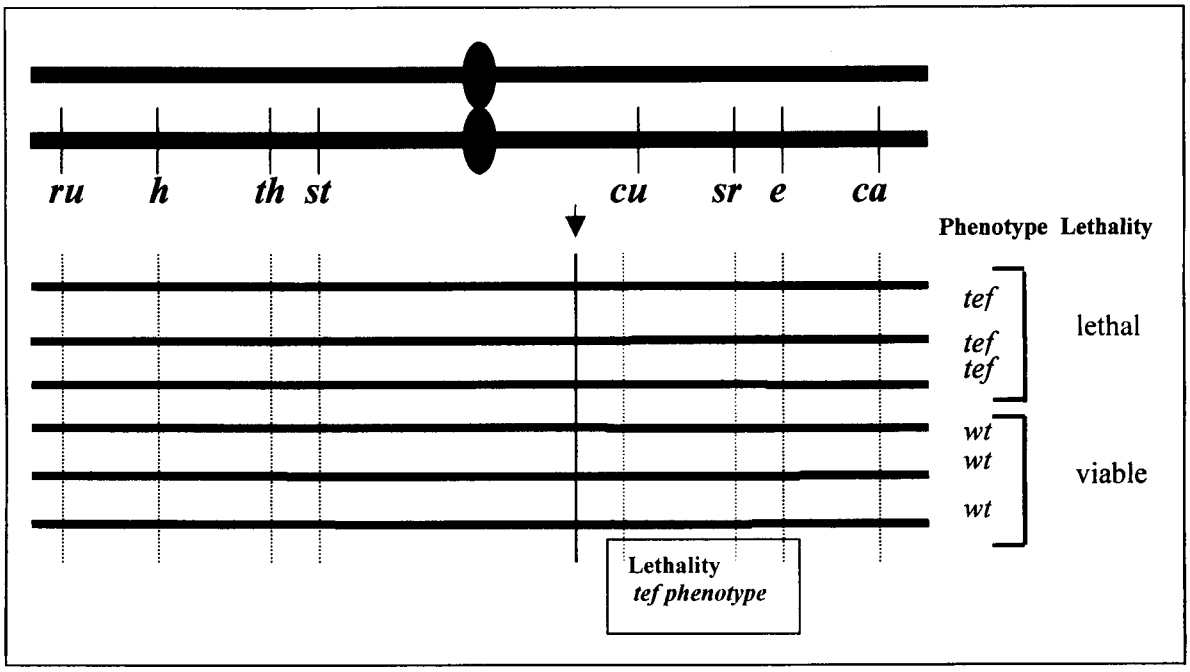

Figure 10: Analysis of the mitotic phenotype and third instar larval lethality of several *tef/rucuca* recombinant lines. Red and black lines represent the *tef* and *rucuca* chromosomes respectively, and circles represent centromeres. The genetic markers (recessive genes) are referred below the *rucuca* chromosome. Recombinant chromosomes are represented with different colours corresponding to both chromosomes. The limit between both colours within two genetic markers is arbitrary. The blue vertical line refers to the P-element insertion. The mitotic phenotypes observed are pointed at the right hand side, in which *tef* corresponds to an abnormal chromosome fusion behaviour and wt to a wild-type phenotype. The viability of these recombinant lines is also referred (adapted from Joana Perdigão, PhD thesis, 1997).

3.1.4.2 Genetic complementation using several deficiency strains mapped between the *cu* and *sr*

To narrow the limits of the cytological region where the *tef* mutation was mapped, several genetic complementation assays were performed with different deficiency strains mapped between the *cu* and *sr* markers (Fig. 11). Taken together the deficiencies cover almost the entire genomic region between those markers. *Df(3R)red31* did not complement the lethality nor the mitotic phenotype observed in homozygous *tef* individuals. These results indicated that the *tef* gene localises between the breakpoints of this deficiency, that is, between 87F12-14 and 88C1-3.

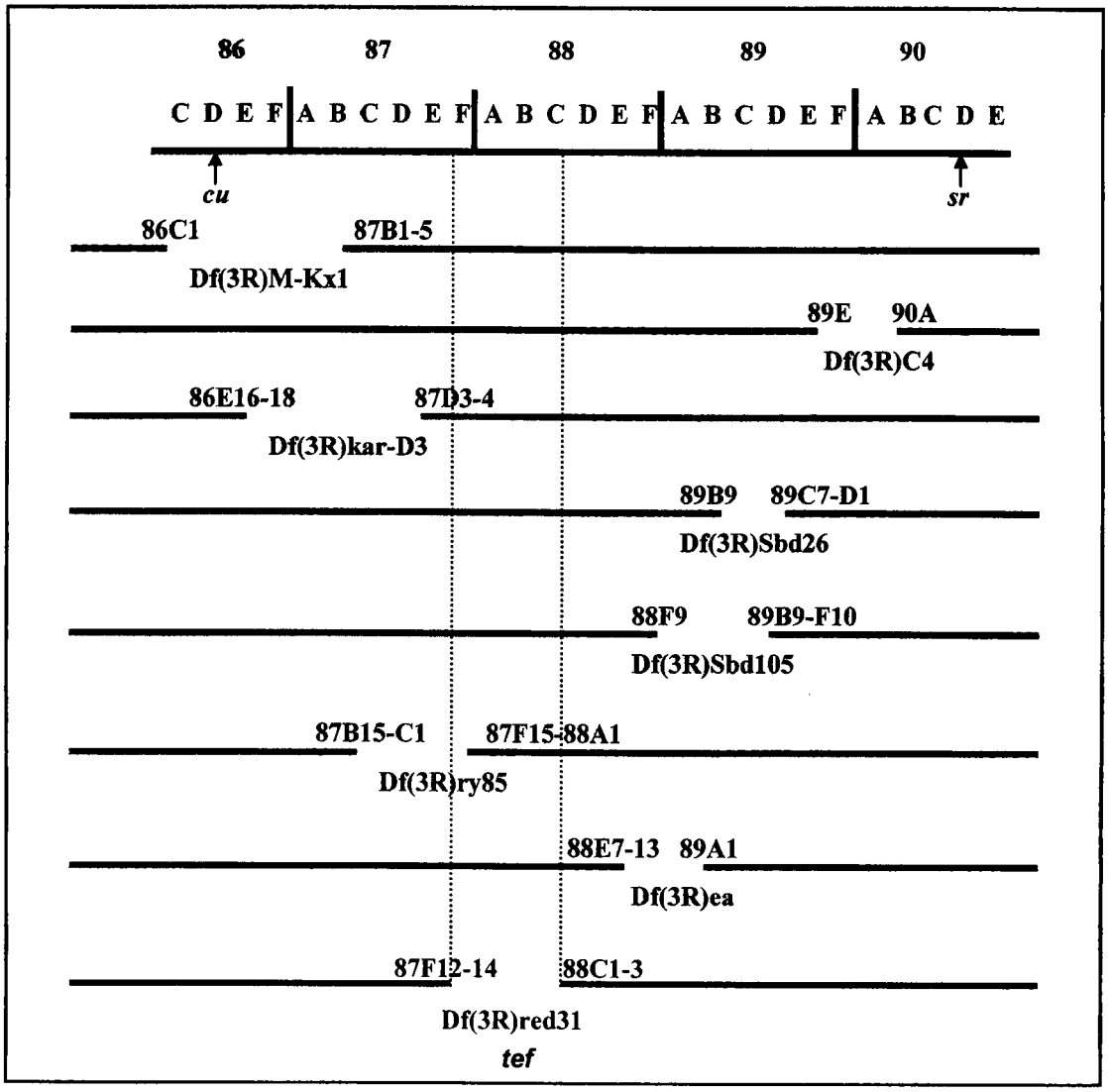

Figure 11: Genetic complementation assays between the *tef* chromosome and several deficiencies mapped within the *cu* and *sr* markers. *Df(3R)red31* (red) was the only deletion that did not complement the mitotic phenotype and the lethality of the *tef* chromosome. The results indicate that the *tef* mutation maps within the breakpoints of *Df(3R)red31*.

Smaller deficiencies localised within the breakpoints of *Df(3R)red31* were also tested. This required careful confirmation of breakpoint sites for each deficiency to ensure that the entire genomic region held between the breakpoints of *Df(3R)red31* was being analysed. Therefore, *in situ* hybridisation with a number of P1 clones was performed to determine the exact limits of each deficiency (Fig. 12).

Analysis of viability and mitotic phenotype of hemizygous individuals *Df/tef* was performed. All of them were viable and did not exhibit abnormal chromosome behaviour. Additionally, hemizygous individuals were fertile. These results allowed us to localise the mutation between the distal breakpoint of *Df(3R)red31* and *Df(3R)su(hw)7*, corresponding to the cytological region 88B5-C4 (Fig.13).

Figure 12: *In situ* hybridisation to *Df(3R)su(Hw)7* using two P1 clones simultaneously (94-46, yellow and 28-52, blue). The 94-46 P1 clone maps within the breakpoints of this deficiency, thus labelling only half of the polytene band corresponding to the loop structure. In contrast, 28-52 maps outside the deleted region, since it labels the entire polytene band.

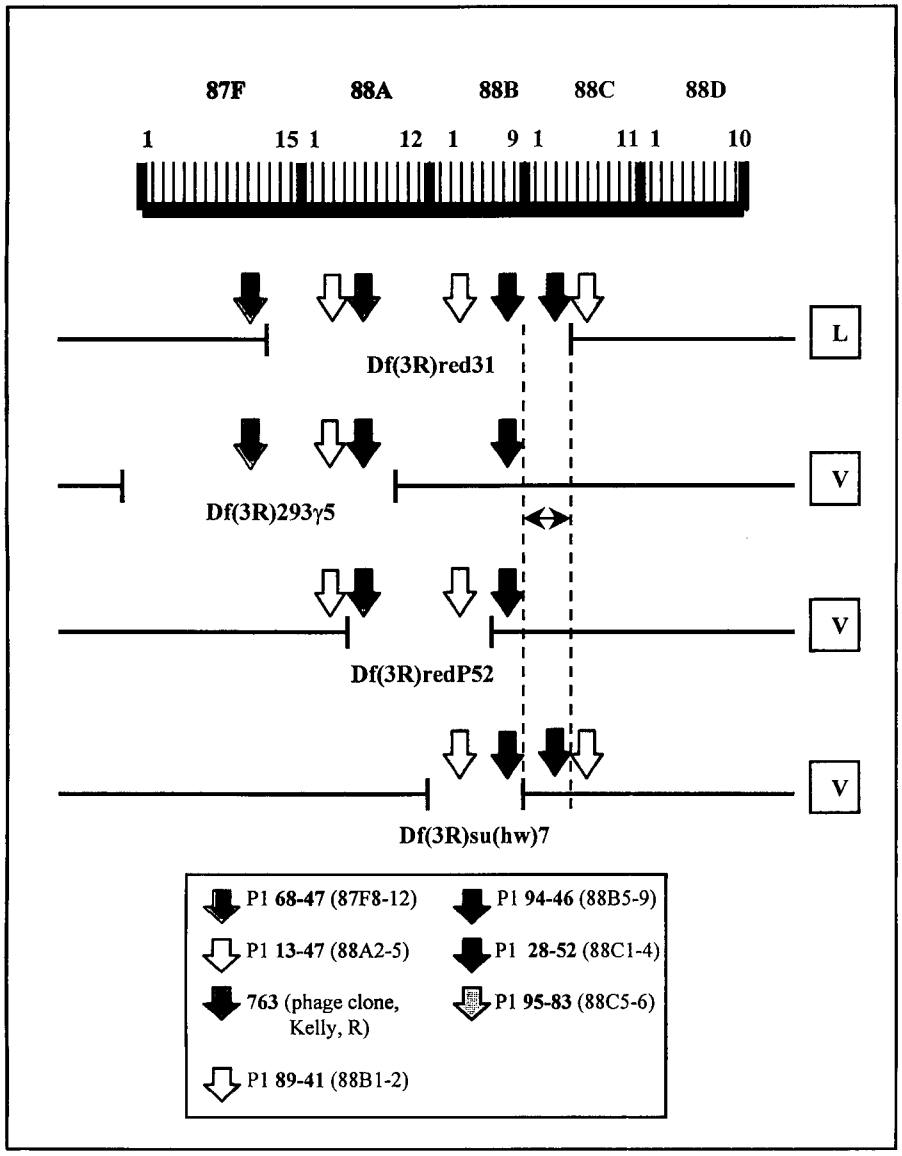

Figure 13: Genetic complementation assays between *tef* and several deficiencies that map within *Df(3R)red31* (L=lethal, showing the same mitotic phenotype as homozygous *tef* cell. V=viable, showing normal mitotic behaviour). *In situ* hybridisation of *+/Df* polytene chromosomes using several P1 clones (see box) was performed in order to confirm overlapping regions between deficiencies. *In situ* localisation of each P1 clone is represented by a distinct patterned arrow in several deficiencies. Taken together, the recombination assays, deficiency mapping and *in situ* hybridisation data, localise *tef* between the distal ends of *Df(3R)su(Hw)7* and *Df(3R)red31* at 88B8-C4.

Since the lethality and mitotic phenotype always segregate together and map to the same cytological region, it is likely that both result of a mutation at a single locus.

Table 2 illustrates the genotype of each deficiency strain used in the genetic complementation assays. *In situ* hybridisation with various P1 clones was performed to precisely determine the breakpoints of some deficiencies.

Table 2: Deficiency strains used in genetic complementation assays. Genotypes and breakpoints are also described. (+) indicates that the deficiency complements both the mitotic phenotype and lethality of the *tef* chromosome, and (–) indicates that the deficiency does neither complement the phenotype nor the lethality of the *tef* chromosome. *(*)* These deficiencies are not represented in figure 13 (♦) Breakpoint limits determined by *in situ* hybridisation of these deficiencies did not match with those indicated in *Drosophila* databases.

Deficiencies	Genotype	Breakpoints	*tef* phenotype Complementation
Df(3R)M-Kx1	Df(3R)M-Kx1/TM3, Sb Ser	86C1; 87B1-5	+
Df(3R)kar-D3	Df(3R)kar-D3 e/cu kar Sb	86E16-18; 87D3-4	+
Df(3R)red31	Df(3R)red31/TM6, Hu Tb e ca	87F12-14; 88C1-3	-
Df(3R)ea	Df(3R)ea ri/TM3 Ser	88E7-13;89A1	+
Df(3R)sbd105	Df(3R)sbd105 sr e/TM6B Hu Tb e ca	88F9; 89A1-B10	+
Df(3R)bd26	Df(3R)sbd26 e/TM2 Ubx e	89B9-10; 89C7-D1	+
Df(3R)C4	Df(3R)C4 p/ Dp(3;3)P5, Sb	89E; 90A	+
Df(3R)urd (*)	Df(3R)urd ru h th st sr e ca /TM3, Sb Ser	87F1; 87F15	+
Df(3R)126C (*)	Df(3R)126C kar/ MKRS, kar ry Sb	87D14-E1; 87F11-12	+
Df(3R)293 γ7 (*)	Df(3R)293 g7/TM6, Hu Tb e ca	88A1; 88A5	+
Df(3R)293γ5	Df(3R)293g5/TM6B, Hu Tb e ca	87E; 88A2-9	+
Df(3R)redP52	Df(3R)redP52 Ubx/TM1, Me Sb	88A5-9; 88B4-5	+
Df(3R)red1(*)	Df(3R)red1/TM1 Me Sb	88A; 88B2-5 (♦)	+
Df(3R)su(Hw)7	Df(3R)su(Hw)7	88B1-2; 88B5-8	+
Df(3R)ry85 (*)	Df(3R)ry85/TM6B, Hu Tb e ca	87B15-C1; 87F15-88A1	+
Df(3R)redP93 (*)	Df(3R)redP93/TM6, Hu Tb e ca	88B1; 88B3-4 (♦)	+
Df(3R)redP1 (*)	Df(3R)redP1/TM6, Hu Tb e ca	88B1; 88B3-4 (♦)	+
Df(3R)redP6	Df(3R)redP6/TM6, Hu Tb e ca	88B1; 88B3-4 (♦)	+

3.1.4.3 Genetic complementation assays between the *tef* mutant and several P-element insertion, inversion or translocation lines

In order to test for eventual transposable element insertions in the *tef* locus, several database stocks from the Bloomington Stock Centre and the Department of Jozsef Attila University, Szeged, Hungary were obtained. Genetic complementation assays were performed with the *tef* mutant and each stock described in Table 3 and 4. *P/tef* individuals were viable and did not show abnormal mitotic phenotype. Accordingly, all P-insertion lines complemented the *tef* mitotic phenotype and the lethality.

Table 3: P-element insertion lines ordered from the Bloomington Stock Centre. Genotypes and P-element insertion genomic sites of *Drosophila* stocks used for genetic complementation assays with the *tef* mutant.

Stock	Genotype	Insertion
P203	Adh[fn6] cn [1]; P{ry[+t7.2]=HBDelta-23}88A,ry[506]	88A
P1091	ry[506] P{ry[+t7.2]=1ArB}A292.2F3	88A-B
P1592	ry[506] P{ry[+t7.2]=PZ}l(3)03477[03477]/TM3 ry[RK] Sb[1]	88A4-5
P2135	y[*] w[*]; P{w[+mC]=lacW}l(3)j1E7 [j1E7]/TM3 Sb	88A4-5
P2136	w[*]; P{w[+mC]=lacW}l(3)s5452 [s5452]/TM6C, Sb[1]	88B1-2
P2137	y[*] w[*]; P{w[+mC]=lacW}l(3)j14A6 [j14A6]/TM6B	88B1-2
P1495	ry[506] P{ry[+t7.2]=PZ}trx[00347]/TM3 ry[RK] Sb[1] Ser[1]	88B1-3
P279	y[1]w[1118]; P{w[+mC]=lacW}l(3)L5340[L5340]/TM3, Ser[1]	88B1-2
P34	mwh[1] red[1] P{hsneo}135 e[1], l(3) *[*]/TM3, Sb[1] Ser[1]	88C
P278	mwh[1] red[1] P{hsneo}l(3)neo41[1] e[1]/TM3, ry[RK]Sb[1] Ser[1]	88C1-10
P1709	ry[506] P{ry[+t7.2]=PZ}l(3)06951[06951]/TM3 ry[RK] Sb[1] Ser[1]	88C1-4
P1745	ry[506] P{ry[+t7.2]=PZ}put[10460]/TM3 ry[RK] Sb[1] Ser[1]	88C9-10
P281	y[1]w[1118]; P{w[+mC]=lacW}l(3)L1231[L1231]/TM3, Ser[1]	88C9-11
P1567	ry[506]P{ry[+t7.2]=PZ}l(3)neo42[02404]/TM3, ry[RK] Sb[1] Ser[1]	88D1-2
P1605	ry[506]P{ry[+t7.2]=PZ}l(3)03719[03719]/TM3, ry[RK] Sb[1] Ser[1]	88D1-2

Table 4: P-element insertion lines ordered from the Szeged Stock Centre. All strains complemented the *tef* phenotype

Stocks:	Insertion
l(3)083710	88C, 93B1-2
l(3)022231	88C, 2R
l(3)026409	85D14-18, 88C
l(3)001620	88C
l(3)094003	88C
l(3)139308	80A, 88B5-9
l(3)105407	88C
l(3)129717	88C
l(3)126201	88C
l(3)086405	88C
l(3)091014	88C
l(3)092708	88C
l(3)020514	88C
l(3)000721	88C
EP(3)3533	88C
EP(3)3074	88C
EP(3)3074	88C
EP(3)3567	88C
EP(3)3711	88C
EP(3)3504	88C

Other genetic approaches using *Drosophila* stocks containing inversions or translocations were also tested (Table 5). Crosses between *tef* and these strains were performed and showed that all of them complemented the mitotic phenotype and the

lethality. These results suggested that none of the breakpoints of these inversions or translocations lead to mutation at the *tef* locus.

Table 5: Stocks harbouring chromosomal rearrangements ordered from the Bloomington Stock Centre. All strains complemented the *tef* phenotype

Stock	Genotype	Breakpoints
1241	In(3LR)252/TM6B	64D3-4;88B
1341	In(3LR)229/TM3, Sb[1]	61F7-62A1;88B
2803	T(Y;3)A173, y[+]/TM6, Ubx[+] e[1]; C(1)RM, y[1]/C(1;Y)1, y[1]	88B
3461	In(3R)iab7[SGA],Abd-B[iab7-SGA]/Ubx[130]	88C;89E
1238	Inv(3LR)273/TM6B	68A;88A
1286	In(3LR)251/TM1	88A5-9; 100C5-D1
3339	T(1;3)OR60/TM3	4B; 88A

3.1.5 Stage of lethality observed in *tef* mutant individuals

In order to determine the lethal period of *tef* mutant individuals, embryos laid by heterozygous adults were collected and the lethal stage determined. Quantification of hatching embryos was performed with crosses between *tef/TM6B* females and *tef/+* males, to avoid *TM6B/TM6B* individuals, which usually die during embryogenesis. The results show that out of 307 embryos 94,5% hatch normally. A similar frequency was obtained for the Oregon-R controls (93% from a sample of 200 embryos). However, the results from crosses between *tef/TM6B* males and females showed that only a small proportion of homozygous mutant third instar larvae/pupae are recovered (5% of 925 embryos). These results suggest that *tef* individuals die mostly during the first and the second instar larvae (~20% out of the 25% expected frequency), and only a few are capable to reach the third instar stage.

3.1.6 Quantification of mitotic parameters in *tef* mutant neuroblasts

Quantitative analysis of mitotic parameters in *tef* homozygous and hemizygous neuroblasts (Table 6) indicates that *tef* causes a reduction in the mitotic index when compared to the wild-type control. Furthermore, there is a reduction in the frequency of anaphases and consequently a higher metaphase/anaphase ratio. A quantitative analysis of abnormal mitotic figures (Table 7) show that the frequency of metaphases

exhibiting fusions is very high (92%). Therefore, most cells that reach mitosis contain one or more chromosomes with fused ends.

Also, in accordance with the frequency of abnormal metaphases, most cells in anaphase (87-95%) display chromatin bridges, indicating that mutant cells are unable to resolve chromosome associations before the metaphase-to-anaphase transition. However, the frequency of polyploid or aneuploid cells is relatively low. A comparison of the data from homozygous and hemizygous mutant cells indicate that *tef* is likely to be a severe hypomorph.

Table 6: Quantification of mitotic parameters in wild-type and *tef* mutant neuroblasts. 7-10 neuroblasts were scored for each genotype. The microscope area was observed under a phase contrast 60x magnification.

	Optical Fields	Mitotic Figures	Prophases N°	%	Metaphases N°	%	Anaphases N°	%	Mitotic Index	Met/Anaph ratio
Oregon	1605	3223	634	19,7	1926	59,7	663	20,6	2,0	2,9
tef/tef	1365	1770	177	10,0	1345	76,0	248	14,0	1,3	5,4
tef/Df(3R)red31	1219	1619	280	17,3	1096	67,7	243	15,0	1,3	4,5

Table 7: Quantification of abnormal mitotic figures in *tef* mutant neuroblasts. 7-10 neuroblasts were scored for each genotype. The microscope area was observed under a phase contrast 60x magnification.

Genotype	Number of metaphases	% Metaphase with fusions	% Poliploid cells	Number of anaphases	% Abnormal anaphases
Oregon	233	0	0	251	0
tef/tef	1345	92,0	1,9	248	87,4
tef/Df(3R)red31	1096	92,3	3,7	243	95,1

3.1.7 Apoptosis in *tef* mutant neuroblasts

Quantitative analysis of mitotic parameters of *tef* mutant neuroblasts shows a reduced mitotic index suggesting that these cells are either delaying progression through interphase or that at some point cells die due to severe chromosome aberrations. Therefore, we isolated *tef* mutant neuroblasts and determined the level of apoptosis using the TUNEL assay. The TUNEL assay adds digoxigenin-nucleotide to

3'-OH ends, which can then be visualised using an antidigoxigenin-Fluorescein conjugated antibody. The results (Fig.15) indicate that *tef* mutant neuroblasts display significantly more TUNEL positive cells than the wild-type control.

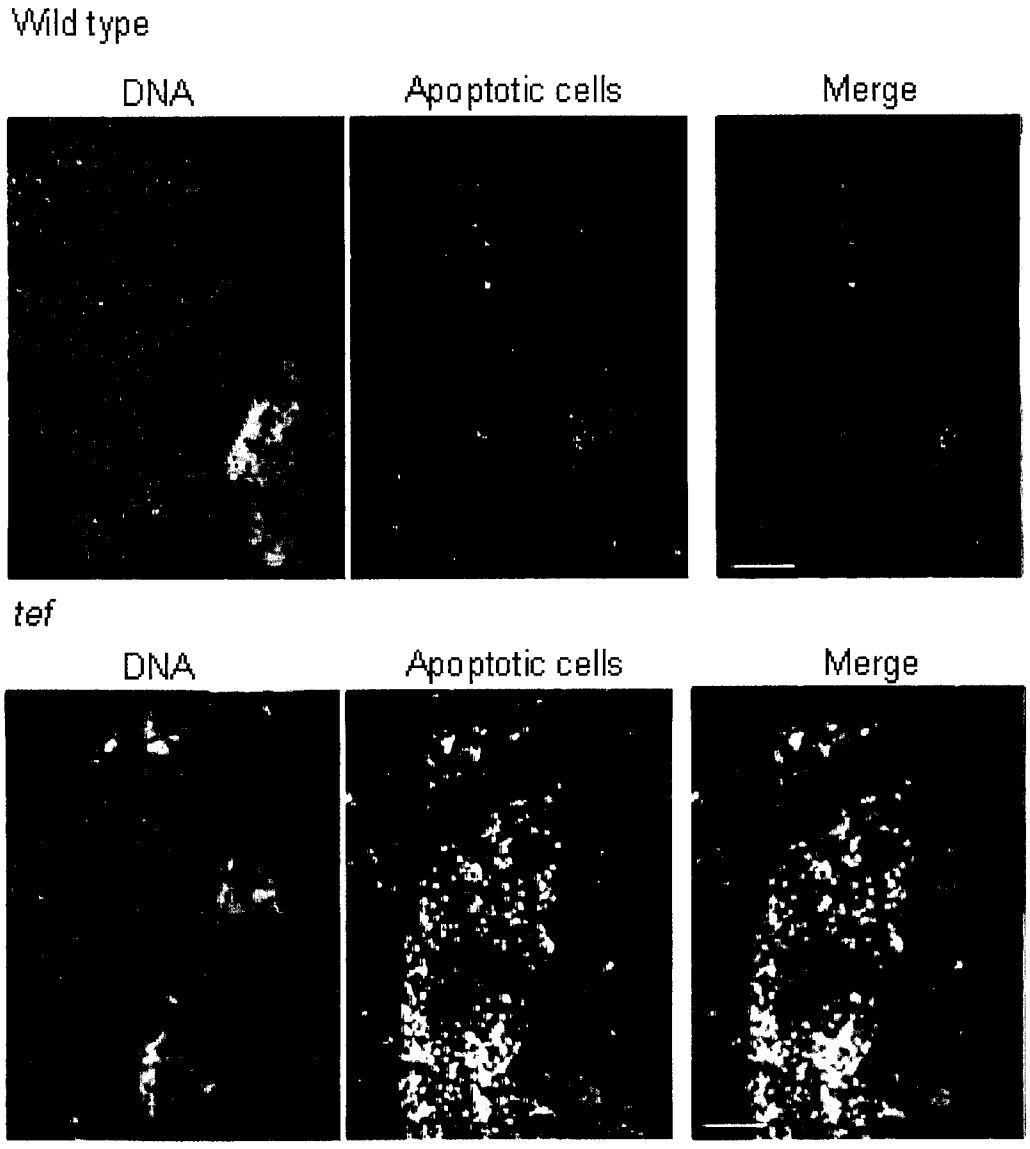

Figure 14: *tef* mutant neuroblasts show significant levels of apoptosis. Wild-type and *tef* mutant neuroblasts were isolated and tested for the presence of TUNEL positive cells as indication of apoptotic cells. DNA was labelled with propidium iodide (red and TUNEL positive cells with FITC (green) in the merged images. Bar is 100μm.

3.1.8 DNA repair in *tef* mutant neuroblasts

In order to test the ability of mutant cells to respond to DNA damage, embryos laid by either wild-type or *tef/TM6 B Tb, e* individuals were irradiated and the survival frequency determined, taking into consideration the number of homozygous mutant individuals that survive to reach the third instar larval or the pupal stage. *mus101* mutant embryos were used as control since this strain exhibits hypersensitivity to chemical mutagens and γ-radiation, due to a deficient post-replication repair pathway (Boyd and Setlow, 1976). The results (Table 8) show that DNA damage caused by 500 rads of γ-radiation was not able to induce a decrease in the viability of either the wild-type control or *tef*, but induced a significant decrease (10 fold) in the survival of *mus 101* individuals. Increasing the dose of γ-irradiation (1200, 2400 rads) decreases the viability of *tef* but also that of the wild-type strains. This suggests that DNA damage caused by an equivalent dose of gamma radiation is more efficiently repaired in either wild-type or *tef* mutant than in *mus101* homozygotes. Furthermore, *tef* mutant cells survive better than wild-type cells to higher doses of radiation. The ability of *tef* mutant cells to survive radiation-induced DNA damage, suggests the existence of a functional DNA-damage checkpoint.

Table 8: Survival of wild-type and mutant individuals after irradiation

		Control	500 rads	1200 rads	2400 rads
Oregon	**N° Embryos**	196	188	187	218
	% Larvae	88	89	13,3	0
Tef	**N° Embryos**	925	791	382	166
	% Homoz. 3rd Instar Larvae	5	4,7	2,4	0
Mus101	**N° Embryos**	256	149	250	59
	% Larvae	50,4	5,4	1	0

3.1.9 Analysis of *tef* checkpoint controls during the cell cycle

In order to evaluate whether the *tef* mutation alters the response to different cell cycle checkpoints, mutant homozygous neuroblasts were challenged with either microtubule depolymerising or DNA damaging agents and the mitotic parameters ascertained.

To determine whether *tef* mutant cells respond normally to the spindle checkpoint, neuroblasts were incubated with colchicine and the frequency of cells in which sister chromatids undergo separation was determined. The results indicate that after 30 minutes incubation, most wild-type (77%, out of 352 cells) or mutant (83%, out of 201 cells) cells in mitosis do not proceed to anaphase. These results indicate that the mutation does not cause any significant alteration to the spindle checkpoint.

It has already been shown above that the low mitotic index in mutant neuroblasts could in part be due to apoptosis, however, one cannot exclude the possibility that cells may take longer to progress through interphase due to the DNA-damage checkpoint being activated. The activation of the DNA damage checkpoint was assessed by exposing mutant or wild-type larvae to γ-radiation (500 rads) and after various time intervals, dissected and the whole brain incubated in colchicine for 30 minutes prior to fixation (Fig.15).

The results show that the mitotic index of wild-type cells decreases 5-fold between 15 minutes (time from irradiation to incubation in colchicine) and 55 minutes (time from irradiation to fixation). The rapid decrease in the mitotic index is likely to reflect an arrest caused by activation of the DNA damage checkpoint during late S or G2 (Hari *et al.*, 1995). However, the *tef* mutant neuroblasts were unable to respond efficiently to DNA damage when compared to the wild-type controls. Mutant cells show a modest 1,5-fold decrease in the mitotic index. Increasing the time between irradiation and the beginning of colchicine incubation, shows that control cells start to recover from the arrest caused by DNA damage. Wild-type neuroblasts show an increase in the mitotic index (1,7-fold) after 30-70 minutes and after 90-130 minutes the mitotic index increases 2,7-fold. This is in agreement with previous studies (Hari *et al.*, 1995). However, *tef* mutant neuroblasts do not show a significant increase in the mitotic index even after 120-160 minutes between irradiation and colchicine incubation. Increasing the dose of radiation induces a more severe mitotic arrest and gives qualitatively similar results (Fig. 16).

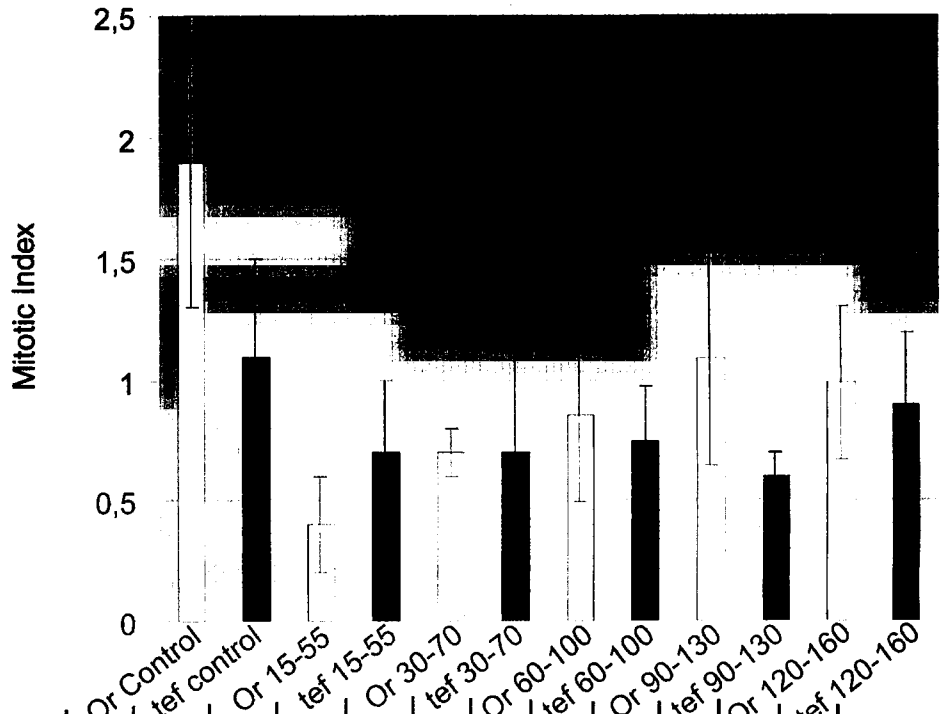

Optical Fields	964	495	605	521	961	609	781	399	412	346	487	360
Mitotic Figures	1793	543	250	380	697	409	663	298	448	193	480	314
Mitotic Index	1.9	1.1	0.4	0.7	0.7	0.7	0.8	0.7	1.1	0.6	1.0	0.9

Figure 15: Detection of DNA damage inducible checkpoint in wild-type and *tef* mutant neuroblasts. Third instar larvae were selected, irradiated with 500 rads and allowed to recover for different periods of time before dissection and incubation in colchicine prior to fixation. Each data point is labelled with a time range. The lower limit is the time from irradiation to addition of colchicine and the upper limit is the total time from irradiation to fixation (including the 30 minutes of colchicine incubation and 10 minutes in a hypotonic solution). Primary data are shown below. 7-10 brains were analysed for each case. The mitotic index was determined by calculating the mean of the mitotic indexes of the total number of brains analysed. The standard deviations are shown on the graphic.

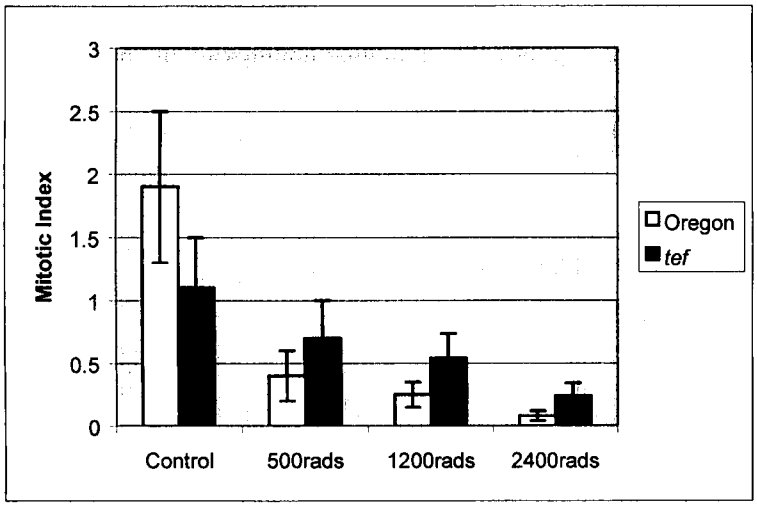

Figure 16: Mitotic index at the time 15-55 minutes, with several doses of γ-radiation. 7-10 brains were analysed for each case. The mitotic index was determined by calculating the mean of the mitotic indexes of the total number of brains analysed.

3.1.10 Quantification of acentric metaphase fragments

There are two possible interpretations for the *tef* mutant chromosome fusions. One could be the existence of extensive mitotic recombination and another the end-to-end fusion hypothesis. Aiming to test this, *in situ* hybridisation with the *Hoppel* transposable element (Coelho et al, 1998), which labels the pericentromeric region of all chromosomes was performed, in order to screen for the appearance of acentric fragments (Fig.17). Although newly formed fragments are thought to be lost during the following cell divisions, it would be likely that, at least a portion of metaphase cells, would harbour these acentric fragments. Out of 200 metaphases analysed, only two contained such fragments (which did not hybridise at all with the *Hoppel* transposable element), suggesting that mitotic recombination is not likely to be the most responsible for the end-to-end chromosome associations observed in *tef* mutant cells.

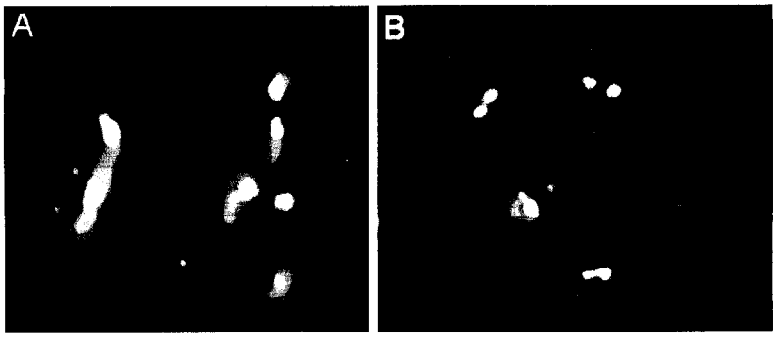

Figure 17: *In situ* hybridisation of *tef* mutant neuroblasts with the *Hoppel* transposable element (green). (A) shows the most abundant type of metaphases, where no acentric fragments were detected. (B) shows two possible acentric fragments (arrows).

3.1.11 Behaviour of chromosomes lacking normal telomere ends in a *tef* mutant background

The data presented so far suggest that the *tef* mutation causes end-to-end chromosome fusions and also that these are unlikely to be the result of a defective DNA repair response. It is therefore reasonable to suppose that the chromosome attachments observed might be mediated by unprotected telomeric ends. In order to test this hypothesis we have quantified the frequency of attachments of a ring chromosome in a *tef* mutant background. We constructed a strain carrying *tef* and a X chromosome (R(1)2) that has a ring conformation and therefore bears no exposed

ends (*In[1] w[vc]/y[1]w[1]/Dp(1;Y)y[+]; tef e/TM6B*) (Fig. 18). Additionally it is deficient for the telomeric region 1A3-A4.

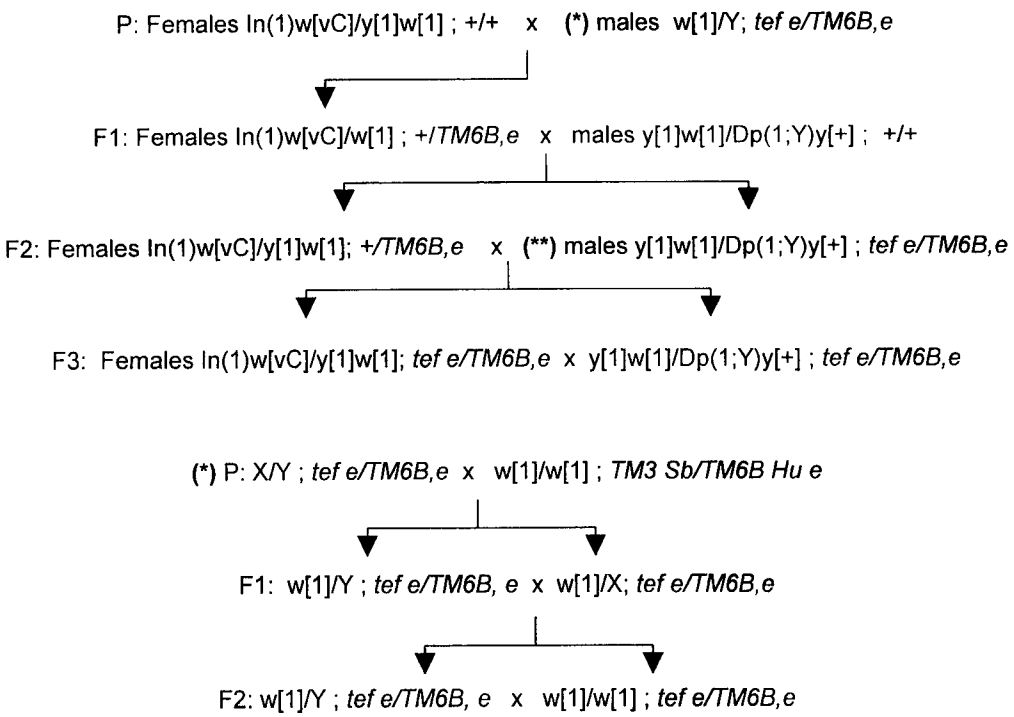

Figure 18: Cross strategy to insert the ring chromosome into the *tef* genetic background.

Third instar neuroblasts from *tef* homozygous larvae carrying R(1)2 were hybridised with a pericentromeric probe specific for the X-chromosome. As a control, the behaviour of a normal X chromosome in the *tef* stock was also assessed. Analysis of the R(1)2 chromosome indicates that there are three types of conformations observed (Fig.19). Cells in which the ring chromosome appeared unaffected (Fig.19A), cells in which the ring chromosome was clearly fused to another chromosome (Fig.19B) and cells in which the conformation of the ring chromosome could not be clearly determined (Fig.19C). The quantification of the data (Fig.19D) shows that in a *tef* mutant background, the normal X chromosome shows end-to-end associations in 28% of cells and no ambiguous conformations was detected. However, in the R(1)2;

tef/tef cells clear fusions involving the ring chromosome were very rarely observed (3%) and ambiguous ring conformation was detected in 10% of cells. The frequency of ambiguous fusions involving the ring chromosome in a wild-type background, was equivalent to those found in the *tef* background (around 11%). These results suggest that the ring chromosome appears to be protected from association to other chromosomes probably due to the absence of exposed ends that are most likely required for end-to-end fusion.

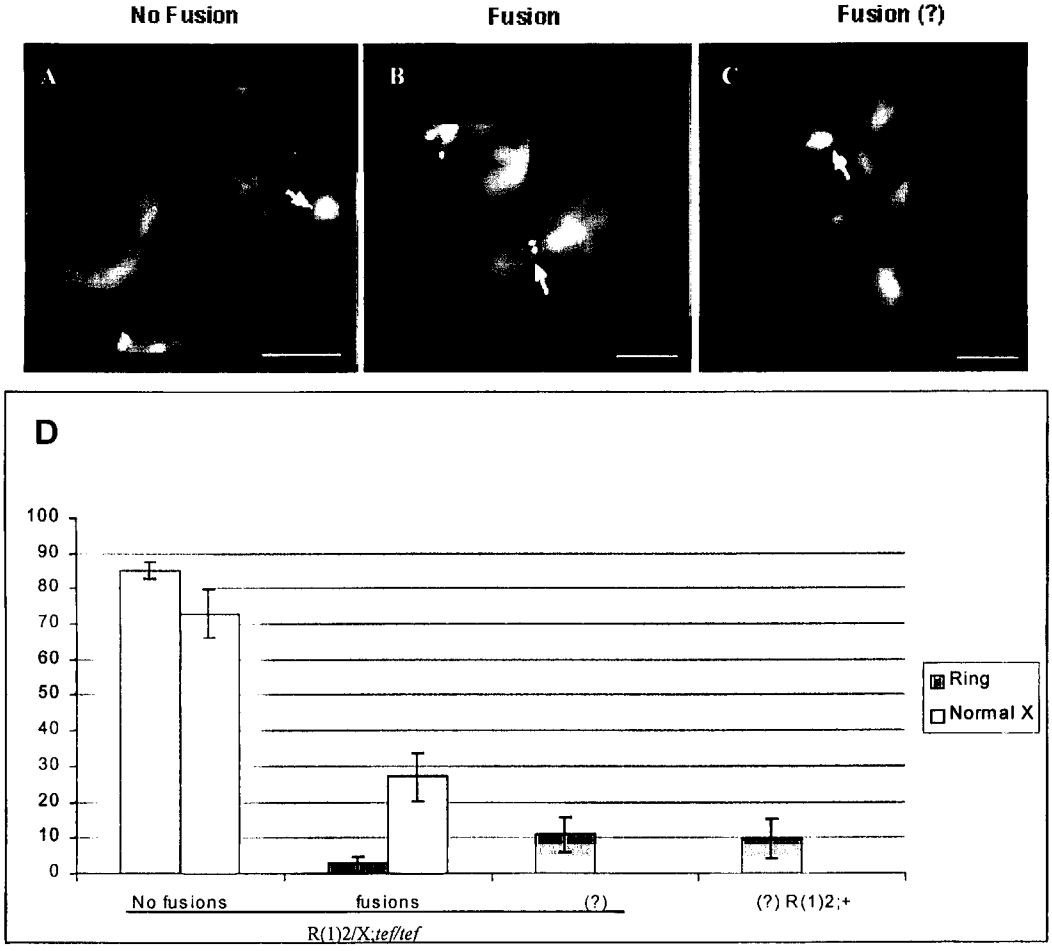

Figure 19: Quantification of fusions of a ring-X chromosome (R(1)2) that does not contain free telomeres in a *tef* mutant background. The frequencies of fusions involving the R(1)2 and the normal X chromosome, in a *tef* background were quantified from fixed preparations hybridised with subtelomeric X-chromosome specific DNA sequence (shown in green). DNA was stained with propidium iodide (red). Three different patterns were observed. The arrows indicate the ring X chromosome and the subtelomeric *in situ* hybridisation signal. (A) Cells in which the R(1)2 chromosomes did not show any kind of association, (B) cells in which the R(1)2 chromosome was fused to other chromosomes and (C) cells in which a fusion event could not be clearly classified. In all preparations the normal X chromosome behaviour was also scored and the quantification of the data is shown in panel (D). The behaviour of the R(1)2 chromosome was scored out of 229 metaphases from 7 brains. The frequency of unclear fusions involving the ring chromosome in a wild-type background (R(1)2;+) was calculated as a control. Bar is 10 μm.

These results are supported by quantification assays of anaphase bridges harbouring the ring chromosome (Table 9), performed in mitotic cells hybridised with a subtelomeric probe for the X chromosome. Anaphase figures that did not involve fusions of the ring chromosome were present in 89,6% of the cases analysed (sum of frequencies (a) and (d) in table 8). This frequency is equivalent to that in figure 19D (86%). The frequency of anaphase bridges clearly involving the ring chromosome was 4,5%, similar to the 3% obtained in metaphase analysis. Unclear anaphase figures were present in 7.3% of the cases analysed. Figure 20 shows an example of each type of anaphase involving DNA bridges quantified in this study.

Table 9: Quantification of anaphase DNA bridges harbouring X ring chromosome. StDev stands for standard deviation

Total nº of anaphases=41	Frequency	StDev
DNA bridge with no ring chromosome (a)	57,5	**9,6**
DNA bridge involving the ring chromosome (b)	4,5	**5,9**
Not classified (c)	**7,3**	**8,6**
Normal anaphases (d)	32,1	6,3

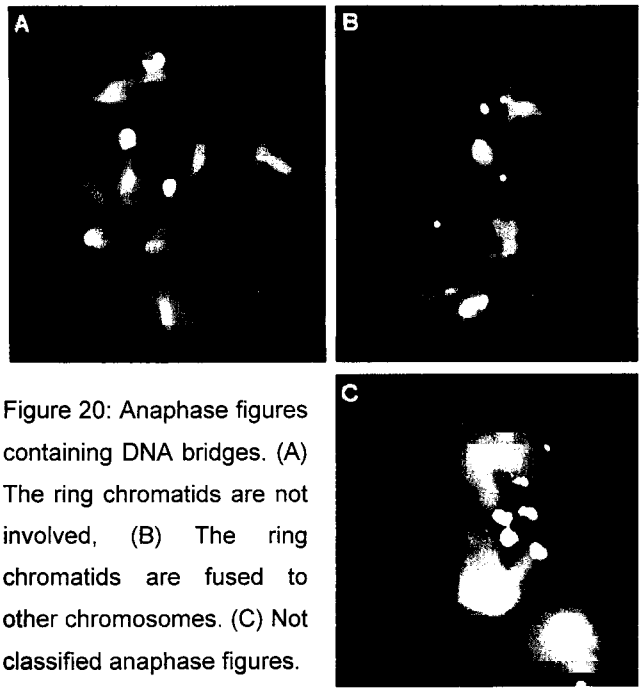

Figure 20: Anaphase figures containing DNA bridges. (A) The ring chromatids are not involved, (B) The ring chromatids are fused to other chromosomes. (C) Not classified anaphase figures.

3.1.12 Localisation of HP1 in *tef* polytene chromosomes

The previous sections indicate that the end-to-end fusions observed in *tef* mutant neuroblasts required exposed ends. Since it has been shown in *Drosophila* that the HP1 protein localises to the telomeres and that mutations cause end-to-end fusions (Fanti *et al.*, 1998), we carried out immunostaining for HP1 on polytene chromosomes isolated from *tef* mutant larvae. The results show that HP1 localises to telomeres in *tef* mutant cells, just like in wild-type cells (Fig. 21).

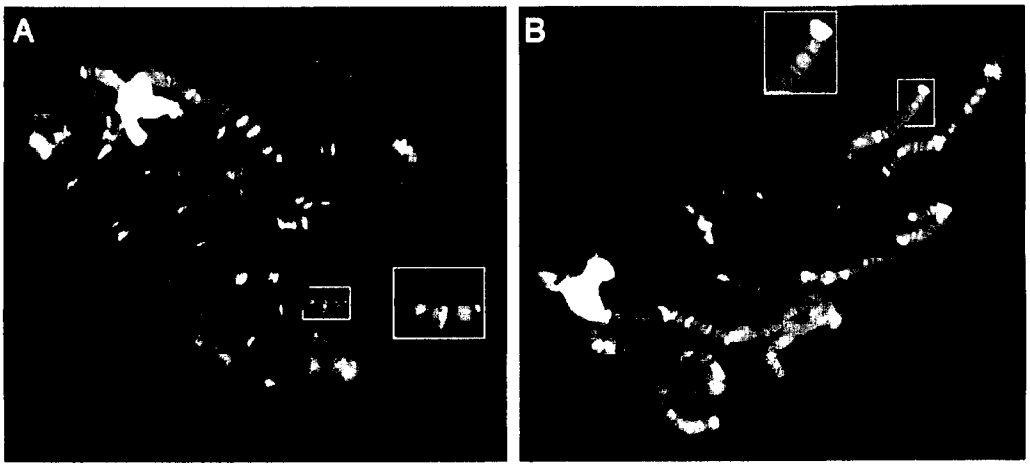

Figure 21: HP1 immunolocalisation to wild-type and *tef* mutant polytene chromosomes. Note that immunostaining signal is somehow not uniformly intense in all wild-type or *tef* chromosomes. In fact a variability of this intensity was observed in different chromosomes of the same neuroblast.

3.1.13 Analysis of spermatogenesis in *tef* mutant individuals

All data presented thus far indicate that the *tef* mutation causes significant alterations during chromosome segregation. In order to determine whether this locus is also required for male meiosis we have analysed spermatogenesis in testes isolated from third instar *tef* mutant larvae. The results indicate that chromosome fusions can be found at all stages of spermatogenesis (Fig.22). We observed cells at different stages of spermatogenesis that contain unresolved chromatin bridges (Fig.22B,D,F,J). Also, we found cells that contain fully formed spindles but either do not contain detectable chromatin, or the karyosome is completely misplaced between 2 spindles (Fig.22D,F). Evidence for chromosome missegregation was also obtained. Phase contrast microscopy of live *tef* testes shows late spermatids at the onion stage containing multiple nuclei associated with a single Nebenkern (Fig. 22H). Nevertheless, complete cysts of onion stage spermatids were found containing 64 cells. At later stages of sperm differentiation, during sperm head elongation, *tef* mutant cells are generally disorganised and sperm heads appear to be interconnected by thin chromatin bridges (Fig. 22J).

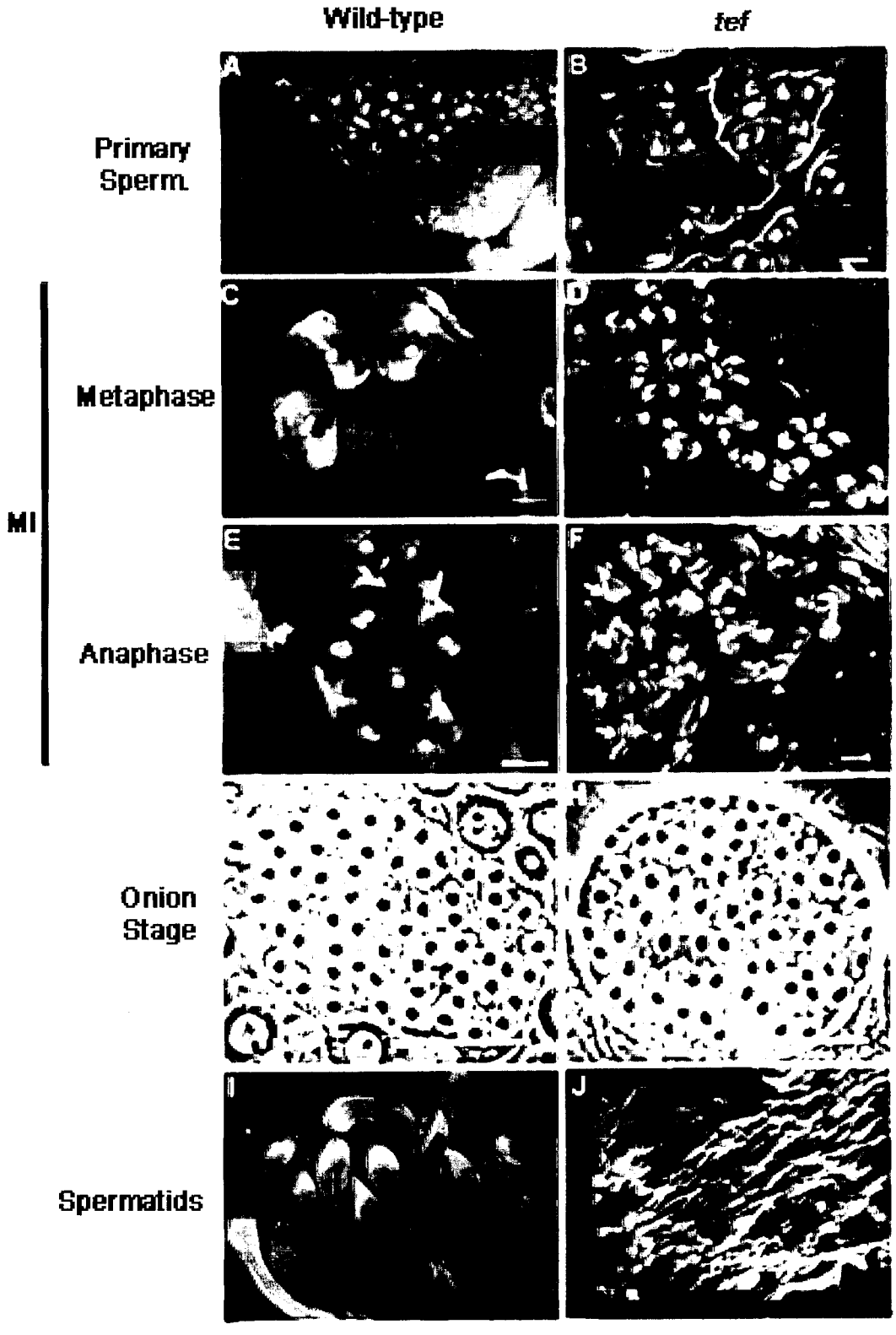

Figure 22: Spermatogenesis in wild-type and *tef* mutant testes are shown. Different stages of spermatogenesis from wild-type (A,C,E,G and I) and *tef* cells (B,D,F,H and J) are shown. Wild-type (A,C,E,I) and mutant cells (B,D,F,J) were stained with propidium iodide to visualise the DNA (red) and with an anti-α-tubulin antibody to visualise microtubules (green). Bar is 10 µm.

3.2. Molecular and genetic approaches to clone the *tef* gene

3.2 Molecular and genetic approaches to clone the *tef* gene

3.2.1 Detection of P-element sequences in the *tef* mutant

In situ hybridisation with P-element probes performed on *tef* polytene chromosomes showed that it contained a unique hybridisation signal at division 84A4-5. Subsequently genetic analysis demonstrated that the P-element insertion was not responsible either for the *tef* mitotic phenotype or the lethality.

These results were confirmed by southern blot analysis. For this genomic DNA from wild-type, the original *tef* mutant and two different recombinant *tef* mutant single flies was extracted, and digested with several restriction enzymes. Wild-type controls included, not only a homozygous Oregon R but also a *TM6B* balanced Oregon R fly, since *tef* genomic DNA was extracted from balanced heterozygous flies. A 7 kb *Sal*I *rosy* fragment was used as a probe for P-element insertions.

Analysis of the southern results (Fig. 23) indicated that the recombinant *ru h th st cu tef*, was identical to the wild-type controls. This recombinant line does not contain the P-element inserted at division 84 of polytene chromosomes. Therefore it is very unlikely that a second P-element insertion is responsible for the *tef* mutation. Accordingly, molecular methods were used to characterise the genomic region previously described by complementation with deletions.

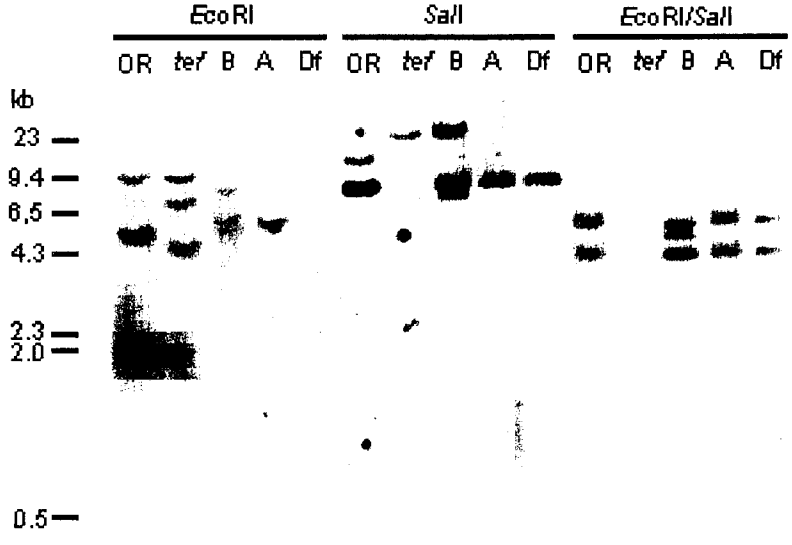

Figure 23: Southern blot hybridisation using a *Sal* I/ *Sal* I rosy DNA fragment (~7 kb). Each lane consists of digested genomic DNA extracted from a single fly. Two lanes did not hybridise. (Or) Oregon (wild-type); (B) recombinant *tef sr e ca/TM6B* (A) recombinant *ru h th st cu tef/TM6B*; (Df) *Df(3R)red31/TM6B* used as a control for the *TM6B* balancer.

3.2.2 Molecular characterisation of genomic regions near the *tef* locus

3.2.2.1 Chromosome walk strategy

The first molecular approach to obtain new clones progressively closer to the 88B8-C4 genomic region was carried out using the 94-46 P1 clone (Fig. 14).

The 94-46 P1clone was mapped by *in situ* hybridisation to be localised, within *Df(3R)su(Hw)7*. From the collection of P1 clones, this was the closest to localise near the 88B8-C4 cytological region. Since a P1 clone contains very large genomic inserts (80-100 Kb), it was essential to determine the orientation of the P1 clone, before starting the chromosome walking assay. Orientation of the P1 clone was determined by performing linear PCR with primers for the T7 and SP6 sites located within the P1 vector at either side of the cloned fragment.

Table 10: PCR reaction conditions tested to amplify genomic DNA sequences adjacent to the SP6 primer in the 94-46 P1 clone

	94-46	SP6	V(buffer10x)	dATP	dCTP	dGTP	dTTP	dUTP-Biotin	Taq	Vtotal
PCR1	200ng	34 pmol	10µl	200µM	200µM	200µM	100µM	100µM	0.5	100 µl
PCR2	600ng	34 pmol	10µl	200µM	200µM	200µM	100µM	100µM	0.5	100 µl
	94-46	**T7**	**V(buffer10x)**	**dATP**	**dCTP**	**dGTP**	**dTTP**	**dUTP-Biotin**	**taq**	**Vtotal**
PCR1	200ng	40 pmol	10µl	200µM	200µM	200µM	100µM	100µM	0.5	100 µl
PCR2	600ng	60 pmol	10µl	200µM	200µM	200µM	100µM	100µM	0.5	100 µl

Two different labelling reactions were tested with both primers (Table 10). *In situ* hybridisation was performed with each of the PCR products and the 94-46 P1 clone simultaneously, directly labelled with dCTP-Fluorescein. PCR was performed by denaturing the reaction at 94°C for 5 min, followed by 35 cycles, which started with denaturation at 94°C for 30 seconds, annealing at 43°C for 30 seconds, and extension at 72°C for 1 minute. A final 5 minutes extension was performed. Previous studies (Innis *et al.*, 1988) showed that *Taq* polymerase extension reactions at 72°C, incorporated 35-100 nucleotides per second. As mentioned already, for synthesising the *in situ* hybridisation probes, PCR extension reactions were performed for 1 minute (corresponding roughly to 1 kb). Probes were not denatured before application on chromosome preparations since PCR products were already single stranded. Therefore the 2x hybridisation solution was denatured separately. Detection of PCR

product hybridisation site was made possible by incubating slides with Avidin conjugated with Cy5. As shown in figure 24, the genomic region adjacent to the T7 primer in the 94-46 P1 clone is located closer to the 88B8-C4 cytological region, compared to the PCR product using the SP6 primer. Accordingly, the PCR product amplified with the T7 primer was used as a starting probe for a chromosome walking strategy. This probe was used to screen a genomic library

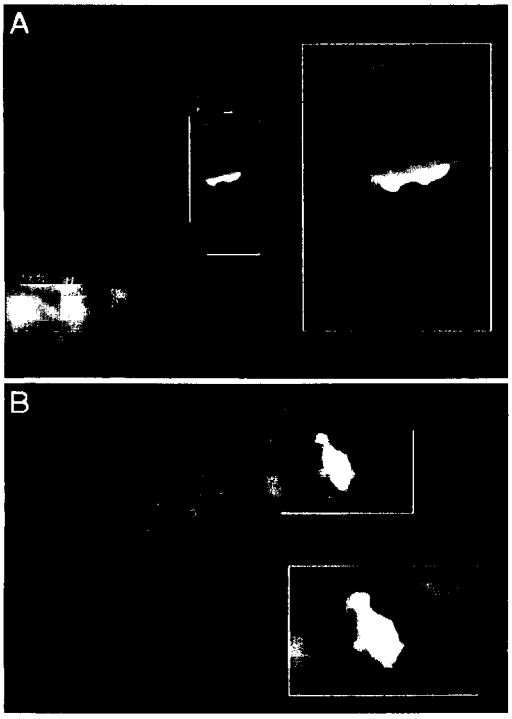

Figure 24: *In situ* hybridisation of wild-type polytene chromosomes using labelled PCR products (blue) and 94-46 P1 clone (green). (A) Double *in situ* hybridisation with PCR product amplified with SP6 primer and the 94-46 P1 clone. (B) Double *in situ* hybridisation with PCR product amplified with T7 primer and the 94-46 P1 clone.

Screening of a genomic λdash library was performed initially with 400.000 phage plaques, using a ^{32}P-labelled PCR reaction product. The labelling reaction was executed by adding the T7 primer and a mixture of dNTPs, which also included the α[^{32}P]-dCTP (Table 11). PCR reaction conditions were the same as described above for the *in situ* hybridisation assay.

Table 11: PCR reaction conditions used to amplify and label genomic sequences adjacent to the T7 primer with α[32P]-dCTP. PCR product was used to screen a genomic library.

	94-46	SP6	V(buffer10x)	dATP	dTTP	dGTP	dCTP	α[32P]-dCTP	taq	Vtotal
PCR1	800ng	60 pmol	10 µl	200µM	200µM	200µM	50µM	150µM	0,5	100 µl

At the end of the third screening a total of eight-isolated phage plaques were grown and used to extract phage DNA. *In situ* hybridisation to hemizygous polytene chromosomes *+/Df(3R)su(Hw)7* was performed. The genomic clones were labelled

using the Bionick (Gibco BRL) and then detected with Avidin conjugated with fluorescein. It was shown that four of the genomic clones mapped within *Df(3R)su(Hw)7* and closer to the 88C cytological region when co-localised with the 94-46 P1 previously labelled directly with dCTP-Cy5.

The chromosome walking strategy was not continued, since the *Drosophila* Genome Project reported a new P1 clone, 28-52 that was shown to localise between the distal breakpoints of *Df(3R)su(Hw)7* and *Df(3R)red3,* and was thus used for subsequent molecular characterisation.

3.2.2.2 Southern blot analysis of wild-type and *tef* genomic DNA within the 88B5-C4 region

As described previously, P1 clone 28-52 mapped within the limits that defined the possible locus of the *tef* gene (88B5-C4 cytological region). As shown in figure 25 a rough calculation of the DNA length estimated for that region was performed and thought to be around 100 kb. P1 clones are known to harbour 80-100 kb genomic inserts, therefore a molecular approach to characterise the DNA within the 28-52 clone was started.

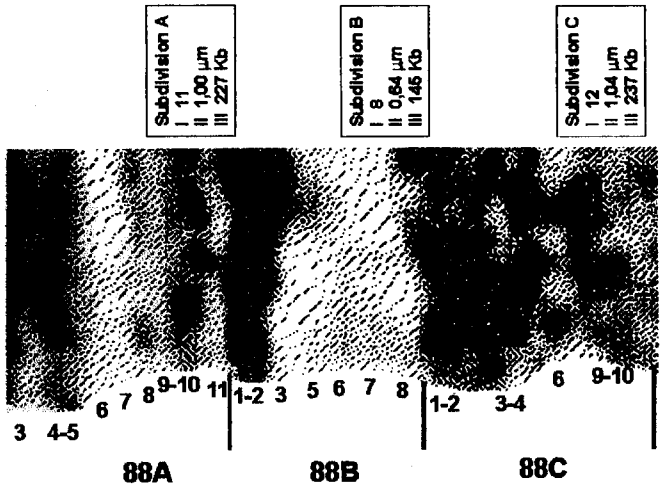

Figure 25: Subdivisions within the genomic 88A-88C cytological region and number of segments (I), DNA length (II) and DNA size (III) (in Heino *et al*, 1994)

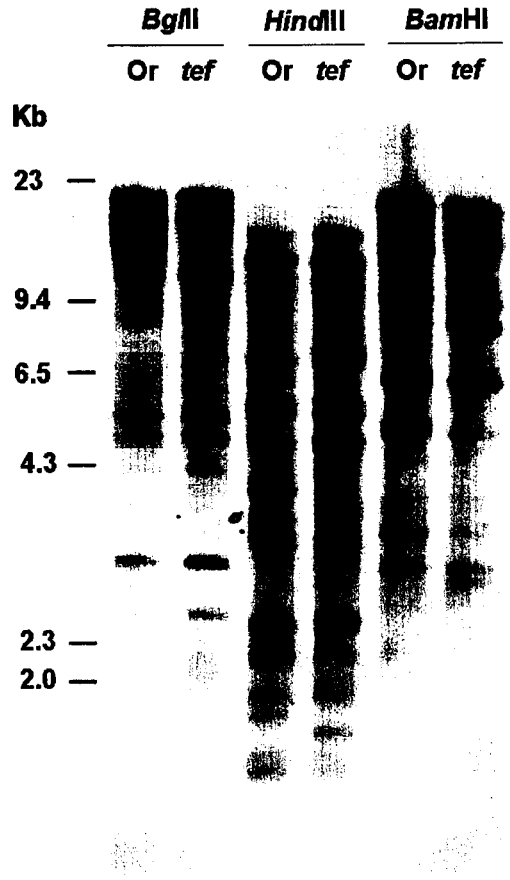

Figure 26: Southern blot hybridisation of Wild-type (Or) and *tef* genomic DNA using the 28-52 P1 clone as a probe. Genomic DNA was obtained from third instar larvae salivary glands and digested with *Bgl*II, *Hind*III and *Bam*HI.

Wild-type and *tef* genomic DNA were digested with several restriction enzymes and a Southern blot was performed using the clone 28-52 as a probe (Fig. 26).

The southern shows that the enzyme restriction pattern revealed by using the P1 clone as a probe, is not identical between wild type and *tef* mutant strains. Digestion with at least three restriction enzymes gives rise to different size bands in wild-type and the *tef* mutant. The results suggest that during the original mutagenesis screen a P-element excised from the *tef* locus in an imperfect manner, either deleting a genomic portion or leaving additional sequences, eventually interrupting the gene and thus modifying the original genomic restriction pattern. The southern hybridisation pattern using the P1 clone as a probe, was found to be highly reproducible.

3.2.2.3 Screening of cDNA libraries

3.2.2.3.1 cDNA screenings of the Uni-Zap™ XR Library

The 28-52 P1 clone was then used to screen cDNA libraries, aiming the isolation of cDNA clones. The first cDNA library to be screened was the *Drosophila melanogaster* (Canton-S) cDNA Uni-Zap™ XR Library, obtained from 2-14 hours developing embryos. This library was cloned unidirectionally in the Uni-Zap™ XR vector at the *Eco*RI and *Xho*I restriction sites (Stratagene, La Jolla, CA).

The first screening was performed with 350 000 phage plaques. 29 of them hybridised to the DNA from 28-52 P1 clone. After a second and a third screen 13 clones were selected.

The pBluescript plasmids containing the cDNA inserts were extracted from the 13 phage clones by *in vivo* excision, performed by co-infecting *E. coli* cells with the ExAssist helper phage (Stratagene, La Jolla, CA). *In situ* hybridisation, using these individual clones, was performed in *Df(3R)red31/+* and *Df(3R)su(Hw)7/+* polytene chromosomes in order to confirm their localisation between the distal breakpoints of both deficiencies. From the 13 positive clones, only 7 mapped within *Df(3R)red31* breakpoints, of which 5 mapped within *Df(3R)su(Hw)7.* This suggests that the 28-52 clone eventually contains DNA sequences of a gene partially interrupted by *Df(3R)su(Hw)7*, although that clone maps between the distal breakpoints of *Df(3R)red31* and *Df(3R)su(Hw)7*,. Therefore, only two cDNA clones were mapped at the 88B8-C4 cytological region.

An equivalent genomic southern as the one used previously with the 28-52 clone was hybridised with the obtained cDNA probes (Fig. 27). The enzyme restriction pattern of *tef* and wild-type genomic DNA was shown to be identical for both cDNA probes. Obviously, these results do not eliminate these two cDNAs as potential candidates for being the *tef* gene. In fact, the genes corresponding to these two cDNAs could eventually be interrupted or deleted at non coding genomic regions such as the promoter, which is not taken into account in southern analysis while using cDNA clones as probes.

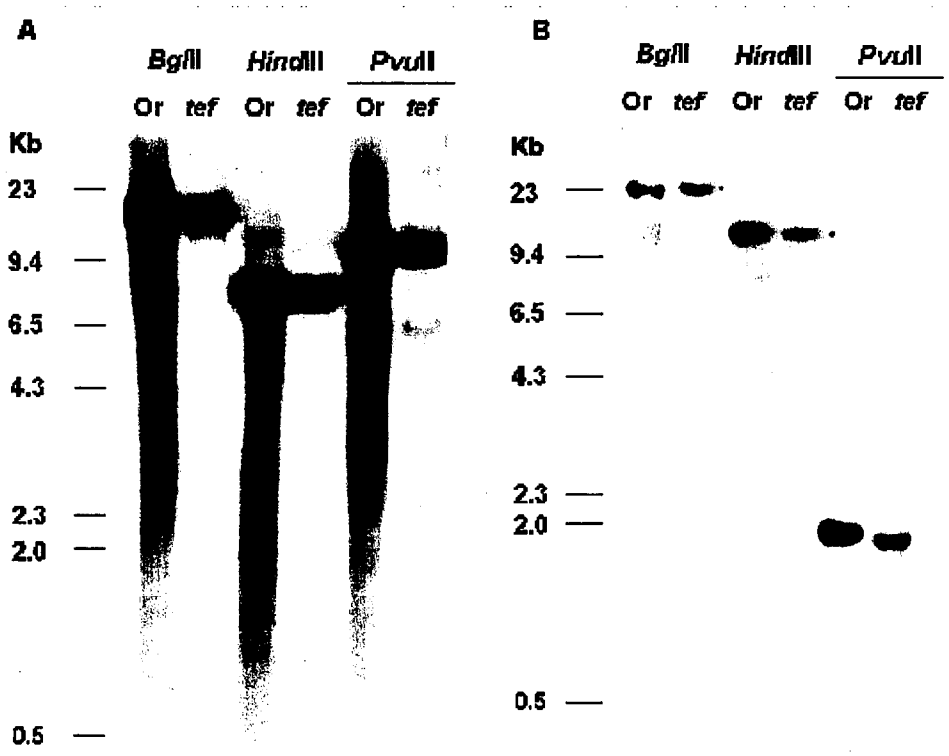

Figure 27: Southern blot hybridisation of wild-type (Or) and *tef* genomic DNA using 7221 (A) and 5211 (B) cDNA clones as probes. Genomic DNA was obtained from third instar larvae salivary glands and digested with *Bgl*II, *Hind*III and *Pvu*II. Wild type lanes contain a higher amount of DNA loaded in the gel slots.

3.2.2.3.2 cDNA screening of λgt10 Library

Subsequently a λgt10 cDNA library from larval brains and imaginal discs was screened using the 28-52 P1 clone as a probe. This library was constructed by cloning cDNA inserts at the *Eco*RI site of the λgt10 vector. Thus, this library was not cloned unidirectionally as in the Uni-Zap^{TM} XR vector.

The first screening was performed with 350 000 phage plaques. 62 of them were isolated as possible positive clones. Out of these, 32 mapped within the *Df(3R)red31,* by *in situ* hybridisation. However, most clones (27) mapped within the limits of *Df(3R)su(Hw)7*, and only 5 clones located within the 88B5-C4 genomic region. This suggests that the genomic region adjacent to the distal breakpoint of *Df(3R)su(Hw)7* is contained within the P1 clone. No cDNA clones were found to localise outside the distal breakpoint of *Df(3R)red31* and therefore it is possible that the

genomic sequence cloned in the 28-52 clone does not cover the entire 88B5-C4 region. The inserts of the 5 λgt10 cDNA clones were isolated and subcloned individually in the pBluescript plasmid and used as probes for southern blotting.

Southern blot hybridisation patterns using 4411 and 6311 cDNA clones were not conclusive (Fig. 29).

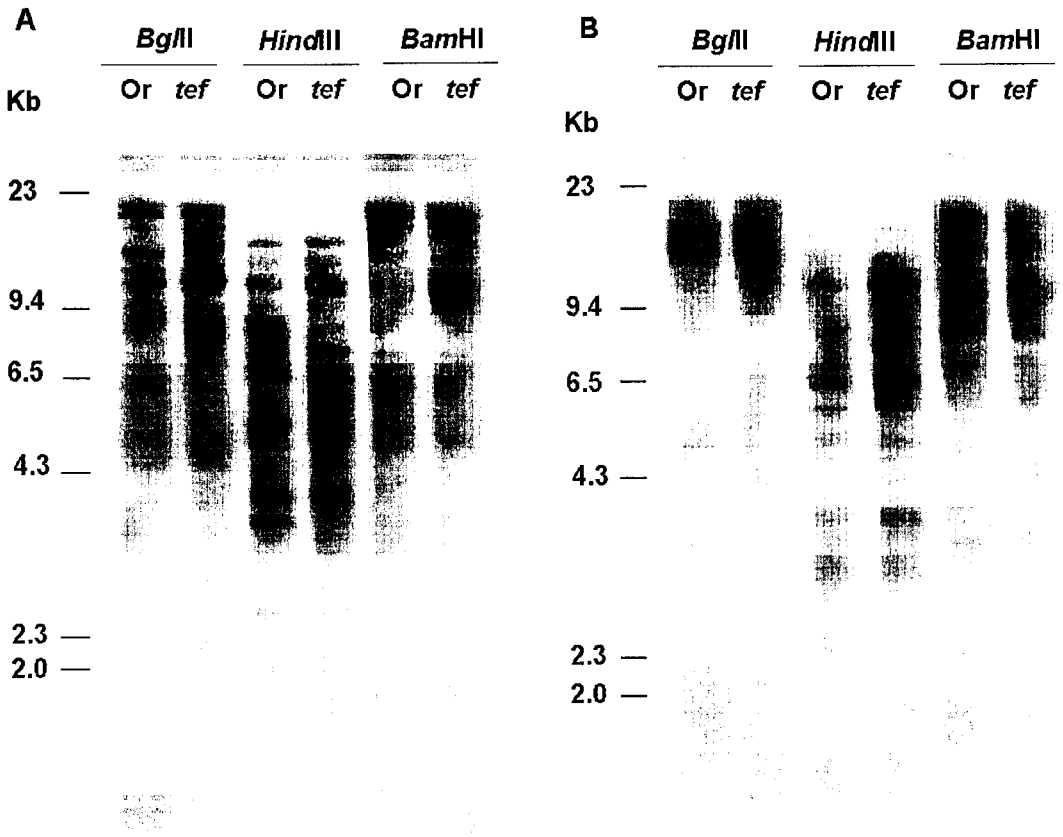

Figure 29: Southern blot hybridisation of wild-type (Or) and *tef* genomic DNA using 4411 (A) and 6311 (B) cDNA clones as probes. Genomic DNA was obtained from third instar larvae salivary glands and digested with *Bgl*II, *Hind*III and *Bam*HI.

Two cDNA clones exhibited different restriction patterns between the wild-type and the *tef* DNA digested with at least two restriction enzymes. Although these results support the existence of a genomic alteration within the 88B5-C4 region, identification of the *tef* gene requires an exhaustive analysis (Fig. 30).

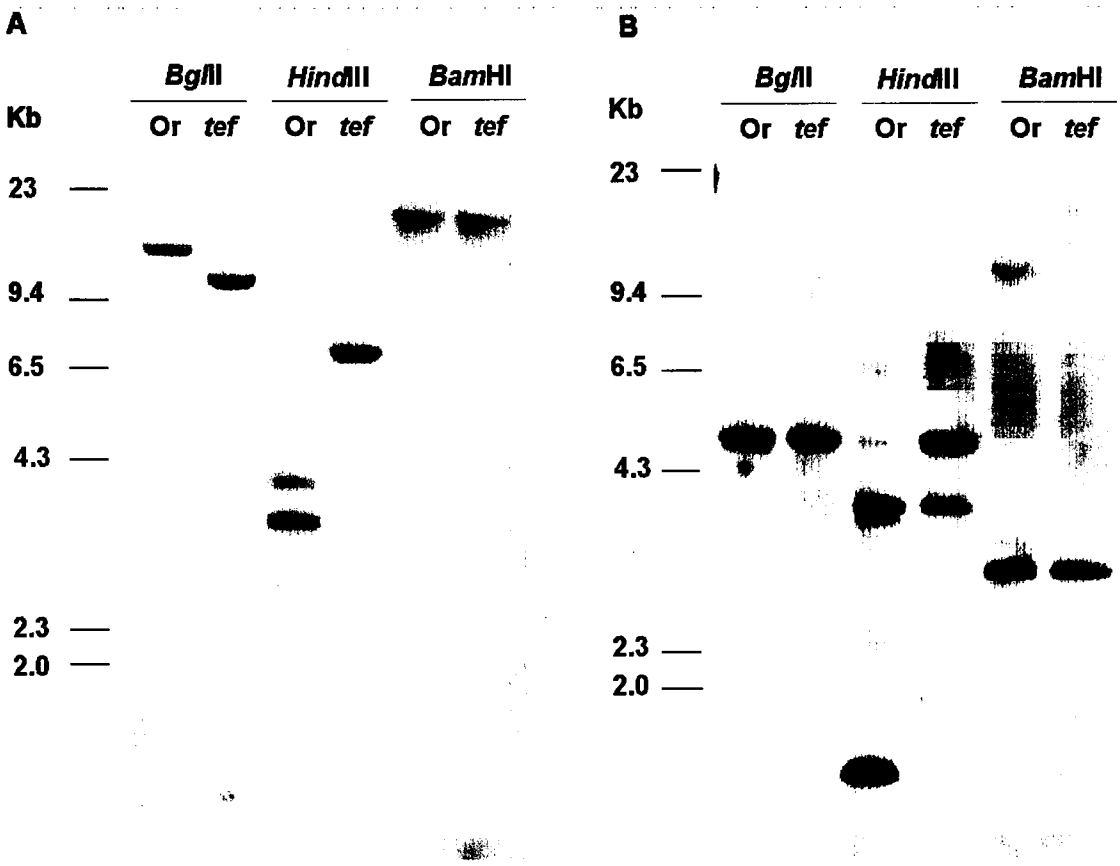

Figure 30: Southern blot hybridisation of wild-type (Or) and *tef* genomic DNA using 1211 (A) and 8523 (B) cDNA clones as probes. Genomic DNA was obtained from third instar larvae salivary glands and digested with *Bgl*II, *Hind*III and *Bam*HI.

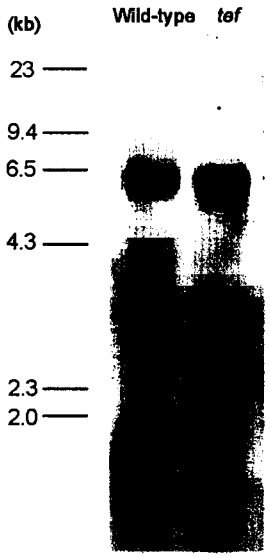

Figure 31: Northern blot hybridisation, using cDNA 8523 as a probe.

Northern blot analysis was only possible with the 8523 cDNA (Fig. 31). However, no significant differences of expression levels or mRNA sizes were detected between the *tef* and the wild-type control. Northern blot with other cDNA probes isolated from the cDNA screen proved to be unsuccessful.

3.2.2.4 *Drosophila* genome sequencing advances and gene prediction for the 88B5-C4 genomic region

The *Drosophila* genome sequencing progress concluded last year enabled the identification of coding sequences by chromosomal map position (Table 12). Most of the predicted genes by computer analysis do not exhibit homology with other known and identified sequences.

Table 12: Estimated genes by computational analysis from the Berkeley *Drosophlia* Genome Project (BDGP)

Gadfly reference	Gene	Map position	Function	mRNA (bp)	Peptide
CG8684		88B5	Enzyme	1131	356aa
CG14840		88B5	unknown	903	300aa
CG14841		88B5	unknown	651	216aa
CG14839		88B5	unknown	802	250aa
CG8651	trx	88B5-B6	Transcription factor	11696	3085aa
CG12207		88B6	unknown	635	?
CG3259		88B7	unknown	1767	588aa
CG8573	su(Hw)	88B7	Transcription factor	3068	941aa
				2870	941aa
CG3284	RpII15	88B7	Enzyme	698	129aa
CG3302	Crz	88B7	Signal transduction	572	154aa
CG3307		88B7	Transcription factor	2598	689aa
CG8538		88B7-B8	Transmembrane receptor	3477	1035aa
CG3321		88B8	Enzyme	571	81aa
CG3325	spn-B	88B8	DNA repair protein	1026	341aa
CG8524	NK7.1	88B8-C1	Transcription factor	2602	722aa
CG8489		88C1	unknown	614	147aa
CG8480		88C1-C2	Signal transduction	2853	950aa
CG14845		88C2	unknown	171	56aa
CG14846		88C2	unknown	1527	508aa
CG14847		88C2	unknown	666	221aa
CG14842		88C2	unknown	534	177aa
CG14843		88C2	unknown	1104	367aa
CG14848		88C2	unknown	714	237aa
CG14849		88C2	unknown	1311	436aa
CG14844		88C3	unknown	162	53aa
CG8464		88C5	unknown	1555	422aa
CG3351		88C5	Ribosomal protein	591	196aa

The cDNAs obtained from our screen using the P1 clone 28-52, were sequenced and homology alignments were performed. The 8523 clone shows homology to a predicted gene in the genomic scaffold AE003704 (Table 13). This clone (CG8480) encodes a product involved in signal transduction mechanisms related to cell growth and maintenance. It has a known homologue in *C. elegans*, *Homo sapiens*,

Mus musculus and rat. The rat homologue, p122-RhoGAP is involved in the Rho signalling pathway, leading to actin-related cytoskeletal changes.

The 7221 clone isolated from the UNIZAP cDNA library shows high homology to a *Drosophila* mitochondrial 16S ribosomal RNA, which is apparently not related to the *tef* mutated mitotic phenotype. No homology alignments were demonstrated with the genomic scaffolds in the BLAST query. The 6311 cDNA clone was found to correspond to the Gadfly CG14849 predicted gene, which has no identified homologous sequence in other organisms so far, and no function was computationally suggested for the predicted gene product (Table 13).

Identification of predicted genes in the AE003704 genomic scaffold that correspond to the other cDNA clones is prone to error. In fact the predicted open reading frames in the genomic scaffolds have undefined limits. An estimation of the first and the last base pair position is assigned in the genomic scaffold (e.g. CG8480: <132548 bp...>136037 bp) for each gene. The sequence homology between the other cDNAs and the genomic scaffold is always located close but outside the assigned limits. The last predicted gene on the AE003704 is the CG14844 and the first coding sequence in the following AE003705 scaffold starts in a distant downstream position (29274 bp). Thus, it seems likely that the 1211 and 4411 cDNAs correspond to the CG14844 gene. Comparison of the genomic southern using these cDNAs as probes reveals a very different restriction pattern, eventually suggesting that they are different portions of the same cDNA. Additionally, hybridisation of a southern blot containing the 28-52 genomic P1 clone digested with several enzymes showed that these two cDNAs hybridised to common heavy weight bands (data not shown).

Table 13: Regions of homology between the cDNAs isolated and the AE003704 genomic scaffold. Only 8523 and 6311 clearly fall within the limits of predicted coding sequences. The other cDNA clones contain sequences that are very close to the predicted coding regions. Two possibilities are estimated for the 5211 gene.

cDNA clones	Predicted Coding Region	Assigned limits (bp)	Homologous region in AE003704
8523	CG8480	<132548...>136037	132250...132697
6311	CG14849	<171270...>173142	167448...172979
1211	CG14844	<190134...>191299	203673...205253
6211	CG14844	<190134...>191299	187926...188625
4411	CG14844	<190134...>191299	206877...208838
5211	CG14849	<171270...>173142	184492...184898
	or CG14844	<190134...>191299	"

3.2.3 Genetic approach for cloning the *tef* gene

3.2.3.1 Mobilisation assay of a P-element inserted close to the *tef* locus

A new attempt to interrupt the *tef* gene, by P-element insertional mutagenesis was carried out. The goal of this experiment was to obtain a new *tef* allele induced by P-element tagging. Therefore, we chose to induce mobilisation of a P-element previously localised very close to the 88B-C region (*ry[506]*P{*ry*[+t7.2]=PZ}l(3)06951 [06951]/*TM3, ry[RK] Sb[1] Ser[1]*). This lethal third instar larvae mutant stock harbours a P-element insertion in the cytological region 88C1-4. Although this P-element stock did complement the *tef* mutation, the insertion site was found to be very close to the *tef* locus, mapped within the 88B8-C4 region. As it was previously demonstrated (Tower *et al*, 1993) *Drosophila* P-elements preferentially transpose into genomic regions close to their starting sites. Accordingly, a P-element mobilisation assay was performed using the P1709 stock, by performing genetic crosses represented in figure 32. The PZ element present in this line contains the lacZ, the kanamycine resistance and the rosy genes. This stock is therefore constructed in a *ry-* background. Previous studies (Zhang and Spradling, 1993) showed that more independent local insertions nearby the starting element were recovered among the progeny of females compared to males. These results may be due to some intrinsic difference between the transposition mechanism or its efficiency in male and female germ lines. Female germ line cells produce less mutations following an equal dosage of radiation, presumably because they repair DNA damage more efficiently than male cells (Ashburner, 1989). Accordingly, a balancer harbouring the *Δ2-3* mutation was used to select females, thus avoiding recombination events.

P: *ry[506] / P{ry[+t7.2]=PZ} / TM6B,Tb Hu e* x *ry[506] / Df(1)ea / Δ2-3 TM3 Sb e*

↓

F1: females *ry[506] / P{ry[+t7.2]=PZ} / Δ2-3 TM3 Sb e* x males *TM3, Sb e / TM6B,Tb Hu e*

↓

F2: *ry[506] / P{ry[+t7.2]=PZ} */ TM6B,Tb Hu e* x *tef, e / TM6B,Tb Hu e* (single cross)

Figure 32: P-element stock was originally crossed with a strain carrying the *Δ2-3* chromosome. In F2, *P{ry[+t7.2]=PZ} /Δ2-3 TM3 Sb e* females were selected and hybrid dysgenisis occurred at the germ line level. These females were crossed to males carrying a third balancer chromosome. Single crosses between balanced P-element chromosome males or females and the *tef* balanced mutant individuals were performed. These crosses were checked for *tef*/P-element lethality (which would correspond to the *Tb*+ larvae).

Out of 900 single F2 crosses a single line was identified that did not complement neither the *tef* lethality nor the end-to-end fusion mitotic phenotype (Fig. 33). This *tef* allele was shown to be more severe, since homozygous larvae for the P-element chromosome were observed only until early stages of development (first and second instar larvae). The new mutant allele was not complemented by *Df(3R)red31* either.

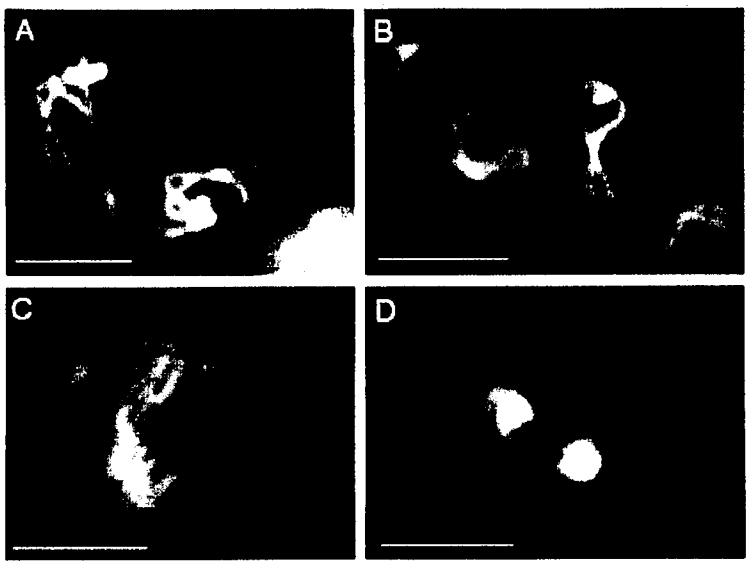

Figure 33: Mitotic phenotype of the $P_{mobilised}$/*tef* strain

Preliminary attempts to determine whether this new allele of *tef* contained a P-element were carried out by *in situ* hybridisation, using *lac-Z* and plasmid sequences as a probe. The results indicate that a substantial part of the original P-element was deleted in the new *tef* allele. One possible interpretation of these results is that the *tef* locus is located very close to the insertion in 88C1-4 and as a result of the mobilisation, part or the whole *tef* locus was deleted.

The P1709 insertion is located at the 220043-220572 bp position in the AE003704 genomic scaffold, which, as predicted by the Gadfly database, is not a coding region. The genes located adjacent to this P element insertion are the CG14844 (present in the AE003704 genomic scaffold) and CG8464 (present in the AE003705 genomic scaffold).

Cloning the *tef* gene will be possible by testing potential candidates individually, using RNA interference approaches, for example. According to the data it would be wiser to start with those DNA sequences adjacent to the P element insertion in the P1709 strain.

4. DISCUSSION

4. DISCUSSION

Here we describe the identification and characterisation of the recessive telomere fusion (*tef*) mutation. In the absence of the *tef* function chromosomes form end-to-end attachments that do not resolve during mitosis or meiosis, leading to chromosome breakage and significant genome rearrangement. We hypothesise that the *tef* gene product is required for the molecular complex that protects telomere ends of linear chromosomes.

tef is required to maintain chromosomal integrity

The most significant aspect of the mitotic abnormalities caused by the *tef* mutation is the fusion of chromosome arms through their ends. Mitotic chromosomes display fusion from very early stages of mitosis suggesting that these occur either during S phase or G2. The frequency of mitotic cells containing fusions is high indicating that the function encoded by *tef* is essential to maintain chromosome integrity. Analysis of anaphase and telophase cells shows that chromatin bridges persist until late mitosis and it is likely that the final events of cytokinesis lead to chromosome breakage since most cells contain abnormally rearranged chromosomes. Similar phenotypes have also been described in a number of other cell types, including human tumours containing cells lacking telomeres (reviewed in de Lange, 1995). Furthermore, it has been shown that senescent cells, which are known to possess critically short telomeres, show chromosome fusions (Saltman *et al*, 1993). It has been proposed that these telomeric associations could promote the formation of dicentric chromosomes that eventually break or missegregate in anaphase, resulting in chromosome rearrangements or loss of heterozygosity (Hastie and Alshire, 1989; de Lange, 1995).

End-to-end associations appear to form before DNA replication and reflect a non-random organisation of telomeres

Analysis of the frequency of attachments of individual chromosomes in *tef* mutant cells shows that all chromosomes are capable of forming associations.

Nevertheless, intrachromosomal associations, such as ring conformations and sister unions, are less frequent than homologous or heterologous interactions, and fusions between chromosome 2 and 3 are the most frequent events. Additionally, single chromatid associations are less frequent than double chromatid associations, suggesting that most fusions occur before DNA has replicated. Similar results were obtained when analysing *Drosophila* strains deficient for the UbcD1 (Cenci *et al*, 1997). It was shown that the most frequent events were DCAs, indicating that the majority of telomere fusions occurred before DNA replication, although absolute frequencies of different types of fusions were lower in those strains than in the *tef* mutant. Taken together these results suggest that in *Drosophila* neuroblasts telomeres of autosomes remain in close proximity after exit from mitosis suggested by the higher frequency of fusion between their telomeres. A detailed analysis of the frequency of associations involving the long arm compared to the short arm of the telocentric X chromosome also supports a clear intranuclear organisation of chromosomes. As previously described for UbcD1 mutants (Cenci *et al*, 1997), the *tef* mutant exhibits a higher frequency of DCA involving the long arm of the X chromosome suggesting that telomeres and centromeres organise in a Rabl orientation.

The *tef* mutation is not associated with a defective DNA repair response and appears to have an active DNA damage inducible checkpoint

One possible interpretation of the mitotic phenotype caused by the *tef* mutation could be that these mutant cells are unable to efficiently repair their DNA. We have tested the ability of *tef* mutant individuals to survive after low doses of γ-radiation. The results indicate that *tef* individuals are no more sensitive to low doses of radiation than the wild-type controls. Therefore, the results support the view that DNA repair pathways induced by γ-radiation have not been compromised in the *tef* mutant individuals. However, *tef* mutants were shown to survive better to higher doses of radiation than wild-type. This is consistent with the reduced mitotic index and slow progression through mitosis observed in mutant neuroblasts, since it is well established that slowly dividing cells survive better high levels of DNA damage than rapidly proliferating cells.

The ability to repair DNA damage induced by radiation is associated with a functional checkpoint that delays progression through interphase, allowing DNA repair mechanisms function. Quantitative analysis of mitotic parameters of *tef* mutant cells

indicates that these cells spend more time in interphase than wild-type cells. This reduction in the mitotic index could represent the activation of the DNA damage checkpoint as a result of the inability to resolve chromosome attachments with a consequent delay of the entry into the next mitosis. However, the reduction in the mitotic index caused by radiation-induced DNA damage in *tef* mutant neuroblasts was shown to be much less significant than in wild-type cells. This result raises the possibility that the *tef* function may be required for the activation of an efficient DNA damage checkpoint that arrests cells before entering the next mitosis. However, the period of time required to repair radiation-induced damage most likely coincides with the time used to repair bridge-induced damage, so that the two occur simultaneously. Thus, the reduction in the mitotic index due to radiation may be masked by the already existing reduction in the mitotic index due to bridges and consequent chromosome breakage.

Mutant neuroblasts also exhibit a higher frequency of apoptotic cells than the wild-type cells. This suggests that when chromosome damage accumulates to a certain degree apoptosis is induced. This is also supported by the low frequency of polyploid cells observed.

End-to-end fusion of chromosomes in *tef* mutant cells requires linear chromosomes

One possible interpretation for the chromosomal phenotype observed in *tef* mutant cells is that chromosomes fuse by extensive mitotic recombination. However, if this is the case, acentric fragments would be produced and should be detected at least at low frequency. Extensive analysis of mitotic figures did not reveal any acentric fragments, suggesting that mitotic recombination is unlikely to underlay the phenotypes we observed. Alternatively, chromosome fusions in a *tef* mutant background might require exposed telomere ends.

In order to test these hypothesis, we studied the behaviour of a ring X chromosome that did not contain exposed ends (R(1)2) in a *tef* mutant background. The results show that the ring X chromosome forms attachments very infrequently compared to the normal X chromosome present in this strain. One explanation for these results is that the ring X chromosome is somewhat unusual and cannot form chromosome-chromosome interactions despite the absence of exposed ends. However, given the fact that the normal X in the stock is able to form fusion, and most importantly, that there is no evidence of mitotic recombination, the simplest

interpretation is that the reduction in the frequency of fusions is related to the lack of exposed ends of the ring chromosome. Accordingly, it is likely that the fusions observed in the *tef* mutant cells occur through the telomeres. It maybe possible that *tef* causes chromosome attachments by somehow inactivating the telomeres. Inactivation of telomere function (Steensel *et al*, 1998) or modification of terminal sequences (Counter *et al*, 1992) has been shown to cause telomere fusion.

HP1 and *tef* gene products function in different pathways

HP1 protein is thought to be required for the protection of telomeres from fusions (Fanti *et al*, 1998). Mutations in HP1 cause extensive chromosome end-to-end attachments in a manner very similar to the *tef* mutant. Therefore, it is possible that loss of the Tef gene product could lead to inappropriate localisation of HP1 and consequently end-to-end fusion. The presence of HP1 in *tef* telomeres of polytene chromosomes suggests that HP1 and Tef may function in different pathways to maintain non-recombinogenic telomeres. Additionally one can not exclude the possibility that Tef could operate downstream of HP1, or that, since immunostaining studies are relatively crude assays for localization of HP1, Tef does affect the localisation or the organization of HP1 but not to a degree that is detectable with this assay.

tef is required during spermatogenesis to maintain chromosomal integrity

The analysis of testes isolated from *tef* mutant individuals indicates that this gene function is also required during spermatogenesis. Mutant testes contain cells that show chromosome fusions at all stages of spermatogenesis. These chromosome associations lead to significant missegregation since spermatids containing irregular size nuclei and micronuclei, were regularly found. The abnormalities observed during early stages of spermatogenesis are reflected during final sperm differentiation, namely during sperm head elongation. Mutant sperm show very disorganised heads that appear to be interconnected by thin chromatin bridges and the overall organisation of sperm bundles is clearly abnormal. Similar results were also obtained after analysis of spermatogenesis in UbcD1 mutant males (Cenci *et al*, 1997), indicating that both mitotic and meiotic chromosomes require similar gene functions in order to maintain telomere integrity.

PART II: Chromosome painting in *Drosophila melanogaster*

1. INTRODUCTION

1. INTRODUCTION

Chromosome painting is a technique of fluorescence *in situ* hybridisation (FISH), using a chromosome-specific DNA library as a probe pool, to identify an entire chromosome or a specific chromosomal region. This technique can detect an individual chromosome from other chromosomes in both metaphase and interphase nuclei. Chromosome painting is now used routinely to enhance the identification of chromosomal rearrangements, the assignment of breakpoints and the determination of the origin of extrachromosomal material. Chromosome painting is used in pre- and post-natal diagnosis, as well as in tumour cytogenetics. Karyotype analysis based on classical chromosomal banding may be time demanding. Additionally, metaphase chromosomes obtained from tumour cells are usually hard to obtain and thus the analysis by classical chromosomal banding techniques shows several limitations. Recent studies in chromosome painting have helped to identify DNA double–strand breaks repair pathways and to characterize different aberration patterns left behind by various kinds of irradiation (reviewed in Sachs *et al*, 2000).

Additionally, advances in protocols for multicolour FISH have enabled a faster karyotype analysis, namely the scanning of human and other genomes for chromosomal rearrangements. This experimental approach allows the recognition of several chromosomes depicted in different colours (Speicher *et al*, 1996, Schrock *et al*, 1996).

The probes used for chromosome painting are often not of sufficient complexity to detect subtle chromosomal changes: small regions of rearranged material can be missed by painting approaches. This has led to the development of sets of subregional FISH probes that stain strongly the chromosomal area of interest. This procedure is often used in diagnosis situations (Fisher *et al*, 1996). The use of chromosome arm painting probes (CAPs) enables the detection of pericentric inversions and interarm exchange that would not be detected using whole chromosome painting probes (WCPs). An exciting example for a probe set designed for the detection of the relevant changes in a diagnostic situation is the use of chromosome end markers, such as subtelomeric fragments. There is an unexpected high frequency of translocations and deletions involving telomeric regions in families with mental retardation and dysmorphic features (Flint *et al*, 1995). This type of chromosomal rearrangements have also been demonstrated in chinese hamster cell lines using subtelomeric region specific painting probes (Xiao and Natarajan, 1998).

Comparative genomic hybridisation (CGH) allows screening for DNA sequence copy-number changes, and provides a map of those chromosomal regions that are gained or lost in a DNA specimen. Because DNA copy-number alterations are of pathogenic importance in cancer, most of the applications of CGH come from cancer research. In CGH, which is based on a modified *in situ* hybridisation, differentially labelled test (green) and reference (red) DNAs (tumour *versus* normal DNA, for example) are co-hybridised to normal metaphase spreads. Copy number differences between the test and reference genomes are seen as green:red fluorescence intensity differences on the metaphase chromosomes, identified using a digital image analysis system.

Because oncogenes and drug-resistance genes are known to be up-regulated by DNA amplifications, it has been speculated that DNA amplification sites in cancer could pinpoint locations of novel genes with important roles in cancer progression. Following the mapping of the telomerase gene to 3q26, the frequent presence of 3q gains in CGH of ovarian and cervical cancers led scientists to discover amplification of telomerase in some tumour types (Soder *et al*, 1997). The discovery of novel small regions of loss of genetic material could help the search for new tumour suppressor genes as suggested by studies of hereditary cancer predisposition (Hemminki *et al*, 1997). CGH also enables the analysis of tumour progression, in the sense that the gain of specific DNA sites are associated to different stages of tumour development.

In addition to genetic aberrations, chromosome painting techniques are also used in comparative cytogenetics in order to address the question of chromosome evolution between related species (reviewed in Forozan *et al*, 1997).

The generation of whole chromosome painting probes (WCPs) is generally performed by chromosome microdissection followed by a PEG/proteinase K treatment and direct amplification by PCR using a degenerate primer (Deng *et al*, 1992; Guan *et al*, 1994). Alternatively, probes may be generated by flow-sorting chromosomes of different size. Accordingly, PCR may be performed with flow-sorted Robertsonian-translocated chromosomes (Telenius *et al*, 1992, Breneman *et al*, 1993).

These technologies have enabled the development of reverse chromosome painting, in which the paint is produced from sorted aberrant chromosomes and hybridised back onto normal metaphase spreads to identify directly the composition of the aberrant chromosome. Reverse painting is able to identify the regions and breakpoints involved in the generation of aberrant chromosomes.

Chromosome painting in *Drosophila melanogaster* is limited by the fact that 30% of the fly genotype is composed of heterochromatin, primarily localised in the pericentromeric and telomeric regions, but also present along the euchromatic arms. Accordingly, the chromosomal specificity is often compromised when DNA probes contain repetitive sequences such as transposable elements, since more hybridisation signals are detected in different chromosomes. The elimination of additional hybridisation signals was tested in human chromosome painting, by incubating the probe mixture with human genomic DNA enriched for repetitive DNA sequences (Nisson *et al*, 1992)

Chromosome painting in *Drosophila* may be used for the analysis of mutants that involve chromosomal abnormalities such as genome rearrangements or condensation failure, thus contributing for the study of mitotic phenotypes associated to a gene mutation.

2. MATERIALS AND METHODS

2. MATERIALS AND METHODS

2.1 Chromosome painting in mitotic chromosomes, using a mixture of biotin-labelled probes

Mitotic chromosomes were treated and denatured as described previously in chapter I. A mixture of P1 DNA probes was concentrated in a Speed-Vacuum apparatus and genomic DNA was added to a final concentration 10-fold higher than the mixture of P1 DNA. After denaturing DNA at 95°C, 5 minutes, the mixture was incubated at 37°C for 2,5 hours. An equal volume of 2xhybridisation solution previously denatured was added to the mixture. 10μL of the final mixture were applied to the denatured chromosomes. Slides were incubated overnight at 58°C in a humid chamber.

Excess of probe was washed away in a 2xSSC solution at 53°C for 2 minutes, followed by 5 minutes successive washes in 4xSSC, 4xSSC with 0.1% Triton X-100, and 4xSSC solutions. Slides were incubated at room temperature in a dark humid chamber for 30 minutes with 2% avidin-Fluorescein conjugate (Vector Laboratories, #A-2001) in 4xSSC. Slides were immersed in 4xSSC solution for 5 minutes and in 4xSSC, 0.1% Triton X-100, 5% BSA solution (previously centrifuged for 30 minutes at 4000 rpm and filtered with a 0,45μm filter) for 15 minutes. Chromosomes were incubated with a 2% anti-avidin biotinylated solution in 4xSSC, 0.1% Triton X-100, 5% BSA for 30 minutes. Slides were washed in 4xSSC solution for 5 minutes and incubated with a 2% avidin-fluorescein in 4xSSC, 0.1% Triton X-100, 5% BSA solution for 30 minutes. Slides were washed 5 minutes in 4xSSC and stained with propidium iodide in an anti-fading mounting medium (Vector laboratories).

2.2 Chromosome painting in mitotic chromosomes using Degenerate Oligonucleotide-Primed PCR (DOP-PCR)

The degenerated primer "CCGACTCGAGNNNNNNATGTGG" was used for PCR reactions using a mixture of P1 clones of a chromosome arm in a 10ng/μL final concentration. PCR reactions were established by adding 2mM of $MgCl_2$, 5U/100μL Taq polymerase, 4 μM of degenerated primer, 300 μM of dATP, dCTP, dTTP and

dGTP. PCR was started with 5 low temperature annealing cycles - 95°C for 1 minute; 30°C for 1,5 minutes; a 3 minutes transition period from 30°C to 72°C; 72°C for 2 minutes – followed by 30 more restringent cycles – 94°C for 1 minute, 62°C for 1 minute and 72°C for 2 minutes. A final extension reaction was performed at 72°C for 5 minutes. 5μL of the PCR product was re-amplified in a PCR reaction containing 50 μM of dTTP and 100μM of a conjugated dUTP-biotin nucleotide. Approximately 500ng of the new PCR product was mixed with 1 volume of 2x hybridisation solution and applied to a slide.

3. RESULTS AND DISCUSSION

3. RESULTS AND DISCUSSION:

3.1 Chromosome painting using a mixture of labelled DNA probes

Chromosome painting was tested with 10 P1 clones for each *Drosophila* chromosome arm (Table 1). P1 clones have approximately 30 kb and are able to comprise DNA fragments up to 100 Kb. Since, they are kept as single copies inside bacteria, these clones are able to maintain stable inserts (Hartl and Lozovskaya, 1995). The localisation of each chromosome probes was confirmed in polytene chromosomes. Subsequently, each probe was hybridised individually against mitotic chromosomes to test for specificity. Some of the clones tested, especially those localised near pericentromeric or telomeric regions, showed multiple hybridisation sites on the same or on different chromosomes. In order to eliminate additional hybridisation signals, unlabelled *Drosophila* genomic DNA was used to inhibit cross-hybridisation of repetitive sequences present in the probe mixture that bind to multiple chromosomes. The remaining single-stranded DNA was hybridised to mitotic chromosomes, and detected by Fluorescein-Biotin conjugates, following post-hybridisation washes. The results showed that multiple hybridisation signals were eliminated, except in a few cases where they were still present although with much lower intensity.

Chromosome painting was successfully accomplished for the X chromosome and the left arms of both autosomes (2L and 3L) (Fig.1). Probes were selected for their specificity, and incubation with genomic DNA was performed when necessary.

Table 1: P1 clones tested for chromosome painting in *Drosophila melanogaster*. Intensity and the number of hybridisation signals in mitotic chromosomes were determined for each individual clone. Genomic DNA incubation was tested individually for each clone: (+) means that multiple hybridisation spots were successfully eliminated, (-) means that probes were sufficiently specific, (change) means that probes were not appropriate.

Chromosome	P1 clones (library reference)	Hybridisation site	Hybridisation signal	Incubation with Genomic DNA
X	26-92	1D1-2	Unique, strong	-
	15-29	3A3-F1	Unique, strong	-
	75-61	5E5-F6	Unique, weak	-
	80-33	7D1-19	Unique, strong	-
	10-58	9E7-10B2	X chromosome - strong 2nd chromosome - centromeric signal	+
	9-75	12E10-13A2	X chromosome - strong Autosomes - pericentromeric signal	+
	74-46	14F6-15A4	Unique, strong	-
	48-69	17D1-6	Labels all chromosomes	+
	32-7	19E7-20A3	Unique, strong	-
2L	9-19	21A1-A5	Unique, strong	-
	7-40	21E3-F3	Unique, strong	-
	43-53	23E1-F6	Unique, strong	-
	83-55	25C6-F3	Unique, strong	-
	75-30	26F1-27C2	Unique, weak	-
	95-14	28E7-29D2	Unique, strong	-
	77-21	31F1-32A2	Unique, strong	-
	58-82	34A3-C2	Unique, strong	-
	12-28	35F1-36C11	Unique, strong	-
	49-30	37D4-38A2	Unique, weak	-
	29-87	40A2-C	Unique, strong	-
2R	55-29	44C4-D2	Unique, strong	-
	76-73	46E1-F9	Unique, strong	-
	37-59	48D-E1	Multiple hybridisation sites	+
	33-91		Unique, strong	-
	66-66	53C1-F	Unique, strong	-
	17-16	55E6-56A2	Unique, strong	-
	94-38	57F8-58A2	Unique, strong	-
	23-74	59B4-C5	Unique, strong	-
	19-32		Unique, strong	-
	91-4	60D15-F5	Unique, strong	-
3L	35-75	61A1-B3	Unique, weak	-
	47-82	63A2-B8	Unique, strong	-
	49-75	64F1-65A2	Unique, strong	-
	40-56	66F4-67B7	Unique, strong	-
	24-55	69A2-B3	Unique, strong	-
	24-75	71B3-C2	Unique, strong	-
	20-76	73E5-74A2	Unique, weak	-
	15-49	77B4-C1	Unique, Strong	-
	51-56	79A1-B3	Unique, strong	-
	94-71	80A3-B2	Multiple hybridisation sites	+
3R	15-86	82A1-B4	Multiple hybridisation sites	change
	64-15	83F1-F2	Unique, strong	-
	73-67	85F8-86A1	Unique, strong	-
	62-6	90E3-F10	Multiple hybridisation sites	+
	5-42	92E4-E14	Unique, strong	-
	80-20	94D2-95A5	Unique, strong	-
	3-49	96F12	Unique, strong	-
	73-53	97A4	Multiple hybridisation sites	+
	72-40	98E3-F2	Unique, strong	-
	93-75	87F8-88A5	Unique, strong	-

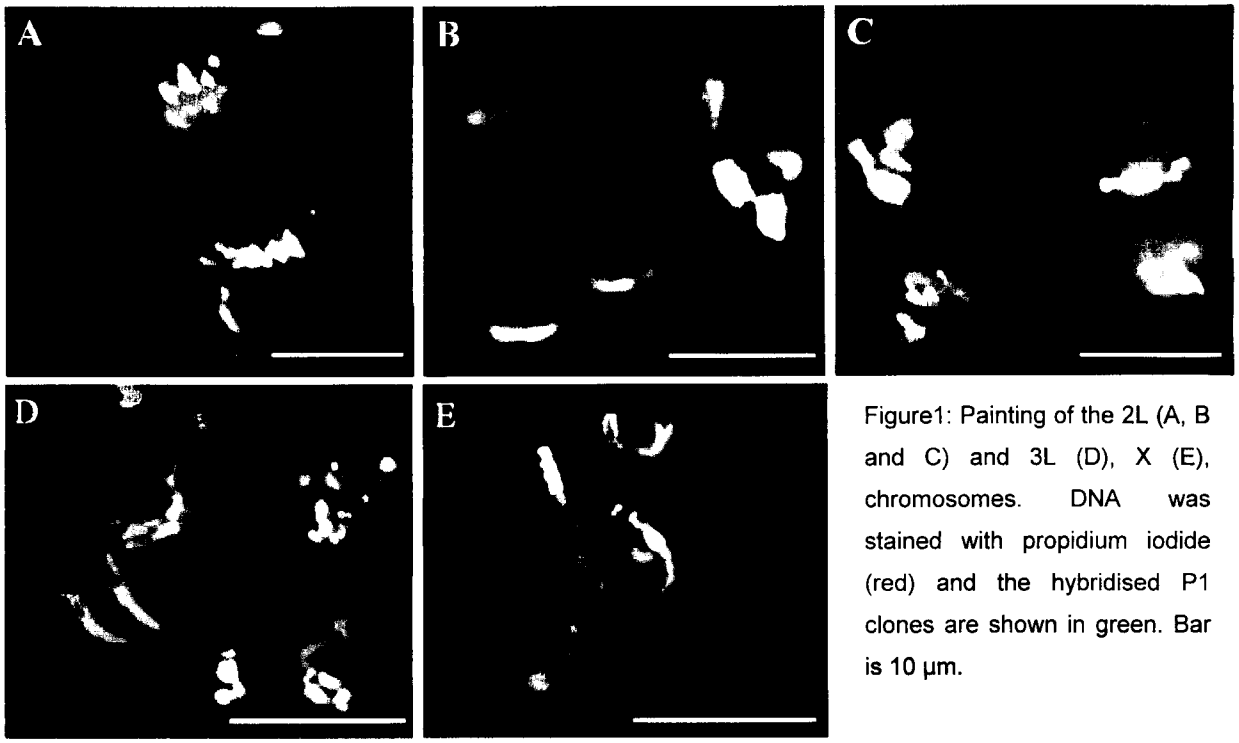

Figure1: Painting of the 2L (A, B and C) and 3L (D), X (E), chromosomes. DNA was stained with propidium iodide (red) and the hybridised P1 clones are shown in green. Bar is 10 µm.

3.2 Chromosome painting by DOP-PCR (Degenerate Oligonucleotide-Primed PCR) labelling reaction

Performing multiple DNA extractions for several chromosome painting assays and labelling each probe individually is time consuming and a fastidious work. In order to reduce the amount of DNA required to paint a chromosome arm and to avoid labelling each P1 clone individually by nick translation, a PCR labelling reaction was developed. PCR was performed with degenerate oligonucleotides (5'-CCGACTCGAGNNNNNNATGTGG-3'), to give general amplification of target DNAs. DOP-PCR (Degenerate Oligonucleotide-Primed PCR) is performed with initial low annealing temperature cycles (30ºC) and subsequently at higher annealing temperature cycles. PCR reaction conditions (see Materials and Methods) were tested initially, using one or a few probes (10 ng/µl). A 100 µM: 50 µM concentration ratio of biotinylated-dUTP: dTTP nucleotides was used.

This chromosome painting approach was tested for the left arm of chromosome 2 (Fig. 2). Nevertheless, a similar procedure can be used to paint other chromosomes, as long as the problem of repetitive sequences is overcome by incubating the probe

with genomic DNA at 37°C before *in situ* hybridisation. Reamplifying once a PCR product was also tested and the resulting chromosome painting was similar (Fig.2).

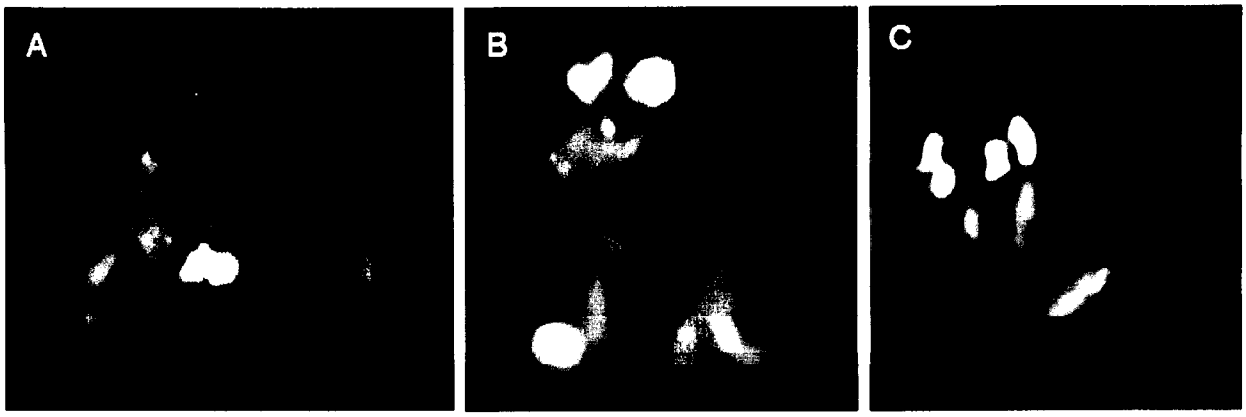

Figure 2: Painting of chromosome 2 using DOP-PCR labelling reaction.

PART III

APPENDIX

1. ABBREVIATIONS

ABBREVIATIONS

APC	Anaphase Promoting Complex
ATP	Adenosine 5' triphosphate
bp	Base pair
BSA	Bovine Serum Albumin
CAK	Cdk-Activating Kinase
Cdc	Cell Division Cycle gene
Cdk	Cyclin-Dependent Kinase
cDNA	Complementary DNA
DAPI	4', 6'-diamidino-2-fenilindole
µL	microlitre
µM	micromolar
clb	Cyclin B
cln	Cyclin
dATP	2'-desoxyadenosine-5'-triphosphate
dCTP	2'-desoxycytosine-5'-triphosphate
ddATP	2',3'-desoxyadenosine-5'-triphosphate
ddCTP	2',3'- desoxycytosine-5'-triphosphate
ddGTP	2',3'- desoxyguanosine-5'-triphosphate
ddTTP	2',3'- desoxytimidine-5'-triphosphate
dGTP	2'- desoxyguanosine-5'-triphosphate
DNA	Desoxyribonucleic acid
Dnase	Desoxyribonuclease
dTTP	2'- desoxytimidine-5'-triphosphate
EDTA	Ethylenediamino Tetracetic Acid
GFP	Green Fluorescent Protein
HP1	Heterochromatin Protein 1
Hsp	Heat Shock Protein
IPTG	Isopropil-β-D-tiogalactopiranoside
kb	Kilobase
kDa	Kilodalton
LB	Luria-Bertani culture medium
M	Molar
MAT1	Ménage à Trois 1
mL	millilitre

mM	Milimolar
MPF	Maturation Promoting Factor
MTOC	Microtubule organising Centres
MRNA	Messanger RNA
PBS	Phosphate Buffer Saline
PCR	Polymerase Chain Reaction
PEV	Position Effect Variegation
PP1	Protein Phosphatase 1
PP2A	Protein Phosphatase 2A
RNA	Ribonucleic Acid
Rnase	Ribonuclease
Rpm	Rotations per minute
SDS	Dodecil (lauril) Sodium Sulfate
SSC	Saline Citrate Buffer
TAE	Electrophoresis buffer containing Tris, Acetate and EDTA
TE	Tris-EDTA buffer
TBE	Electrophoresis buffer containing Tris, Borate and EDTA
Tris	Tris (hidroxymetyl)aminomethane
X-Gal	5-bromo-4-cloro-3-indol-β-D-galactoside

2. REFERENCES

2. REFERENCES

Abad JP, Carmena M, Baars S, Saunders RDC, Glover DM, Luden P, Sentis C, Tyler-Smith C and Villasante A (1992) *Dodecasatellite*: a conserved G+C rich satellite from the centromere heterochromatin of *Drosophila melanogaster*. Proc Natl Acad Sci USA 98: 4663-4667

Abad JP and Villasante A (1999) The 3' non-coding region of the Drosophila melanogaster Het-A telomeric retrotransposon contains sequences with propensity to form G-quadruplex DAN. FEBS Lett 453(1-2): 59-62

Abruzzo MA, Miller JA and Singer VL (1991) Telomeric associations involving Yq12 in a lymphoblastoid cell line. Cytogenet Cell Genet 56: 149-151

Acevedo OL, Dickinson LA, Macke TJ and Thomas CA (1991) The coherence of synthetic telomeres. Nucleic Acids Res 20: 507-511

Adamczewski JP, Rossignol M, Tassan JP, Nigg EA, Moncollin V and Egly JM (1996) MAT1, cdk7 and cyclin H form a kinase complex which is UV light sensitive upon association with TFIIH. EMBO J 15: 1877-1884

Adams Martin A, Dionne I, Wellinger RJ and Holm C (2000) The function of DNA polymerase alpha at telomeric G tails is important for telomere homeostasis. Mol Cell Biol 20: 786-796

Ahmad K and Golic KG (1998) The transmission of fragmented chromosomes in *Drosophila melanogaster*. Genetics 148: 775-792

Ahmad K and Golic KG (1999) Telomere loss in somatic cells of *Drosophila* causes cell cycle arrest and apoptosis. Genetics 151: 1041-1051

Allshire RC, Dempster M and Hastie ND (1989) Human telomeres contain at least three types of G-rich repeat distributed non randomly. Nucleic Acids Res 17: 4611-4627

Araki H, Leem SH, Phongdara A and Sugino A (1995) Dpb11, which interacts with DNA polymerase II (ε) in *S. cerevisiae* has a dual role in S-phase progression and at a cell cycle checkpoint. Proc Natl Acad Sci USA 92:11791-11795

Artandi SE and DePinho RA (2000) A critical role for telomeres in suppressing and facilitating carcinogenesis. Curr Opin Gen Dev 10: 39-46

Ashburner M (1989) *Drosophila* - A Laboratory Handbook. Cold Spring Harbor Laboratory Press

Ashley T and Ward DC (1993) A "hot spot" of recombination coincides with an interstitial telomeric sequence in the Armenian hamster. Cytogenet Cell Genet 62(2-3): 169-171

Barlow C, Brown KD, Deng CX, Tagle AA and Wynshaw-Boris A (1997) Atm selectively regulates distinct p53-dependent cell cycle checkpoint and apoptotic pathways. Nature Genetics 17:453-456

Basu J, Bousbaa H, Logarinho E, Li Z, Williams BC, Lopes C, Sunkel CE and Goldberg ML (1999) Mutations in the essential spindle checkpoint gene *bub1* cause chromosome missegregation and fail to block apoptosis in *Drosophila*. J Cell Biol 146: 13-28

Benn PA (1976) Specific chromosome aberrations in senescent fibroblast cell lines derived from human embryos. Am J Hum Genet 28: 465-473

Bennett CB, Lewis AL, Baldwin KK and Resnick MA (1993) Lethality induced by a single site-specific double-strand break in a dispensable yeast plasmid. Proc Natl Acad Sci USA 90(12): 5613-56137

Bentley NJ, Holtzman DA, Flaggs G, Keegan KS, Demaggio A, Ford JC, Hoekstra M and Carr AM (1996) The *Schizosaccharomyces pombe* rad3 checkpoint gene. EMBO J 15: 6641-6651

Bianchi A, Smith S, Chong L, Elias P and de Lange T (1997) TRF1 is a dimmer and bends telomeric DNA. EMBO J 16: 1785-1794

Biessmann H and Mason J M (1988) Progressive loss of DNA sequences from terminal chromosome deficiencies in *Drosophila melanogaster*. EMBO J 7: 1081-1088

Biessmann H, Carter SB and Mason J M (1990a) Chromosome ends in *Drosophila* without telomeric sequences. Proc Natl Acad Sci USA 87: 1759-1761

Biessmann H, Mason JM, Kristian, F, d'Hulst M, Valgeirsdottir, Traverse KL and Pardue ML (1990b) Addition of telomere-associated Het DNA sequences "heals" broken chromosome ends in *Drosophila*. Cell 61: 663-673

Biessmann H, Valgeirsdottir K, Lofsky A, Chin C, Ginther B, Levis RW, Pardue ML (1992a) HeT-A, a transposable element specifically involved in "healing" broken chromosome ends in *Drosophila melanogaster*. Mol Cell Biol 12(9): 3910-8

Biessmann H, Champion LE, O'Hair M, Ikenaga K, Kasravi B and Mason JM (1992b) Frequent transpositions of *Drosophila melanogaster* Het-A transposable elements to receding chromosome ends. EMBO J 11: 4459-4469

Biessmann H and Mason JM (1994) Telomeric repeat sequences. Chromosoma 103: 154-161

Biessmann H, Kasravi B, Bui T, Fugiwara G, Champion LE and Mason JM (1994) Comparison of two active Het-A retroposons of *Drosophila melanogaster*. Chromosoma 103: 90-98

Biessmann H and Mason JM (1997) Telomere maintenance without telomerase. Chromosoma 106: 63-69

Blackburn EH and Gall JG (1978) A tandemly repeated sequence at the termini of the extrachromosomal ribosomal RNA genes in *Tetrahymena*. J Mol Biol 120: 33-53

Blackburn EH and Chiou S (1981) Non-nucleosomal packaging of a tandemly repeated DNA sequence at termini of extrachromosomal DNA coding for the rRNA of *Tetrahymena*. Proc Natl Acad Sci 78: 2263-2267

Blackburn EH (2000) Telomere states and cell fates. Nature 408: 53-56

Blasco MA, Lee HW, Hande MP, Samper E, Lansdorp PM, DePinho RA and Greider CW (1997) Telomere shortening and tumor formation by mouse cells lacking telomerase RNA. Cell 91: 25-34

Bodnar AG, Ouellette M, Frolkis M, Holt SE, Chiu CP, Morin GB, Harley CB, Shay JW, Lichtsteiner S and Wright WE (1998) Extension of life span by introduction of telomerase into normal human cells. Science 279: 349-352

Bouffler S, Silver A and Cox R (1993) The role of DNA repeats and associated secondary structures in genomic instability and neoplasia. Bioessays 15: 409-412

Boulton SJ and Jackson SP (1998) Components of the Ku-dependent non-homologous end-joining pathway are involved in telomeric length maintenance and telomeric silencing. EMBO J 17(6): 1819-28

Bourns BD, Alexander MK, Smith AM and Zakian VA (1998) Sir proteins, Rif proteins, and Cdc13p bind *Saccharomyces* telomeres in vivo. Mol Cell Biol 18: 5600-5608

Boyd JB and Setlow RB (1976) Characterization of post-replication repair in mutagen-sensitive strains of *Drosophila melanogaster.* Genetics 84: 507-26

Breneman JW, Ramsey MJ, Lee DA, Eveleth GG, Minkler JL and Tucker JD (1993) The development of chromosome-specific composite DNA probes for the mouse and their application to chromosome painting. Chromosoma 102: 591-598

Bryan TM, Englezou A, Gupta J, Bacchetti S and Reddel RR (1995) Telomere elongation in immortal human cells without detectable telomerase activity. EMBO J 14: 4240-42.48

Bryan TM, Englezou A. Dalla-Pozza L, Dunham MA and Reddel RR (1997) Evidence for alternative mechanism for maintaining telomere length in human tumors and tumor-derived cell lines. Nat Med 3: 1271-1274

Bryan TM and Cech TR (1999) Telomerase and the maintenance of chromosome ends. Curr Opin Cell Biol 11: 318-324

Cardenas ME, Bianchi A and de Lange T (1993) A *Xenopus* egg factor with DNA-binding properties characteristic of terminus-specific telomeric proteins. Genes Dev 7: 883-894

Carmena M, Riparbelli MG, Minestrini G, Tavares AM, Adams R, Callaini G and Glover DM (1998) *Drosophila* Polo kinase is required for cytokinesis. J Cell Biol 143: 659-671

Cavalier-Smith T (1974) Palindromic base sequences and replication of eukaryotic chromosome ends. Nature 250: 467-470

Cenci G, Rawson RB, Belloni G, Castrillon DH, Tudor M, Petrucci R, Goldberg ML, Wasserman AS and Gatti M (1997) UbcD1, a *Drosophila* ubiquitin-conjugating enzyme required for proper telomere behaviour. Genes Dev 11: 863-875

Chan CS and Tye BK (1983a) A family of *Saccharomyces cerevisiae* repetitive autonomously replicating sequences that have very similar genomic environments. J Mol Biol 168: 505-523

Chan CS and Tye BK (1983b) Organization of DNA sequences and replication origins at yeast telomeres. Cell 33: 563-573

Chin L, Artandi SE, Shen O, Tam A, Lee SL, Gottlieb GJ, Greider CW and DePinho RA (1999) p53 deficiency rescues the adverse defects of telomere loss and cooperates with telomere dysfunction to accelerate carcinogenesis. Cell 97: 527-538

Choi KH and Choi BS (1994) Formation of hairpin structure by telomere 3' overhang. Biochem Biophys Acta 1217: 341-344

Chong L, van Steensel B, Broccoli D, Erdjument-Bromage H, Hanish J, Tempst P and de Lange T (1995) A human telomeric protein. Science 270: 1663-1667

Chua PR and Roeder GS (1997) Tam1, a telomere-associated meiotic protein, functions in chromosomes synapsis and crossover interference. Genes Dev 11: 1786-1800

Ciosk R, Zachariae W, Michaelis C, Shevchenko A, Mann M and Nasmyth K (1998) An ESP1/PDS1 complex regulates loss of sister chromatid cohesion at the metaphase to anaphase transition in yeast. Cell 93: 1067-1076

Clarke DJ and Giménez-Abián JF (2000) Checkpoints controlling mitosis. BioEssays 22: 351-363

Clute P and Pines J (1999) Temporal and spatial regulation of cyclin B destruction in metaphase. Nature Cell Biol 1: 82-87

Coelho PA, Queiroz-Machado J, Hartl D and Sunkel CE (1998) Pattern of chromosomal localization of the *Hoppel* transposable element family in *Drosophila melanogaster* subgroup. Chromosome Res 6: 385-395

Cohen-Fix O, Peters JM, Kirschner MW and Koshland D (1996) Anaphase initiation in *S. cerevisiae* is controlled by the APC-dependent degradation of the anaphase inhibitor Pds1p. Genes Dev 10: 3081-3093

Cohen LH and Gotchel BV (1971) Histones of polytene and nonpolytene nuclei of *Drosophila melanogaster*. J Biol Chem 246(6): 1841-8

Cohn M and Blackburn EH (1995) Telomerase in yeast. Science 269: 396-400

Coleman MJ, McHale MT, Arnau J, Watson A and Oliver RP (1993) Cloning and characterisation of telomeric DNA from *Cladosporium fulvum*. Gene 132: 67-73

Coleman TR, Tang Z and Dunphy WG (1993) Negative regulation of Wee1 protein kinase by direct action of nim1/cdr1 mitotic-inducer. Cell 72: 919-929

Collins K, Kobayashi R and Greider CW (1995) Purification of *Tetrahymena* telomerase and cloning of genes encoding the two protein components of the enzyme. Cell 81: 677-686

Collins K and Gandhi L (1998) The reverse transcriptase component of the *Tetrahymena* telomerase ribonucleoprotein complex. Proc Natl Acad Sci USA 95: 8485-8490

Conrad MN, Wright JH, Wolf AJ and Zakian VA (1990) RAP1 protein interacts with yeast telomeres *in vivo*: overproduction alters telomere structure and decreases chromosome stability. Cell 63: 739-750

Conrad MN, Dominguez AM and Dresser ME (1997) Ndjp, a meiotic telomere protein required for normal chromosome synapsis and segregation in yeast. Science 276: 1252-1255

Counter CM, Avilion AA, LeFeuvre CE, Stewart NG, Greider CW, Harley CB and Bacchetti S (1992) Telomere shortening associated with chromosome instability is arrested in immortal cells which express telomerase activity. EMBO J 11: 1929-1992

Counter CM, Hahn, WC, Wei W, Caddle SD, Beijersbergen RL, Lansdorp PM, Sedivy JM and Weinberg RA (1998) Dissociation among *in vitro* telomerase activity, telomere maintenance and cellular immortalisation. Proc Natl Acad Sci USA 95: 14723-14728

Cooke HJ, Brown WR and Rappold GA (1985) Hypervariable telomeric sequences from the human sex chromosomes are pseudoautosomal. Nature 317: 687-692

Cooper JP, Nimmo ER, Allshire RC and Cech TR (1997) Regulation of telomere length and function by a Myb-domain protein in fission yeast. Nature 385: 744-747

Cooper JP, Watanabe Y and Nurse P (1998) Fission yeast Taz1 protein is required for meiotic telomere clustering and recombination. Nature 392: 828-831

Cooper JP (2000) Telomere transitions in yeast: the end of the chromosome as we know it. Curr Opinion Gen Dev 10: 169-177

Cristofalo VJ, Allen RG, Pignolo RJ, Martin BG and Beck JC (1998) Relationship between donor age and the replicative lifespan of human cells in culture: a reevaluation. Proc Natl Acad Sci USA 95: 10614-10619

Danilevskaya ON, Petrov DA, Pavlova MA Koga A, Kurenova EV and Hartl DL (1992) A repetitive DNA element associated with telomeric sequences in *Drosophila melanogaster*, contains open reading frames. Chromosoma 102: 32-40

Danilevskaya ON, Lofsky A, Kurenova EV and Pardue ML (1993) The Y chromosome of *Drosophila melanogaster* contains a distinctive subclass of Het-A-related repeats. Genetics 134: 531-543

Danilevskaya ON, Slot F, Traverse KL, Hogan NC and Pardue ML (1994) The *Drosophila* telomere transposons Het-A produces a transcript with tightly bound protein. Proc Natl Acad Sci USA 91: 6679-6682

Danilevskaya ON, Arkhipova IR, Traverse KL and Pardue ML (1997) Promoting in tandem: the promoter for telomere transposons Het-A and implications for the evolution of retroviral LTRs. Cell 88: 647-655

Davis FM, Tsao TY, Fowler SK and Rao PN (1983) Monoclonal antibodies to mitotic cells. Proc Nat Acad Sci USA 80: 2924-2930

de Bruin D, Lanzer M and Ravetch JV (1994) The polymorphic subtelomeric regions of Plasmodium falciparum chromosomes contain arrays of repetitive sequence elements. Proc Natl Acad Sci 91:619-623

de Lange T (1995) Telomere dynamics and genome instability in human cancer. *In* Telomeres (ed. EH Blackburn and CW Greider). Cold Spring Harbor Laboratory Press. Cold Spring Harbor, NY,pp295-338

de Lange T and Jacks T (1999) For better or worse? Telomerase inhibition and cancer. Cell 98: 273-275

Deng H, Yoshiura K, Dirks RW, Harada N, Hirota T, Tsukamoto K, Yoshihiro J and Niikawa N (1992) Chromosome-band–specific painting: chromosome *in situ* suppression hybridisation using PCR products from a microdissected chromosome band as a probe pool. Hum Genet 89: 13-17

DePamphilis ML (2000) Review: Nuclear structure and DNA replication. J Struct Biol 129: 186-197

Dernburg AF, Sedat JW, Cande WZ and Bass HW (1995) Cytology of telomeres. *In* Telomeres (ed. EH Blackburn and CW Greider) Cold Spring Harbor Laboratory Press, Cold Spring Harbor, NY, pp295-338

Devault A, Martinez AM, Fesquet D, Labbé JC, Morin N, Tassan JP, Nigg EA, Cavadore JC and Dorée M (1995) MAT1 (ménage à trois) anew RING-Finger protein subunit stabilising cyclin H-cdk7 complexes in starfish and *Xenopus* CAK. EMBO J 14: 5027-5037

Diede SJ and Gottschling DE (1999) Telomerase-mediated telomere addition in vivo requires DNA primase and DNA polymerase alpha and delta. Cell 99: 723-733

Dunphy WG, Brizuela L, Beach D and Newport J (1988) The *Xenopus* cdc2 protein is a component of the MPF, a cytoplasmic regulator of mitosis. Cell 54: 423-431

El-Deiry WS, Harper JW, O'Connor PM, Velculescu VE, Canman CE, Jackman J, Pietenpol JA, Burrel M, Hill DE, Wang J, Wiman KG, Mercer WE, Kastan MB, Kohn KW, Elledge SJ, Kinzler KW and Vogelstein B (1994) Waf1/Cip1 is induced in p53-mediated G1 arrest and apoptosis. Cancer Res 54: 1169-1174

Emili A (1998) MEC1-dependent phosphorylation of Rad9p in response to DNA damage. Mol Cell : 173-182

Engels WR, Johnson-Schlitz DM, Eggleston WB, and Sved J (1990) High frequency P-element loss in *Drosophila* is homologue dependent. Cell 62: 515-525

Evans SK and Lundblad V (1999) Est1 and Cdc13 as comediators of telomerase access. Science 286: 117-120

Evans SK and Lundblad V (2000) Positive and negative regulation of telomerase access to the telomere. J Cell Science 113: 3357-3364

Evans T, Rosenthal ET, Youngblom J, Distel D and Hunt T (1983) Cyclin: A protein specified by maternal mRNA in sea urchin eggs that is destroyed at each cleavage division. Cell 33: 389-396

Fang G and Cech TR (1993) *Oxytricha* telomere-binding protein: DNA-dependent dimerization of the α and β subunits. Proc Natl Acad Sci 90: 6056-6060

Fang G and Cech TR (1995) Telomere proteins. *In* Telomeres (ed. EH Blackburn and CW Greider) Cold Spring Harbor Laboratory press. Cold Spring Harbor, NY, pp 69-105

Fang G, Yu H and Kirschner MW (1998) Direct binding of CDC20 protein family members activates the anaphase-promoting complex in mitosis and G1. Mol Cell 2: 163-171

Fanti L, Giovinazzo G, Berloco M and Pimpinelli S (1998) The heterochromatin protein 1 prevents telomere fusion in *Drosophila*. Mol Cell 2: 527-538

Featherstone C and Russel P (1991) Fission yeast p107 wee1 mitotic inhibitor is a tyrosine/serine kinase. Nature 349: 808-811

Feilotter H, Nurse P and Young PG (1991) Genetic and molecular analysis of cdr1-7nim1 in *S. pombe*. Genetics 127: 309-318

Fesquet D, Labbe JC, Derancourt J, Capony JP, Galas S, Girard F, Lorca T, Shuttleworth J, Doree M and Cavadore JC (1993) The MO15 gene encodes the catalytic subunit of a protein kinase that activates cdc2 and other cyclin-dependent kinases (CDKs) through phosphorylation of Thr 161 and its homologues. EMBO J 12: 3111-3121.

Fisher K, Scholl C, Salat J, Frohling S, Schlenk R, Bentz M, Stilgenbauer S, Lichter P and Dohner H. (1996) Design and validation of DNA probe sets for a comprehensive interphase cytogenetic analysis of acute myeloid leukemia. Blood 88(10): 3962-71

Fisher RP and Morgan DO (1994) A novel cyclin associates with MO15/CDK7 to form the CDK-activating kinase. Cell 78: 713-724

Fisher RP, Jin P, Chamberlain HM and Morgan DO (1995) Alternative mechanisms of CAK assembly require an assembly factor or an activating kinase. Cell 83: 47-57

Fitzgerald PH and Moris C (1984) Telomeric association of chromosomes in B-cell lymphoid leukemia. Hum Genet 67: 385-390

Flint J, Wilkie AO, Buckle VJ, Winter RM, Holland AJ and McDermid HE (1995) The detection of subtelomeric chromosomal rearrangements in idiopathic mental retardation. Nat Genet Feb 9(2): 132-40

Fogarty P, Kalpin RF and Sullivan W (1994) The *Drosophila* maternal effect mutation grapes causes a metaphase arrest at nuclear cycle 13. Development 120: 2131-2142

Forozan F, Karhu R, Kononen J, Kallioniemi A and Kallioniemi OP (1997) Genome screening by comparative genomic hybridisation. Trends Genet 13(10): 405-409

Frank-Kamenetskii M (1989) DNA structure. The turn of the quadruplex? Nature 342: 737

Friedberg EC, Walker GC and Siede W (1995) DNA repair and mutagenesis. Washington DC American Society for microbiology. pp 662-669

Froelich-Ammon SJ, Dickinson BA, Bevilacqua JM, Shultz SC and Cech TR (1998) Modulation of telomerase activity by telomere DNA binding proteins in *Oxytricha*. Genes Dev 12: 1504-1514

Gall JG (1995) Beginning of the end: origins of the telomere concept. *In* Telomeres (ed. EH Blackburn and CW Greider) Cold Spring Harbor Laboratory press. Cold Spring Harbor, NY, pp1-10

Gautier J, Norbury C, Lohka M, Nurse P and Maller J (1988) Purified maturation-promoting–factor contains the product of a *Xenopus* homologue of the fission yeast cell cycle control gene *cdc2+*. Cell 54: 433-439

Gerhart J, Wu M and Kirschner MJ (1984) Cell cycle dynamics of M phase-specific cytoplasmic factor in *Xenopus laevis* oocytes and eggs. J Cell Biol 98: 1247-1255

Gilson E, Roberge M, Giraldo R, Rhodes D and Gasser SM (1993) Distortion of the DNA double helix by RAP1 at silencers and multiple telomeric binding sites. J Mol Biol 231: 293-310

Girard F, Strausfeld U, Fernandez A and Lamb NJ (1991) Cyclin A is required for the onset of DNA replication in mammalian fibroblasts. Cell 67: 1169-1179

Glotzer M, Murray A and Kirschner MW (1991) Cyclin is degraded by the ubiquitin pathway. Nature 349: 132-138

Goldstein S (1990) Replicative senescence: the human fibroblasts comes of age. Science 249: 1129-1133

Gorbsky GJ and Ricketts WA (1993) Differential expression of a phosphoepitope at the kinetochores of moving chromosomes. J Cell Biol 122: 1311-1321

Gottschling DE and Cech TR (1984) Chromatin structure of the molecular ends of *Oxytricha* macronuclear DNA: Phased nucleosomes and a telomeric complex. Cell 38: 501-510

Gould KL and Nurse P (1989) Tyrosine phosphorylation of the fission yeast cdc2+ protein kinase regulates entry into mitosis. Nature 342: 39-45

Grandin N, Reed SI and Charbonneau M (1997) Stn1, a new *Saccharomyces cerevisiae* protein, is implicated in telomere size regulation in association with Cdc13. Genes Dev 11: 512-527

Gravel S, Larrivee M, Labrecque P and Wellinger RY (1998) Yeast Ku as a regulator of chromosomal DNA end structure. Science 280: 741-744

Greenberg RA, Allsopp RC, Chin L, Morin GB and DePinho RA (1998) Expression of mouse telomerase reverse transcriptase during development, differentiation and proliferation. Oncogene 16: 1723-1730

Greider CW (1995) Telomerase Biochemistry and Regulation. In *Telomeres* (ed. EH Blackburn and CW Greider) Cold Spring Harbor Laboratory press. Cold Spring Harbor, NY, pp35-68

Greider CW and Blackburn EH (1985) Identification of a specific telomere transferase activity in *Tetrahymena* extracts. Cell 43: 405-413

Greider CW and Blackburn EH (1989) A telomeric sequence in the RNA of *Tetrahymena* telomerase required for telomere repeat synthesis. Nature 337: 331-337

Greider CW (1996) Telomere length regulation Annu Rev Biochem 65: 337-365

Greider CW (1999) Telomerase activation. One step on the road to cancer? Trends Genet 15: 109-112

Griffith JD, Bianchi A and de Lange T (1998) TRF1 promotes parallel pairing of telomeric tracts *in vitro*. J Mol Biol 278: 79-88

Griffith JD, Comeau L, Rosenfield S, Stansel RM, Bianchi A, Moss H and de Lange T (1999). Mammalian telomeres end in a large duplex loop. Cell 97: 503-514

Guan XY, Meltzer PS and Trwent JM (1994) Rapid generation of whole chromosome painting probes (WCPs) by chromosome microdissection. Genomics 22(1): 101-107

Haber JE (1998) The many interfaces of Mre11. Cell 95: 583-586

Hagan I, Hayles J and Nurse P (1988) Cloning and sequencing of the cyclin-related cdc13+ gene and cytological study of its role in fission yeast mitosis. J Cell Sci 91: 587-595

Hahn WC, Stewart SA, Brooks MW, York SG, Eaton E, Kurachi A, Beijersbergen RL, Knoll JHM, Meyerson M and Weinberg RA (1999) Inhibition of telomerase limits the growth of human cancer cells. Nat Med 5: 1164-1170

Hardwick KG and Murray AW (1995) Mad1p, a phosphoprotein component of the spindle assembly checkpoint in budding yeast. J Cell Biol 131: 709-720

Hardwick KG, Weiss E, Luca FC, Winey M and Murray AW (1996) Activation of the budding yeast spindle assembly checkpoint without mitotic spindle disruption. Science 273: 953-956

Hardy CFJ, Balderes D and Shore D (1992) A RAP1-interacting protein involved in transcriptional silencing and telomere length regulation. Genes Dev 6: 801-814

Hari KL, Santerre A, Sekelsky JJ, McKim KS and Boyd JB (1995) The *mei-41* gene of *Drosophila melanogaster* is a structural homologue of the human ataxia telangiectasia gene. Cell 82: 815-821

Harley CG (1995) Telomeres and Aging. In *Telomeres* (ed. EH Blackburn and CW Greider) Cold Spring Harbor Laboratory press. Cold Spring Harbor, NY, pp247-263

Harrington JJ, Van Bokkelen G, Mays RW, Gustashaw K and Willard HF (1997) Formation of *de novo* centromeres and construction of first-generation human artificial microchromosomes. Nat Genet 15(4): 345-55

Harrington L, Zhou W, McPhail T, Oulton R, Yeung DS, Mar V, Bass MB and Robinson MO (1997) Human telomeres contains evolutionary conserved catalytic and structural subunits. Genes Dev 11: 3109-3115

Hartl DL and Lozovskaya ER (1995) The *Drosophila* genome map: a practical guide. Berlin: Springer-Verlag

Hartwell LH and Kastan MB (1994) Cell cycle control and Cancer. Science 266:1821-1828.

Hastie ND and Allshire RC (1989) Human telomeres: fusion and interstitial sites. Trends Genet 5: 326-331

Hayflick L (1965) The limited *in vitro* lifetime of human diploid cell strains. Exp Cell Res 37: 614-636

Hecht A, Strahl-Bolsinger S, Gasser SM and Grunstein M (1996) Spreading of transcriptional repressor SIR3 from telomeric heterochromatin. Nature 383: 92-95

Heino TI, Saura AO and Sorsa V (1994) Maps of the salivary gland chromosomes of *Drosophila melanogaster*. Drosophila Information Service (73)

Hemminki A, Tomlinson I, Markie D, Jarvinen H, Sistonen P, Bjorkqvist AM, Knuutila S, Salovaara R, Bodmer W, Shibata D, de la Chapelle A and Aaltonen LA. (1997) Localization of a susceptibility locus for Peutz-Jeghers syndrome to 19p using comparative genomic hybridization and targeted linkage analysis. Nat Genet 15(1): 87-90

Henderson EH, Hardin CC, Walk SK, Tinoco IJ and Blackburn EH (1987) Telomeric DNA oligonucleotides form novel intramolecular structures containing guanine-guanine base pairs. Cell 51: 899-908

Henderson EH, Larson D, Melton W, Shampay J, Spangler E, Greider C, Ryan T and Blackburn EH (1988) Structure, synthesis and regulation of telomeres. Cancer Cells 6: 453-461

Henderson E (1995) Telomere DNA structure. In *Telomeres* (ed. EH Blackburn and CW Greider) Cold Spring Harbor Laboratory press. Cold Spring Harbor, NY pp11-34

Herbert BS, Pitts AE, Baker SI, Hamilton SE, Wright WE, Shay JW and Corey DR (1999) Inhibition of human telomerase in immortal human cells leads to progressive telomere shortening and cell death. Proc Natl Acad Sci USA 96: 14276-14281

Herrmann S, Amorim I and Sunkel CE (1998) The POLO kinase is required at multiple stages during spermatogenesis in *Drosophila melanogaster*. Chromosoma 107: 440-451

Hochstrasser M, Mathog D, Gruenbaum Y, Saumweber H and Sedat J (1986) Spatial organization of chromosomes in the salivary gland nuclei of *Drosophila melanogaster*. J Cell Biol 102: 112-123

Hochstrasser M (1996) Ubiquitin dependent protein degradation. Annu Rev Genet 30: 405-439

Holt SE, Wright WE and Shay JW (1996) Regulation of telomerase activity in immortal cell lines. Mol Cell Biol 16: 2932-2939

Holt SE, Aisner DL, Baur J, Tesmer VM, Dy M, Ouellette M, Trager JB, Morin GB, Toft DO, Shay JW, Wright WE and White MA (1999) Functional requirement of p23 and Hsp90 in telomerase complexes. Genes Dev 13(7): 817-826

Horvath MP, Schweiker VL, Bevilacqua JM, Ruggles JA and Schultz SC (1998) Crystal structure of the *Oxytricha nova* telomere end binding protein complexed with single strand DNA. Cell 95: 963-974

Hoyt MA, Totis L and Roberts BT (1991) *S. cerevisiae* genes required for cell cycle arrest in response to loss of microtubule function. Cell 66: 507-517

Hughes TR, Evans SK, Weilbaecher RG and Lundblad V (2000) The Est3 protein is a subunit of yeast telomerase. Curr Biol 10: 809-812

Hwang LH, Lau LF, Smith DL, Mistrot CA, Hardwick KG, Hwang ES, Amon A and Murray AW (1998) Budding yeast Cdc20: a target of the spindle checkpoint. Science 279: 1041-1044

Innis MA, Myambo KB, Gelfand DH and Brow (1988) DNA sequencing with Thermus aquaticus DNA polymerase and direct sequencing of polymerase chain reaction-amplified DNA. Proc Natl Acad Sci USA 85: 9436-9440

Izumi T, Walker DH and Maller JL (1992) Periodic changes in phosphorylation of the *Xenopus* cdc25 phosphatase regulate its activity. Mol Biol Cell 3: 927-939

Izumi T and Maller JL (1993) Elimination of cdc2 phosphorylation sites in the cdc25 phosphatase blocks initiation of M phase. Mol Biol Cell 4: 1337-1350

Jaspersen SL, Charles JF and Morgan DO (1999) Inhibitory phosphorylation of the APC regulator Hct1 is controlled by the kinase Cdc28 and the phosphatase Cdc14. Curr Biol 9: 227-236

Jeggo AP, Taccioli GE and Jackson SP (1995) Menage à trois: double strand break repair, V(D)J recombination and DNA-PK. BioEssays 17: 949-957

Jiang XR, Jimenez G, Chang E, Frolkis M, Kusler B, Sage M, Beeche M, Bodnar AG, Wahl GM, Tisty TD and Chiu CP (1999) Telomerase expression in human somatic cells does not induce changes associated with a transformed phenotype. Nat Genet 21: 111-114

Johnson RT and Rao PN (1970) Mammalian cell fusion: induction of premature chromosome condensation in interphase nuclei. Nature 226: 717-722

Jorgensen PM, Brundell E, Starborg M and Hoog C (1998) A subunit of the anaphase-promoting complex is a centromere-associated protein in mammalian cells. Mol Cell Biol 18:468-476

Kamnert I, Lopez CC, Rosen M and Edstrom JE (1997) Telomeres terminating in long complex tandem repeats. Hereditas 127: 175-180

Kamnert I, Nielsen L and Edstrom JE (1998) A concertedly evolving region in *Chironomus*, unique within the telomere. J Mol Evol 46: 562-570

Kang SS, Kwon T, Kwon DY and Do SI (1999) Akt protein kinase enhances human telomerase activity through phosphorylation of telomerase reverse transcriptase subunit. J Biol Chem 274: 13085-13090

Karlseder J, Broccoli D, Dai Y, Hardy S and de Lange T (1999) p53 and ATM-dependent apoptosis induced by telomeres lacking TRF2. Science 283: 1321-1325

Karpen GH and Spradling AC (1992) Analysis of subtelomeric heterochromatin in the *Drosophila* minichromosome Dp1187 by single P element insertional mutagenesis. Genetics 132: 737-753

Katinka MD and Bourgain FM (1992) Interstitial telomeres are hotspots for illegitimate recombination with DNA molecules injected into the macronucleus of *Paramecium primaurelia*. EMBO J 11: 725-732

Kilian A, Bowtell DDL, Abud HE, Hime GR, Venter DJ, Keese PK, Duncan EL, Reddel RR and Jefferson RA (1997) Isolation of a candidate human telomerase catalytic subunit gene, which reveals complex splicing patterns in different cell types. Hum Mol Genet 6: 2011-2019

Kim S, Kaminker P and Campisi J (1999) TIN2, a new regulator of telomere length in human cells. Nat Genet 23: 405-412

King RW, Jackson PK and Kirschner MW (1994) Mitosis in transition. Cell 79: 563-571

King RW, Peters JM, Tugendreich S, Rolfe M, Heiter P and Kirshner MW (1995) A20S complex containing CDC27 and CDC16 catalyzes the mitosis-specific conjugation of ubiquitin to cyclin B. Cell 81: 279-288

Kiser GL and Weinert TA (1996) Distinct roles of yeast MEC and RAD checkpoint genes in transcriptional induction after DNA damage and implications for function. Mol Biol Cell 7: 703-718

Klobutcher LA, Swanton MT, Donini P and Prescott DM (1981) All gene-sized DNA molecules in four species of hypotrichs have the same terminal sequence and an unusual 3' terminus. Proc Natl Acad Sci. 78: 3015-3019

Kondo T, Matsumoto K and Sugimoto K (1999) Role of a complex containing Rad17, Mec3 and Ddc1 in the yeast DNA damage checkpoint pathway. Mol Cell Biol 19: 1136-1143

Kovacs G, Muller-Brechlin R and Szucs S (1987) Telomeric association in two human renal tumors. Cancer Genet Cytogenet 28: 363-366

Krek W and Nigg EA (1991) Mutations of p34cdc2 phosphorylation sites induce premature mitotic events in HeLa cells: evidence for double block to p34 cdc2 kinas activation in vertebrates. EMBO J 10: 3331-3341

Kuang J and Ashorn CL (1993) At least two kinases phosphorylate the MPM-2 epitope during *Xenopus* oocyte maturation. J Cell Biol 123: 859-868

Kumagai A and Dunphy WG (1996) Purification and molecular cloning of Plx1, a cdc25-stimulatory kinase from *Xenopus* egg extracts. Science 273: 1377-1380

Kyrion G, Boakye KA and Lustig AJ (1992) C-terminal truncation of *RAP1* results in the deregulation of telomere size, stability and function in *Saccharomyces cerevisiae*. Mol Cell Biol 12: 5159-5173

Lee HW, Blasco MA, Gottlieb GJ, Horner JW, Greider CW and DePinho RA (1998) Essential role of mouse telomerase in highly proliferative organs. Nature 392: 569-574

Lendvay TS, Morris DK, Sah J, Balasubramanian B and Lundblad V (1996) Senescence mutants of *Saccharomyces cerevisiae* with a defect in telomere replication identify three additional EST genes. Genetics 144: 1399-1412

Levis RW (1989) Viable deletions of a telomere from a *Drosophila* chromosome. Cell 58: 791-801

Levis RW, Ganesan R, Houtchens K, Tolar LA and Sheen FM (1993) Transposons in place of telomeric repeats at a *Drosophila* telomere. Cell 75: 1083-1093

Li H, Zhao L, Yang Z, Funder JW and Liu J (1998) Telomerase is controlled by protein kinase C in human breast cancer cells. J Biol Chem 273: 33436-33442

Li R and Murray Aw (1991) Feedback control of mitosis in budding yeast. Cell 66: 519-531

Li R, Waga S, Hannon GJ, Beach D and Stillman B (1994) Differential effects by the p21 CDK inhibitor on PCNA-dependent DNA replication and repair. Nature 371: 534-537

Lieber MR, Grawunder U, Wu X and Yaneva M (1997) Tying loose ends: roles of Ku and DNA-dependent protein kinase in the repair of double strand breaks. Curr Opin Genet Dev 7: 99-104

Lin JJ and Zakian VA (1996) The *Saccharomyces* CDC13 protein is a single-strand TG1-3 telomeric DNA-binding protein *in vitro* that affects telomere behaviour *in vivo*. Proc Natl Acad Sci USA 93: 13760-13765

Lingner J and Cech TR (1996) Purification of telomerase from *Euplotes aediculatus*: requirement of a primer 3' overhang. Proc Natl Acad Sci USA 93: 10712-10717

Lingner J, Hughes TR, Shevchenko A, Mann M, Lundblad V and Cech TR (1997a) Reverse transcriptase motifs in the catalytic subunit of telomerase. Science 276: 561-567

Lingner J, Cech TR, Hughes TR and Lunblad V (1997b) Three Ever Shorter Telomere (*EST*) genes are dispensable for in vitro yeast telomerase activity. Proc Nat Acad Sci USA 94: 11190-11195

Lipps HJ, Gruissem W and Prescott DM (1982) Higher order DNA structure in macronuclear chromatin of the hypotrichous ciliate *Oxytricha nova*. Proc Natl Acad Sci 79: 2495-2499

Liu K, Schoonmaker MM, Levine BL, June CH, Hodes RJ and Weng N (1999) Constitutive and regulated expression of telomerase reverse transcriptase (hTERT) in human lymphocytes. Proc Natl Acad Sci USA 96: 5147-5152

Logarinho E and Sunkel CE (1998) The *Drosophila* POLO kinase localises to multiple compartments of the mitotic apparatus and is required for the phosphorylation of MPM2 reactive epitopes. J Cell Science 111: 2897-2909

Lohka ML, Hayes MK and Maller J (1988) Purification of maturation promoting factor, an intracellular regulator of mitotic events. Proc Natl Acad Sci USA 85: 3009-3013.

Longhese MP, Fraschini R, Plevani P and Lucchini G (1996) Yeast pip3/mec3 mutants fail to delay entry into S phase and to slow DNA replication in response to DNA damage, and they define a functional link between Mec3 and DNA primase. Mol Cell Biol 16: 3235-3244

Longhese MP, Paciotti V, Neecke H and Lucchini G (2000) Checkpoint proteins influence telomeric silencing and length maintenance in budding yeast. Genetics 155: 1577-1591

Louis EJ and Haber JE (1992) The structure and evolution of subtelomeric Y' repeats in *Saccharomyces cerevisiae*. Genetics 131:559-574

Luan DD, Korman MH, Jakubczak JL and Eickbush TH (1993) Reverse transcriptase of R2Bm RNA is primed by a nick at the chromosomal target site: a mechanism for non-LTR retrotransposition. Cell 72: 595-605

Lundblad V and Szostak JW (1989) A mutant with a defect in telomere elongation leads to senescence in yeast. Cell 57: 633-643

Lundblad V and Wright WE (1996) Telomeres and telomerase: a simple picture becomes complex. Cell 87: 369-375

Lundblad V and Blackburn EH (1993) An alternative pathway for yeast telomere maintenance rescues *est1*-senescence. Cell 73: 347-360

Lyndall D and Weinert T (1995) Yeast checkpoint genes in DNA damage processing: implications for repair and arrest. Science 270: 1488-1491

Maercker C and Lipps HJ (1993) Analysis of the subtelomeric regions of macronuclear gene-sized DNA molecules of the hypotrichous ciliate *Stylonychia lemnae*: Implications for the DNA fragmentation process during macronuclear development? Dev Genet 14: 378-384

Makarov VL, Lejnine S, Bedoyan J and Langmore JP (1993) Nucleosomal organization of telomere specific chromatin in rat. Cell 73: 775-787

Mandahl N, Heim S, Arheden K, Rydholm A, Willen H and Mitelman F (1988) Rings, dicentrics and telomeric association in histiocytomas. Cancer Genet Cytogenet 30: 23-33

Maniatis et al (1989) Molecular cloning: a laboratory manual, 2nd ed., Cold Spring Harbor Laboratory press

Mantell LL and Greider CW (1994) Telomerase activity in germline and embryonic cells in *Xenopus*. EMBO J 13: 3211-3217

Marcand S, Gilson E and Shore D (1997) A protein-counting mechanism for telomere length regulation in yeast. Science 275: 986-990

Martin SG, Laroche T, Suka N, Grunstein M and Gasser SM (1999) Relocalization of telomeric Ku and SIR proteins in response to DNA strand breaks in yeast. Cell 97: 621-633

Mason JM and Biessmann H (1995) The unusual telomeres of *Drosophila*. Trends Genet 11: 58-62

Matsumoto T, Fukui K, Niwa O, Sugawara N, Szostak JW and Yanagida M (1987) Identification of healed terminal DNA fragments in linear minichromosomes of *Schizosaccharomyces pombe*. Mol Cell Biol 7: 4424-4430

McAinsh AD, Scott-Drew S, Murray JAH and Jackson SP (1999) DNA damage triggers disruption of telomeric silencing and Mec1p-dependent relocation of Sir3p. Curr Biol 9: 963-966

McClintock B (1941) The stability of broken ends of chromosomes in *Zea mays*. Genetics 26: 234-282

McClintock B (1942) The fusion of broken ends of chromosomes following nuclear fusion. Proc Natl Acad Sci USA 28: 458-463

McEachern MJ and Blackburn EH (1994) A conserved sequence motif within the exceptionally diverse telomeric sequences of budding yeasts. Proc Natl Acad Sci 91: 3453-3457

McEachern MJ and Blackburn EH (1996) Cap-prevented recombination between terminal telomeric repeat arrays (telomere cpr) maintains telomeres in *Kluyveromyces lactis* lacking telomerase. Genes Dev 10: 1822-1834

Mills KD, Sinclair DA and Guarente L (1999) MEC1-dependent redistribution of the Sir3 silencing proteins from telomeres to DNA double strand breaks. Cell 97: 609-620

Mitchell JR, Cheng J, and Collins K (1999a) A box H/ACA small nucleolar RNA like domain at the human telomerase RNA 3' end. Mol Cell Biol 19: 567-576

Mitchell JR, Wood E and Collins K (1999b) A telomerase component is defective in the human disease dyskeratosis congenital. Nature 402: 551-555

Morales CP, Holt SE, Ouellette M, Kaur KJ, Yan Y, Wilson KS, White MA, Wright WE and Shay JW (1999) Absence of cancer-associated changes in human fibroblasts immortalized with telomerase. Nat Genet 21: 115-118

Moretti P, Freeman K, Coodly L and Shore D (1994) Evidence that a complex of SIR proteins interact with the silencer and telomere-binding protein RAP1. Genes Dev 8: 2257-2269

Morin GB (1989) The human telomere terminal transferase enzyme is a ribonucleoprotein that synthesises TTAGGG repeats. Cell 59: 521-529

Morgan, DO (1999) Regulation of the APC and the exit from mitosis. Nature Cell Biol 1: E47-E53

Muller HJ (1938) The remaking of chromosomes. Collecting Net 13: 182-198

Muller HJ (1941) Induced mutations in *Drosophila*. Cold Spring Harbor Symp Quant Biol 9: 151-167

Muller F, Wicky C, Spicher A, and Tobler H (1991) New telomere formation after developmentally regulated chromosomal breakage during the process of chromatin diminution in *Ascaris lumbricoides*. Cell 67: 815-822

Muller R, Mumberg D and Lucibello FC (1993) Signals and genes in the control of cell cycle progression. Biochem Biophys Acta 1155: 151-179

Murray AW and Hunt T (1993) The cell cycle: An introduction. pp1-251. Freeman and Company, New York

Murray A (1995) Cyclin ubiquitination: the destructive end of mitosis. Cell 81: 149-152

Nakamura TM, Morin GB, Chapman KB, Weinrich SL, Andrews WH, Lingner J, Harley CB and Cech TR (1997) Telomerase catalytic subunit homologs from fission yeast and human. Science 277: 955-959

Navas TA, Zhou Z and Elledge SJ (1995) DNA polymerase ε links the DNA replication machinery to the S phase checkpoint. Cell 80: 29-39

Navas TA, Sanchez Y and Elledge SJ (1996) *RAD9* and DNA polymerase ε form parallel sensory branches for transducing the DNA damage checkpoint signal in *S. cerevisiae*. Genes Dev 10: 2632-2643

Neufeld TP and Rubin GM, (1994) The *Drosophila* peanut gene is required for cytokinesis and encodes a protein similar to yeast putative bud neck filament proteins. Cell 77: 371-379

Nicklas RB, Ward SC and Gorbsky GJ (1995) Kinetochore chemistry is sensitive to tension and may link mitotic forces to a cell cycle checkpoint. J Cell Biol 130: 929-939

Nigg EA (1995) Cyclin-dependent protein kinases: key regulators of the eucaryote cell cycle. Bioessays 17: 471-480

Nigg EA (1998) Polo-like kinases: positive regulators of cell division from start to finish. Curr. Opinion Cell Biol 10: 776-783

Nimmo ER, Pidoux AL, Perry PE and Allshire RC (1998) Defective meiosis in telomere-silencing mutants of *Schizosaccharomyces pombe*. Nature 392: 825-828

Nisson P, Watkins P, Meninger J and Ward D (1992) Improved suppression hybridisation with human DNA (Cot-1 DNA) enriched for repetitive DNA sequences. Focus 13(2): 42-45

Nugent CI, Hughes TR, Lue NF and Lundblad V (1996) Cdc13p: a single-strand telomeric DNA binding protein with a dual role in yeast telomere maintenance. Science 274: 249-252

Ohkura H, Hagan IM and Glover DM (1995) The conserved *S. pombe* kinase plo1, required to form a bipolar spindle, the actin ring, and septum, can drive septum formation in G1 and G2 cells. Genes Dev 9: 1059-1073

Oka Y, Shiota S, Nakai S, Nishida Y and Okubo S (1980) Inverted terminal repeat sequence in the macronuclear DNA of *Stylonychia pustulata*. Gene 10: 301-306

Oka Y and Thomas CA (1987) The cohering telomeres of *Oxytricha*. Nucleic Acids Res 15: 8877-8898

Ostler EL, Wallis CV, Aboalchamat B and Faragher RG (2000) Telomerase and the cellular lifespan: implications of the aging process. J Pediatr Endocrinol Metab 13:1467-76

Paciotti V, Lucchini G, Plevani P and Longhese MP (1998) Mec1p is essential for phosphorylation of the yeast DNA damage checkpoint protein Ddc1p, which physically interacts with mec3p. EMBO J 17(14):4199-209

Pan ZQ, Amin A and Hurwitz J (1993) Characterization of the *in vitro* reconstituted cyclin A or B1- dependent cdk2 and cdc2 kinase activities. J Biol Chem 268: 20443-20451

Pardee AB (1989) G1 events and regulation of cell proliferation. Science 246: 603-608

Pardue ML (1995) *Drosophila* telomeres: Another way to end it all. In Telomeres (ed. EH Blackburn and CW Greider). Cold Spring Harbor Laboratory Press, Cold Spring Harbor, New York, NY, pp 339-370

Pardue ML and DeBaryshe PG (1999) Telomeres and telomerase: more than the end of the line. Chromosoma 108: 73-82

Paulovich AG, Margulies RU, Garvik BM and Hartwell LH (1997a) RAD9, RAD17 and RAD24 are required for S phase regulation in *S. cerevisiae* in response to DNA damage. Genetics 145: 45-62

Paulovich AG, Toczyski DP and Hartwell LH (1997b) When checkpoints fail. Cell 88: 315-321

Perdigão J (1997) Análise genética e molecular de genes envolvidos no ciclo celular de *Drosophila melanogaster*. PhD Thesis.

Pluta AF, Kaine BP and Spear BB (1982) The terminal organization of macronuclear DNA in *Oxytricha fallax*. Nucleic Acids Res 10: 8145-8154

Pluta AF, Cooke CA and Earnshaw WC (1990) Structure of the human centromere at metaphase. TIBS 15: 181-185

Pologe LG and Ravetch JV (1988) Large deletions result from breakage and healing of *P. falciparum* chromosomes. Cell 55: 869-874

Polotnianka RM, Li J and Lustig AJ (1998) The yeast Ku heterodimer is essential for protection of the telomere against nucleolytic and recombinational activities. Curr Biol 8: 831-834

Poon RY, Yamashita K, Adamczewski JP, Hunt T and Shuttleworth J (1993) The cdc2-related protein p40 MO15 is the catalytic subunit of a protein kinase that can activate $p33^{cdk2}$ and $p34^{cdc2}$. EMBO J 12: 3123-3132

Prescott J and Blackburn EH (1997) Telomerase RNA mutations in *Saccharamyces cerevisiae* alter telomerase action and reveal nonprocessivity *in vivo* and *in vitro*. Genes Dev 11: 528-540

Price CM and Cech TR (1987) Telomeric DNA-protein interactions of *Oxytricha* macronuclear DNA. Genes Dev 1: 783-793

Price CM and Cech CR (1989) Properties of the telomeric DNA-binding protein from *Oxytricha nova*. Biochemistry 28: 769-774

Prowse KR, Avilion AA and Greider CW (1993) Identification of a nonprocessive telomerase activity from mouse cells. Proc Natl Acad Sci USA 90: 1493-1497

Qi H and Zakian VA (2000) The Saccharomyces telomere-binding protein Cdc13p interacts with both the catalytic subunit of DNA polymerase alpha and the telomerase-associated Est1 protein. Genes Dev 14: 1777-1788

Ray A and Runge K (1998) The C terminus of the major yeast telomere binding protein Rap1p enhances telomere formation. Mol Cell Biol 18: 1284-1295

Ray A and Runge K (1999) The yeast telomere length counting machinery is sensitive to sequences at the telomere-nontelomere junction. Mol Cell Biol 19(1): 31-45

Rao PN and Johnson RT Mammalian cell fusion studies on the regulation of DNA synthesis and mitosis. Nature 225: 159-164

Reddel RR (1998) A reassessment of the telomere hypothesis of senescence. BioEssays 20: 977-984

Resnitzy D, Gossen M, Bujard H and Reed SI (1994). Acceleration of G1/S phase transition by expressing of cyclins D1 and E with an inducible system. Mol Cell Biol 14: 1669-1679

Rieder CL (1982) The formation, structure and composition of the mammalian kinetochore and kinetochore fiber. Int Rev Cytol 79: 1-58

Rieder CL, Cole RW, Khodjakov A and Sluder G (1995) The checkpoint delaying anaphase in response to chromosome monoorientation is mediated by an inhibitory signal produced by unattached kinetochores. J Cell Biol 130: 941-948

Rieder CL, Khodjakov A, Paliulis LV, Fortier TM, Cole RW and Sluder G (1997) Mitosis in vertebrate somatic cells with two spindles implications for the metaphase/anaphase transition checkpoint and cleavage. Proc Natl Acad Sci USA 94: 5107-5112

Rockmill B and Roeder GS (1998) Telomere-mediated chromosome pairing during meiosis in budding yeast. Genes Dev. 12: 2574-2586

Roy J, Fulton TB and Blackburn EH (1998) Specific telomerase RNA residues distant from the template are essential for telomerase function. Genes Dev 12: 3286-3300

Rudolph KL, Chang S, Lee HW, Blasco M, Gottlieb GJ, Greider C and DePinho RA (1999) Longevity, stress response and cancer in aging telomerase-deficient mice. Cell 96: 701-712

Sachs RK, Hlatky LR and Trask BJ (2000) Radiation-produced chromosome aberrations: Colourful clues. Trends Genet 16(4): 143-146

Saltman D, Morgan R, Cleary ML, de Lange T (1993) Telomeric structure in cells with chromosome end associations. Chromosoma 102(2): 121-128

Sanchez Y, Bachant J, Wang H, Hu F, Liu D, Tetzlaff M and Elledge S (1999) Control of the DNA damage checkpoint by Chk1 and Rad53 protein kinases through distinct mechanisms. Science 286:1166-1171

Sandell LL and Zakian VA (1993) Loss of a yeast telomere: arrest, recovery and chromosome loss. Cell 75: 729-739

Savitsky K Bar-Shira A, Gilad S, Rotman G, Ziv Y, Vanagaite L, Tagle DA, Smith S, Uziel T, Sfez S, et al. (1995) A single ataxia telangiectasia gene with a product similar to PI-3 kinase. Science 286: 1749-1753

Schild D and Byers B (1980) Diploid spore formation and other meiotic effects of two cell division cycle mutations of *Saccharomyces cerevisiae*. Genetics 96: 859-876

Schrock E, du Manoir S, Veldman T, Schoell B, Wienberg J, Ferguson-Smith MA, Ning Y, Ledbetter DH, Bar-Am I, Soenksen D, Garini Y and Ried T (1996) Multicolor spectral karyotyping of human chromosomes. Science 273(5274): 494-497

Shay JW, Pereira-Smith O and Wright WE (1991) A role for both Rb and p53 in the regulation of human cellular senescence. Exp Cell Res 196: 33-39

Sheen FM and Levis RW (1994) Transposition of the LINE-like retrotransposons TART to *Drosophila* chromosome termini. Proc Natl Acad Sci USA 91: 12510-12514

Shippen-Lentz D and Blackburn EH (1989) Telomere terminal transferase activity from *Euplotes crassus* adds large numbers of TTTTGGGG repeats onto telomeric primers. Mol Cell Biol 9: 2761-2764

Shippen DE, Blackburn EH and Price CM (1994) DNA bound by the *Oxytricha* telomere protein is accessible to telomerase and other DNA polymerases. Proc Natl Acad Sci USA 91: 405-409

Shore D (1994) RAP1: a protein regulator in yeast. Trends Genet 10(11): 408-12

Shore D (1997) Telomere length regulation: getting the measure of chromosome ends. Biol Chem 378: 591-597

Shuttleworth J, Godfrey R and Colman A (1990) P40 MO15, a cdc2-related protein kinase involved in negative regulation of meiotic maturation of *Xenopus* oocytes. EMBO J: 3233-3240

Sidorova JM and Breeden LL (1997) Rad53-dependent phosphorylation of Swi6 and down-regulation of *CLN1* and *CLN2* transcription occur in response to DNA damage in *Saccharomyces cerevisiae*. Genes Dev 11: 3032-3045

Siede W, Friedberg AS and Friedberg EC (1993) RAD9-dependent G1 arrest defines a second checkpoint for damaged DNA in the cell cycle of *S. cerevisiae*. Proc Natl Acad Sci USA 90: 7985-7989

Singer MS and Gottschling DE (1994) *TLC1*: template RNA component of *Saccharomyces cerevisiae* telomerase. Science 266: 404-409

Smith S, Giriat I, Schmitt A and de Lange T (1998) Tankyrase, a poly(ADP-ribose) polymerase at human telomeres. Science 282: 1484-1487

Smorgorzewska A, van Steensel B, Bianchi A, Oelmann S, Schaefer MR, Schnapp G and de Lange T (2000) Control of human telomere length by TRF1 and TRF2. Mol Cell Biol 20: 1659-1668

Soder AI, Hoare SF, Muir S, Going JJ, Parkinson EK and Keith WN (1997) Amplification, increased dosage and *in situ* expression of the telomerase RNA gene in human cancer. Oncogene 14(9): 1013-1021

Solomon MJ, Glotzer M, Lee TH, Philipe M and Kirschner MW (1990) Cyclin activation of $p34^{cdc2}$. Cell 63: 1013-1024

Solomon MJ, Harper JW and Shuttleworth J (1993) CAK, the p34 ^{cdc2} activating kinase, contains a protein identical or closely related to p40^{MO15}. EMBO J 12: 3133-3142

Speicher MR, du Manoir S, Schrock E, Holtgreve-Grez H, Schoell B, Lengauer C, Cremer T and Ried T (1993) Molecular cytogenetic analysis of formalin-fixed, paraffin-embedded solid tumors by comparative genomic hybridization after universal DNA-amplification. Hum Mol Genet 2(11): 1907-1914

Speicher MR, Jauch A, Walt H, du Manoir S, Ried T, Jochum W, Sulser T and Cremer T (1995) Correlation of microscopic phenotype with genotype in a formalin-fixed, paraffin-embedded testicular germ cell tumor with universal DNA amplification, comparative genomic hybridization, and interphase cytogenetics. Am J Pathol 146(6): 1332-1340

Speicher MR, Gwyn Ballard S and Ward DC (1996) Karyotyping human chromosomes by combinatorial multi-fluor FISH. Nat Genet 12(4): 368-75

Steensel B, Smogorzewska A and de Lange T (1998) TRF2 protects human telomeres from end-to-end fusions. Cell 92: 401-413

Sternberg N, Ruether J, deReil K (1990) Generation of a 50 000-member human DNA library with an average insert size of 75-100 kb in a bacteriophage P1 cloning vector. New Biologist 2: 151-162

Sugimoto K, Shimomura T, Hashimoto K, Araki H, Sugino A and Matsumoto K (1996) Rfc5, a small subunit of replication factor C complex, couples DNA replication and mitosis in budding yeast. Proc Natl Acad Sci USA 93: 7048-7052.

Sun Z, Fay DS, Marini F, Foiani M and Stern DF (1996) Spk1/Rad53 is regulated by Mec1-dependent protein phosphorylation in DNA replication and damage checkpoint pathways. Genes Dev 10: 395-406

Sunkel CE and Glover DM (1988) *polo* a mitotic mutant of *Drosophila* displaying abnormal spindle poles. J Cell Sci 89: 25-38

Tassan JP, Jaquenou M, Fry AM, Frutiger S, Hughes G and Nigg EA (1995) *In vitro* assembly of a functional human cdk7-cyclin H complex requires MAT1, a novel 36 kDa ring finger protein. EMBO J 14: 5608-5617

Telenius H, Pelmear AH, Tunnacliffe A, Carter NP, Behmel A, Ferguson-Smith MA, Nordenskjold M, Pfragner R and Ponder BA (1992) Cytogenetic analysis by chromosome painting using DOP-PCR amplified flow-sorted chromosomes. Genes Chromosomes Cancer 4(3): 257-263

Terada Y, Tatsuka M, Jinno S and Okayama H (1995) Requirement for tyrosine phosphorylation of Cdk4 in G1 arrest induced by ultraviolet irradiation. Nature 376: 358-362

Tower J, Karpen GH, Craig N and Spradling AC (1993) Preferential transposition of *Drosophila* P-elements to nearby chromosomal sites. Genetics 133: 347-359

Traverso EE, Baskerville C, Liu Y, Shou W, James P, Deshaies RJ and Charbonneau H (2001) Characterization of the net1 cell cycle-dependent regulator of the Cdc14 phosphatase from budding yeast. J Biol Chem [epub ahead of print]

Tugendreich S, Tomkiel J, Earnshaw W and Hieter P (1995) CDC27Hs colocalizes with CDC16Hs to the centrosome and mitotic spindle and is essential for the metaphase to anaphase transition. Cell 81: 261-268

Uhlmann F, Lottspeich F and Nasmyth K (1999) Sister-chromatid separation at anaphase onset is promoted by cleavage of the cohesion subunit Scc1. Nature 400: 37-42

Ulaner GA, Hu J, Vu TH, Giudice LC and Hoffman AR (1998) Telomerase activity in human development is regulated by human telomerase reverse transcriptase (hTERT) transcription and by alternative splicing of hTERT transcripts. Cancer Res 58: 4168-4172

van Steensel B and de Lange T (1997) Control of telomere length by the human telomeric protein TRF1. Nature 385: 740-743

van Steensel B, Smogorzewska A and de Lange T (1998) TRF2 protects human telomeres from end-to-end fusions. Cell 92(3): 401-413

Vaziri H and Benchimol S (1998) Reconstitution of telomerase activity in normal human cells leads to elongation of telomeres and extended replicative life span. Curr Biol 8: 279-282

Vermeesch JR and Price CM (1994) Telomeric DNA sequence and structure following de novo telomere synthesis in *Euplotes crassus*. Mol Cell Biol 14(1): 554-66

Vialard JE, Gilbert CS, Green CM and Lowndes NF (1998) The budding yeast Rad9 checkpoint protein is subjected to Mec1/Tel1-dependent hyperphosphorylation and interacts with Rad53 after DNA damage. EMBO J 17: 5679-5688

Virta-Pearlman V, Morris DK and Lundblad V (1996) Est1 has the properties of a single-stranded telomere end-binding protein. Genes Dev. 10: 3094-3104

Visintin R, Prinz S and Amon A (1997) CDC20 and CDH1: a family of substrate specific activators of APC-dependent proteolysis. Science 278: 460-463

Walmsley RM, Chan CS, Tye BK and Petes TD (1984) Unusual DNA sequences associated with the ends of yeast chromosomes. Nature 310: 157-160

Wang J, Xie LY, Allan S, Beach D and Hannon GJ (1998) Myc activates telomerase. Genes Dev 12: 1769-1774

Wang SS and Zakian VA (1990) Telomere-telomere recombination provides an express pathway for telomere acquisition. Nature 345: 456-458

Watson JD (1972) Origin of concatameric T4 DNA. Nat New Biol 239: 197-201

Weinert TA and Hartwell LH. (1988) The RAD9 gene controls the cell cycle response to DNA damage in *S. cerevisiae*. Science 241: 317-322

Weinert TA, Kiser GL and Hartwell LH (1994) Mitotic checkpoint genes in budding yeast and the dependence of mitosis on DNA replication and repair. Genes Dev 8: 652-665.

Weinrich SL, Pruzan R, Ma L, Ouellette M, Tesmer VM, Holt SE, Bodnar AG, Lichtsteiner S, Kim NW, Trager JB, Taylor RD, Carlos R, Andrews WH, Wright WE, Shay JW, Harley CB and Morin GB (1997) Reconstitution of human

telomerase with the template RNA component hTR and the catalytic protein subunit hTRT. Nat Genet 17(4): 498-502

Williamson JR, Raghuraman MK and Cech TR (1989) Monovalent cation-induced structure of telomeric DNA: The G-quartet model. Cell 59: 871-880

Wotton D and Shore D (1997) A novel Rap1p-interacting factor, Rif2p, cooperates with Rif1p to regulate telomere length in *Saccharomyces cerevisiae*. Genes Dev 11: 748-760

Wright JH, Gottschling DE and Zakian VA (1992) *Saccharomyces* telomeres assume a non-nucleosomal chromatin structure. Genes Dev 6: 197-210

Wu CI, Lyttle TW, Wu ML and Lin GF (1988) Association between a satellite DNA sequence and the Responder of Segregation Distorter in *D. melanogaster*. Cell 54(2): 179-89

Xiao Y and Natarajan AT (1998) Development of arm-specific and subtelomeric region-specific painting probes for Chinese hamster chromosomes and their utility in chromosome identification of Chinese hamster cell lines. Cytogenet Cell Genet 83(3-4): 208-213

Yu GL, Bradley JD, Attardi LD and Blackburn EH (1990) *In vivo* alteration of telomere sequences and senescence caused by mutated *Tetrahymena* telomerase RNAs. Nature 344: 126-132

Yu GL and Blackburn EH (1991) Developmentally programmed healing of chromosomes by telomerase in *Tetrahymena*. Cell 67: 823-832

Zahler AM and Prescott DM (1988) Telomere terminal transferase activity in the hypotrichous ciliate *Oxytricha nova* and a model for replication of the ends of linear DNA molecules. Nucleic Acids Res 16: 6953-6972

Zahler AM, Williamson JR, Cech TR and Prescott DM (1991) Inhibition of telomerase by G-quartet DNA structures. Nature 350: 718-720

Zakian VA (1995) Telomeres: beginning to understand the end. Science 270: 1601-1607

Zhang P and Spradling AC (1993) Efficient and dispersed local P element transposition from *Drosophila* females. Genetics 133(2): 361-73

Zhang X, Mar V, Zhou W, Harrington L and Robinson MO (1999) Telomere shortening and apoptosis in telomerase-inhibited human tumor cells. Genes Dev 13: 2388-2399

Zheng P, Fayn DS, Burton J, Xiao H, Pinkham JL and Stern DF (1993) *SPK1* is an essential S phase specific gene of *S. cerevisiae* that encodes a nuclear serine/threonine/ tyrosine kinase. Mol Cell Biol 13: 5829-5842

Zhou J, Monson EK, Teng S, Schulz VP and Zakian VA (2000) Pif1p helicase, a catalytic inhibitor of telomerase in yeast. Science 289: 771-774

Zhu J, Wang H, Bishop JM and Blackburn EH (1999) Telomerase extends the lifespan of virus transformed human cells without net telomere lengthening. Proc Natl Acad Sci USA 96: 3723-3728

Zou H, McGarry TJ, Bernal T and Kirschner (1999) Identification of a vertebrate sister-chromatid separation inhibitor involved in transformation and tumorigenesis. Science 285: 418-422